Design and application of a hydrodynamic cavitation system in textile wastewater treatment

by

Ninette Irakoze

Thesis submitted in the fulfilment of the requirements of the degree

Master of Engineering: Chemical Engineering

In the
Faculty of Engineering and the Built Environment

At the
Cape Peninsula University of Technology

Supervisor: Prof. T.V. Ojumu

Co-Supervisor: Prof L.F. Petrik

Bellville Campus

2020

DECLARATION

I, Ninette Irakoze, declare that the contents of this thesis represented my own unaided work, and that the thesis has not previously been submitted for academic examination towards any qualification. Furthermore, it represents my own opinions and not those of the Cape Peninsula University of Technology.

Signed: _____ **Date:** _____

ABSTRACT

The industrial sector has been growing in South Africa and in Africa in general. This has caused an increase in generation of wastewater which needs to be treated to avoid polluting the environment and those living in it. Textile industry is one of the major polluting industries and textile dyes such as azo dyes are among dyes that are hard to degrade due to their low biodegradability.

The azo dyes are among persistent organic pollutants (POPs) which are hard to treat using conventional treatment methods namely biological methods, coagulation/flocculation, chlorination, adsorption, reverse osmosis etc. This issue has created a need for the development of advanced treatment methods. Advanced oxidation processes (AOPs) are among advanced treatment methods that are effective in the removal of POPs from wastewater. In recent years, one form of AOPs has emerged as a simple method, that is energy-efficient and that has proved to be successful in the degradation of textile dyes. The technology is cavitation, which is a technique that involves the generation, growth and collapse of cavities/bubbles caused by rapid pressure changes. The collapse of the cavities/bubbles produces high amount of energy releasing highly reactive free radicals (hydroxyl radicals) that are generated through the dissociation of water molecules. Cavitation can be generated in different ways and the names of the different types of cavitation are based on the way the cavitation is generated. The common types of cavitation are hydrodynamic cavitation and acoustic cavitation.

In this study, a hydrodynamic cavitation (HC) jet loop system with different cavitating devices was designed and his performance in the treatment of simulated textile wastewater was investigated. A 10 L of 20 ppm of Orange II sodium (OR2) dye solution was used as simulated textile wastewater and its decolouration was monitored. The cavitating devices used were a 10 mm throat diameter venturi and 5 orifice plates with different hole diameters (2 mm, 3 mm, 4 mm, 5 mm, and 6 mm). The different cavitating devices were each used in the HC jet loop system to determine their efficiency in decolourising OR2 dye. The combination of the venturi and the best performing orifice plate in the HC jet loop system was also investigated. In the study different inlet pressures (200 kPa, 300 kPa, and 400 kPa) were also investigated to determine how they affect the performance of the HC jet loop system. Lastly, the energy consumption and the cost of using the HC jet loop system as an extension on to an existing plant was also determined.

Results have shown that the HC jet loop system performs best at an inlet pressure of 400 kPa. For the cavitating devices, the orifice plate having a 2 mm orifice plate was found to be the best cavitating device among all the cavitating devices tested. It has allowed for a 91.11% decolouration in 10 min when using 400 kPa inlet pressure. The combination of the 10 mm throat diameter venturi and the 2 mm hole diameter orifice plate provided an intermediate performance with a 74.08% decolouration while the 10 mm throat diameter venturi provided the poorest performance with a 58.73% decolouration in 10 min at an inlet pressure of 400 kPa.

With regards to the consumption of energy, the HC jet loop system was found to use 0.548 kW/m^3 for dye decolouration which is a relatively low energy consumption compared to the energy consumption incurred by the UV for instance for dye decolouration. Regarding costs, the investment costs was estimated to be R 104 843.00 for an HC jet loop system with a capacity to decolourise 500 L of dye contaminated wastewater. The operating costs were estimated at R 127.24 for the decolouration of 500 L of dye contaminated water when considering that the system will be an extension to an existing plant.

Overall the designed HC jet loop system was found to be an effective technique to use for the decolouration of textile dyes found in textile wastewater such as Orange II sodium salt.

Keywords: Textile wastewater, Azo dyes, Hydrodynamic cavitation, AOPs, POPs.

DEDICATION

This thesis is dedicated to my loving parents

Astère Kibuka

And

Frédérique Ntezahorirwa

For their endless love, support and encouragement

ACKNOWLEDGEMENTS

First of all, I would like to thank my parents for always being there, for their love and support throughout my life. Thank you for inspiring me and giving me the strength to chase my dreams. To my brothers and sister, you deserve my heartfelt thank you for your love, support and understanding throughout my studies.

I also would like to sincerely thank my supervisor Prof. Tunde Ojumu for his support and guidance throughout my studies.

To my co-supervisor Prof. Leslie Petrik, I wish to express my heartfelt gratefulness for providing me with the opportunity to join the Environmental and NanoScience (ENS) research group, for her support and guidance during my research. Her insight into my research topic and advice have been invaluable.

To my mentor Dr. Kassim Badmus, a special thank you to him for his assistance and advice throughout my research project.

I would like to acknowledge the ENS research group for the warm welcome and support I have received since joining the group. I would like to especially thank Mrs Natacha Kakama for her assistance with my lab work, Mrs Vanessa Kellerman, Mrs Ilse Wells and Mr. Denzil Bent for the administrative assistance, Dr. Emile Massima for his advice and Dr. Guillaume Ndayambaje for introducing me to ENS research group.

I would like to also acknowledge Sam Lucas and Geoff Busch from the technical team at the University of the Western Cape (UWC). I am truly grateful for their assistance in constructing and assembling the system used in this study.

To my friends, especially Inès Niragira and Alida Divine Irambona, I would like to thank them for always being supportive, understanding and for their encouragement in my many moments of crisis.

Last but certainly not least, I would like to thank God for **always** being there for me.

TABLE OF CONTENTS

TABLE OF FIGURES

TABLE OF TABLES

LIST OF SYMBOLS AND ABBREVIATIONS

Symbol	Description	Units
English symbols		
H_D	Pumping head	m
H_L	Head loss	m
$\dot{V}$	Volumetric	m^3/s
A	Area	m^2
D	Diameter	m
f	Friction loss	j/kg
g	Gravitational acceleration	m/s^2
L	Length	m
P	Pressure	Pa
v	Velocity	m/s
Z	Elevation	m
Greek symbols		
ϵ	Relative roughness	No units
ε	Absolute roughness	m
μ	Viscosity	Pa.s
π	Pie	No units
ρ	Density	kg/m^3

Abbreviations

AOP:	Advanced oxidation process
BOD:	Biochemical Oxygen Demand
COD:	Chemical Oxygen Demand
HC:	Hydrodynamic Cavitation
HTA:	Hydroxyterephthalic Acid
O.P.:	Orifice plate
OH:	Hydroxyl
OR2:	Orange II Sodium

TA:	Terephthalic Acid
TDS:	Total dissolved solids
TOC:	Total organic carbon
TSS:	Total suspended solids
UV:	Ultra-violet
V.:	Venturi

CHAPTER 1: INTRODUCTION

Introduction

The following chapter gives a brief background of the research, the problem statement of the research and the research questions. Furthermore, the aim and objectives of the study will be outlined, as well as the delineation and significance of this study. The chapter will be concluded with the thesis outline.

1.1. Background

As the population and industries grow, the quality of drinking water has been declining due to pollution. Pollution from sewage is one of the major causes of declining drinking water quality (Jyoti &, Pandit, 2000). Beside reducing pollution, effective treatment of wastewater helps to improve drinking water quality.

Water/wastewater treatment consists of different steps aimed at removing physical, chemical and biological pollutants from the wastewater. Some of the conventional methods used in water treatment have drawbacks that at times outweigh their efficacy and others are not efficient in treating emerging pollutants, which creates a need for advanced methods of treatment.

The following study investigates the use of hydrodynamic cavitation as a textile wastewater treatment method.

The textile industry is among industries that use large amounts of water (Buthelezi et al., 2012) and consequently produces large amounts of wastewater that contain complex chemicals (Wang et al., 2011). In cotton wet processing, the water usage (L/kg) of product is as follows:

the dyeing process uses 8-300 L/Kg of product, the mercerising process uses 232-308 L/Kg of product while the bleaching process uses 3-124 L/Kg of product (Carmen & Daniela, 2012). Textile wastewater contaminants such as dyes are hard to treat, and are toxic, carcinogenic and the effluents contain high COD and BOD (Wang et al., 2011; De Jager, 2013). Textile wastewater therefore requires treatment before being discharged into the environment or reused/recycled (Teodosiu & Petronela, 2007). Methods used in the treatment of textile wastewater to remove dyes such as activated carbon or electrochemical destruction are expensive (Robinson et al., 2001). The azo dyes contained in textile wastewater are hard to treat using conventional methods (De Jager, 2013).

Advanced oxidation processes (AOPs) are some of the advanced methods of treatment of wastewater.

According to Deng & Zhao (2015), AOPs were introduced around the 1980s and they encompass oxidation processes that produce hydroxyl radicals (ºOH) and sulfate radicals ($SO4\cdot^-$) for the treatment of water and wastewater containing organic and inorganic pollutants. Some of the AOPs are photocatalytic oxidation, Fenton oxidation, acoustic cavitation, hydrodynamic cavitation. Hydrodynamic cavitation is one of the energy-efficient AOPs (Rajoriya et al., 2016).

Cavitation has for a long time been known for its disadvantages such as plumbing issues like erosion, noise and vibration. These can negatively affect the functioning of a variety of machines such as turbomachines and positive displacement machines. Cavitation can nevertheless have some positive effect in certain cases. It can in fact lead to a drag reduction or to a better liquid atomisation in submarine vehicles or in fuel injector holes respectively (Ferrari, 2017). It can also be used in ultrasonic cleaning baths, in enhancing chemical reactions, in medical treatments and in wastewater treatment (Mecholic, 2018).

Hydrodynamic cavitation (HC) takes place when a liquid passes through a constriction created by a venturi, a throttling valve or orifice (Tao et al., 2016), which causes an increase in kinetic energy and a decrease in pressure. The pressure at the throat of the constriction drops below or to the same pressure as that of the vapour pressure of the liquid, causing the liquid to vaporise which generates cavities (Saharan et al., 2012; Tao et al., 2016). When the pressure recovers at the end of the constriction the cavities collapse, generating hot spots, releasing highly reactive radicals (Saharan et al., 2012). In those hot spots temperatures can be as high as 10000 K and the pressure at about 1000 atmosphere (Terán et al., 2016).

According to Rajoriya et al. (2016), the degradation of pollutants using AOPS can occur through two mechanisms, namely thermal decomposition (pyrolysis) of the pollutants, and OH radical reactions with the pollutants.

1.2. Problem statement

Hydrodynamic cavitation (HC) is an advanced oxidation process (AOP) used in wastewater treatment. There are limited studies that compare and/or combine different cavitating devices. It will be important to explore the comparison and/or combination of different cavitating devices such as orifice plates and venturis to improve the performance of an HC jet loop system.

1.3. Research questions

This study intends to answer the following questions:

1. What cavitating device is best suited to generate OH radicals in the hydrodynamic cavitation jet loop system?
2. At what operating pressure is the hydrodynamic cavitation jet loop system most effective in generating OH radicals?
3. Can hydrodynamic cavitation treat textile wastewater?
4. What are the energy consumption and operating costs of treating textile wastewater using hydrodynamic cavitation?

1.4. Aim and objectives of the research

The aim of this study is to design an effective hydrodynamic cavitation jet loop system with a view to improving its performance in the treatment of textile wastewater.

The objectives of this study are as follows:

- To determine which orifice plate among various types of orifice plates with different hole diameters is more effective in treating simulated textile wastewater using a hydrodynamic cavitation jet loop system.
- To combine the venturi and the orifice plate to determine the effectiveness of simulated textile wastewater treatment using the 2 types of cavitating devices simultaneously in the hydrodynamic cavitation jet loop system.
- To determine at what inlet pressure the hydrodynamic cavitation jet loop is more effective in treating simulated textile wastewater.
- To determine the OH radicals produced by the hydrodynamic cavitation jet loop system when applying the optimum operating conditions and optimum design conditions.
- To determine the energy consumption and cost of using the hydrodynamic cavitation jet loop system for the treatment of simulated textile wastewater when applying the optimum operating conditions and the optimum design conditions.

1.5. Research approach

The study begun with machining of the cavitating devices that were used in the hydrodynamic cavitation jet loop system.

Upon completion of the machining of the cavitating devices, the effectiveness of simulated textile wastewater treatment through the decolouration of Orange II sodium (OR2) dye solution was determined using the different cavitating devices in the hydrodynamic cavitation jet loop system. The cavitating devices that were used were one venturi and five different orifice plates, then a combination of the venturi and the orifice plates. Operating conditions such as pressure were then varied to determine the optimum operating conditions for the decolouration of OR2 dye solution. After that, a quantification of OH radicals generated by the hydrodynamic cavitation jet loop system under optimum operating and design conditions was done.

To determine the extent of decolouration of the OR2 dye solution, the UV-spectrophotometry technique was used. This technique is used to determine the amount of ultraviolet or visible radiation a substance in solution absorbs. The instrument used is a UV-spectrophotometer. In quantitative analysis, a UV-spectrophotometer can be used to identify organic compounds. It helps to determine the absorption intensity of a given organic compound at a given wavelength. The use of spectrophotometric analysis also implies the use of the Beer-Lambert law which relates the absorbance of a solution to the concentration of the solution, stating that the former is directly proportional to the latter (Behera et al., 2012; Badmus et al., 2016; Peralta et al., 2014).

To determine the amount of OH radicals produced a spectrofluorometer was used. A spectrofluorometer is an instrument used to measure the fluorescence of certain compounds and based on the fluorescence intensity, the concentration of the fluorescent compound and its chemical environment can be determined. When using a spectrofluorometer, a sample is excited at a certain wavelength using a light source and the fluorescence emission of the sample can be observed at another wavelength. The latter can be a single wavelength or a scan can be done by recording the intensity versus wavelength, also known as emission spectra (Genovesi, 2015).

1.6. Delineation of the research

This study mainly focused on the optimisation of the HC jet loop system for the treatment of textile wastewater. Selected cavitating devices and different operating conditions such as pressure were optimised through the treatment of OR2 dye solution and quantification of the amount of OH radicals generated by the HC jet loop system under different conditions. In addition to that, the energy consumption and the cost of operating the hydrodynamic cavitation jet loop system were also investigated.

1.7. Significance of the research

This research will help to advance knowledge of wastewater treatment using advanced oxidation processes, particularly using hydrodynamic cavitation. The successful completion of the study will shed light on what cavitating device between the venturi and orifice plate is best at generating ºOH radicals for the treatment of textile wastewater; on what are the best cavitating device combinations between a venturi and different orifice plates in generating OH radicals; on what is the best inlet pressure in generating OH radicals for the treatment of textile wastewater; and on what are the energy consumption and the cost of treating textile wastewater using hydrodynamic cavitation.

1.8. Thesis outline

This thesis is structured as follows: Chapter 1 consists of an introduction to the research. Chapter 2 is a literature review of the research topic; it gives an overview of the hydrodynamic cavitation phenomenon and the use of hydrodynamic cavitation in wastewater treatment. Chapter 3 provides the research design and methodology used to conduct this study. Chapter 4 compares the performances of an HC jet loop system equipped with a single cavitating device and an HC jet loop system equipped with combined cavitating devices in decolourising OR2 dye solution and in generating OH radicals. Chapter 5 looks at the energy consumption and Chapter 6 covers the cost of using HC jet loop system in the decolouration of OR2 dye solution. Lastly, Chapter 7 draws conclusions on the study conducted and will provide recommendations for future work.

CHAPTER 2: LITERATURE REVIEW

Introduction

This chapter reviews the work that has been done by others in terms of textile wastewater treatment. It covers the characteristics of textile wastewater and the different techniques used in its treatment. Chapter 2 goes into detail on how advanced oxidation is used to treat wastewater and how hydrodynamic cavitation in particular is used in textile wastewater treatment. A description of the characterisation techniques that were used in this study is found in this section. Lastly the gap in literature related to HC as a wastewater treatment method is discussed.

The textile industry was reported to be the 2nd largest producer of effluent in Cape Town in the 2010 Water Research Commission report (Cloete et al., 2010). Water used per day by an average sized textile manufacturer is estimated to be 200L per kg of fabrics processed. The textile dyeing and finishing processes generate 17 to 20 percent of industrial wastewater (Holkar et al., 2016). Effluent from textile processes contains high chemical oxygen demand (COD) (537 to 9553 mg/litre) that is harmful to aquatic life and the environment and could lead to oxygen depletion (Cloete et al., 2010). The authors further state that the pH of most textile effluent is 8, but can vary from 5 to 12.

With the water scarcity faced by South Africa, effective treatment of wastewater is critical to economic growth (Anjum et al., 2016). Shortage and compromised quality of water will aggravate other risks that the South African business sector is facing (Le Roux, 2017). Among other causes of the water crisis in South Africa is underinvestment in wastewater treatment plants, which results in discharge of close to 4 billion litres of untreated or partially treated sewage, causing eutrophication of most major dams (Petrie, 2016). Given the increasing water demand and impacts of climate change it is recommended to continue investing in best water management practices (UNU-WIDER, 2016) such as wastewater reuse, as it is a source that is available all year round (Skosana, 2015).

2.1. Textile industry operations

The textile industry is involved with the preparation and transformation of fibres into yarn. The latter is further transformed by the industry into fabrics which in turn go through several other stages of transformations involving wet processes. Those wet processes are (Holkar et al., 2016):

a. Sizing

This process consists of applying a protective adhesive coating upon the surfaces of the yarn during weaving. After the weaving process, the fabric is desized (Garlick, 1986).

b. Desizing

The dyeing and printing processes are affected by sizing chemicals which makes desizing an important process preceding the dyeing and printing processes. Desizing is a process of removing non-fibrous substances such as starch by converting them into a soluble form using hydrolysis. Desizing can be achieved using two methods, acidic and enzymatic methods. Effluents from desizing have a high biochemical oxygen demand (BOD) content (Masupha, 2007; Holkar et al., 2016).

c. Bleaching

For the production of bright and pale fabrics, the yarn needs to be bleached (Babu et al., 2007). The bleaching process is a wet process performed at pH 9-11 at room temperature. Hydrogen peroxide and peracetic acid can be used for this process. Peracetic acid is believed to give a higher lustre and cause less destruction to the yarn (Masupha, 2007; Holkar et al., 2016).

d. Mercerizing

This operation involves the treatment of cotton material with a sodium hydroxide solution having an 18% to 24% concentration followed by washing off the sodium hydroxide solution after 1 to 3 min while the cotton material is held under tension. This process is used to provide lustre, increase dye uptake, and increase strength (Babu et al., 2007).

e. Dyeing

This process consists of the treatment of fibre or fabric using pigments to provide colour to the fabric or fibre (Babu et al., 2007). This wet operation is carried out at a pH ranging from 6 to 12 and a temperature ranging from room temperature to boiling temperature. The operation is performed using water, a paste of dye, dye assistants, hygroscopic substances, thickener and other chemicals (Masupha, 2007).

f. Printing

Printing is a branch of dyeing defined as localised dyeing. Printing differs from dyeing in that when applying colour in the dyeing process a solution of dye is used while for the printing process a thick paste of dye is used (Babu et al., 2007).

g. Finishing

Textile products are subjected to finishing processes to soften, cross-link and waterproof them. Finishing processes are known to cause water pollution. (Babu et al., 2007).

2.2. Characteristics of textile wastewater

Textile industry products are developed using organic and inorganic chemicals in bleaching, colouring, designing and in finishing processes (Imtiazuddin et al., 2012).

Not all the organic and inorganic chemicals are used in the process of textile manufacturing, as some are washed off in the process. Imtiazuddin et al. (2011) states that the inorganic chemicals in the textile wastewater contain heavy metals and the organic chemicals contain toxic dyes and pigments that can cause cancer, tumours, and other diseases if they find their way into ground water and are consumed by human beings.

Some of the heavy metals contained in the textile wastewater are Cr, As, Cu and Zn (Ghaly et al., 2013). And because of the organic chemicals used in the textile industry, its wastewater contains high levels of chemical oxygen demand (COD), biochemical oxygen demand (BOD), total organic carbon (TOC), total suspended solids (TSS), and oil & grease (O&G) (Ahmed, 2007). Textile effluent also contains microbial impurities (Ghaly et al., 2013).

Table 2-1 shows values of different parameters in untreated textile wastewater reported in literature.

Table 0-1: Characteristics of textile wastewater

Process	Parameters	Minimum value	Maximum value	Authors
Textile wastewater	pH	6	10	(Ghaly et al., 2013)
	COD (mg/L)	150	12000	
	BOD (mg/L)	80	6000	
	TDS (mg/L)	8000	12000	
Dyeing	pH	6.5	12.1	(Savin & Butnaru, 2008)
	COD (mgO_2/D)	458	7561	
	BOD (mgO_2/L)	230	410	
	TSS (mg/L)	175	325	
Dyeing	pH	5	10	(Carmen & Daniela, 2012)
	COD (gO_2/L)	1.1	4.6	
	BOD (gO_2/L)	0.01	1.8	
	TDS (g/L)	0.05	0.05	
Bleaching	pH	8.5	9.6	(Carmen & Daniela, 2012)
	COD (gO_2/L)	6.7	13.5	
	BOD (gO_2/L)	0.1	1.7	
	TDS (g/L)	4.8	19.5	
Desizing	pH	-	-	(Bisschops & Spanjers, 2003)
	COD (mg/L)	950	20000	
	BOD (mg/L)	200	5200	
	TSS (mg/L)	400	4000	
Printing	pH	-	-	(Bisschops & Spanjers, 2003)
	COD (mg/L)	785	49170	
	BOD (mg/L)	600	1800	
	TDS (mg/L)	-	-	
Bleaching	pH	-	-	(Bisschops & Spanjers, 2003)
	COD (mg/L)	288	13500	
	BOD (mg/L)	90	1700	
	TDS (mg/L)	4760	19500	

2.3. Environmental impact of textile wastewater

Some of the major pollutants in textile wastewater are dyes, and the major environmental concern associated with textile wastewater worldwide is water pollution (Khan & Malik, 2014). Dyes found in textile effluent can inhibit the sunlight from penetrating the water surface, which disturbs the aquatic ecosystem (Ghaly et al., 2013). Textile effluents contain hydrosulphides that cause reduction in the oxygen concentration (Khan & Malik, 2014). Some colourants used in the textile industry go into the wastewater and they contain organically bound chlorine which is known to be carcinogenic (Khan & Malik, 2014).

Inorganic pollutants contained in textile effluent are constituted of soluble salts which render water inappropriate for use. The organic pollutants contained in textile effluent, if left untreated, can gradually degrade into undesirable conditions such as gases, odours, floating solids and disagreeable appearance (Masupha, 2007).

Thus, untreated or partially treated textile wastewater is a threat to human and aquatic life (Khan & Malik, 2014).

2.4. Textile dyeing wastewater treatment

Colour is a key element in creating a successful textile product. To give colour to fabrics, dyes are used in the textile industry. For a given type of fibre, a certain type of dye is used to ensure that the characteristics of the textile product are of a certain standard in terms of colour and texture. The consumer looks for a product that can withstand washing and prolonged use and the fabric used in textile products must be resistant to fading, and must have a high affinity and uniform colour (Chequer et al., 2013).

In terms of dyes used to colour fibres, for cotton fibre for instance, direct dyes, reactive dyes, vat dyes and azo dyes can be used. On the other hand, acid dyes are used to give colour to wool. For silk, acid and direct dyes can be used and for polyester, disperse and azo dyes are used (Holkar et al., 2016). As stated above, the textile industry uses a considerable amount of water, thus generating large quantities of wastewater containing dyestuff. For different types of dyes contained in a given textile wastewater, different techniques are required to degrade the different dyes (Gosavi & Sharma, 2014).

Textile dyeing wastewater treatment can be divided into 3 major categories, namely physical methods, biological methods and chemical methods. The physical methods involve techniques such as flocculation-coagulation, adsorption and filtration. The biological methods use enzymes and microorganisms, while the chemical methods are concerned with the use of oxidation or electrochemical techniques, to name a few.

Each of these methods has its own limitations and often cannot be used individually to successfully degrade textile wastewater. However, in combination, these processes give suitable results (Gosavi & Sharma, 2014; Holkar et al., 2016). Physical methods are often simple processes but they can be costly to maintain, can generate sludge and can require high energy investment. Biological methods are also simple to use and economically appealing. However, biological processes can be slow, require pre-treatment, need a favourable environment for their use, and create a biological sludge. Chemical methods have the advantage of being simple, rapid and efficient processes. Chemical processes do not often produce sludge, but the use of chemicals in these types of processes can be costly, and these methods also require pre-treatment (Crini & Lichtfouse, 2019). In terms of limitations, besides the fact that the physical, chemical and biological methods cannot be used individually for efficient treatment of textile wastewater, it is clear that they can all be costly to use, either due to energy consumption or chemical consumption, and they all are prone to generating sludge. It would be cost-effective if these methods could be improved, whether be by reducing energy consumption, chemical consumption, or sludge generation.

The different textile dyeing wastewater treatment methods are reviewed in the following sections.

2.4.1. Physical methods

There are various types of physical methods used in textile wastewater treatment. Some of those are: sedimentation, filtration, flotation, coagulation, reverse osmosis, adsorption, membrane filtration, foam fractionation, and membrane treatment (Kant, 2012). Coagulation-flocculation has proven to be an easy process to operate. It is cost-effective and energy-saving method to remove particles in wastewater using inexpensive particle-separation procedures such as gravity, sedimentation and filtration. It is considered efficient in decolourising disperse dyes but when it comes to reactive dyes and vat dyes, this method is of low efficiency. Some of the most commonly used coagulants are alum ($Al_2(SO_4)_3.4H_2O$ and PAC (poly aluminium chloride). The disadvantages of coagulation-flocculation are that beside being ineffective in treating a wide variety of dyes, it also generates large amounts of sludge (Liang et al., 2014). Adsorption as a textile wastewater treatment technique has the advantage of being a simple process and does not generate sludge but it is expensive, the adsorbent needs regeneration and it can easily clog the reactor. The most widely used adsorbent for industrial applications is activated carbon (Galán et al., 2013). There are more adsorbents such as silica gel, activated alumina, zeolites, clay, polymer and resins (Visual Encyclopedia of Chemical Engineering, 2020; Crini & Lichtfouse, 2019). Membrane technologies such as reverse osmosis and membrane filtration produce high quality treated effluent and are effective in decolourising all types of dyes. They do not require chemicals and they have low solid waste generation.

Their disadvantages are that they have high investment costs both for small industries and medium industries; the membranes tend also to be easily clogged; they have high energy requirements; and high maintenance and operation costs (Crini & Lichtfouse, 2019).
The use of physical methods is important in wastewater treatment. However cheaper, less energy-intensive and more efficient processes still need to be developed.

2.4.2. Biological methods

When degrading dyes in textile wastewater using biological methods, the efficiency of this method depends on the scale of organic load such as dye and microorganism load, the temperature, and the oxygen concentration in the system. There many microorganisms that can degrade dyes and some of those are bacteria, fungi, and algae. When using bacteria, the biological methods used can be classified in two main categories based on oxygen requirements. The first class is aerobic methods and the second class is anaerobic methods. The aerobic methods use microbes for the treatment of textile wastewater in the presence of oxygen while the anaerobic methods use microbes for textile wastewater treatment in the absence of oxygen. At times the two methods can be combined (Wang et al., 2011). For decolourisation, a number of bacteria can achieve azo dye reduction. This occurs in the absence of oxygen through the breaking of azo bonds into a colourless solution of aromatic amine. The aromatic amines can be further catabolised under an aerobic process. For the anaerobic process, there is a need for energy to achieve azo bond reduction, which can be supplied by organic carbon. For the aerobic process, some bacteria have been able to break the azo bonds in azo dyes by using the carbon in the azo complex as a source of energy. Some of the anaerobic bacteria are *Escherichia coli*, *Pseudomonas sp*., *Pseudomonas aeruginosa*, *Clostridium perfringens,* to name a few. Some of the aerobic bacteria are *Klebsiella sp*., *Bacillus subtilis*, *Staphylococcus lentus*, *Lysinibacillus sp*. and *Pseudomonas luteola*.
Fungi have also proved to be able to degrade azo dyes. Some of the fungi used are white rot fungi *Coriolopsis sp*., *Penicillium simplicissimum*, or *Pleurotus eryngii*. The use of fungi has the disadvantage of being unstable, causing bacteria to grow in the system after a certain amount of time (20-30 days) which will then result in the non-degradation of dyes. Algae are also microorganisms that are effective in degradation of dyes. The latter can occur through transformation of dyes to non-coloured intermediates, or CO_2 and H_2O (biodegradation) chromophore adsorption on algae (biosportion) and consumption of dyes for their growth (Meng et al., 2014). Some of the algae used in biosorption are brown alga, *Stoechospermummarginatum*, *Xanthophyta* alga and *Vaucheria* species. For biodegradation the types of algae used are green macroalga *Enteromorpha sp*., *Shewanella* algae (SAL) and green macroalgae *Cladophora* species.

Green macroalgae *Cladophora* species have been found to be particularly successful in degrading azo dyes. This is due to the fact that the algae contains an azoreductase enzyme (Bhatia et al., 2017).

Biological methods require pre-treatment with careful management and maintenance of the microorganisms which constitute some of the disadvantages of this method. Pollutants with low biodegradability are also be difficult to treat and there might be generation of biological sludge.

2.4.3. Chemical methods

Oxidation, ozonation, photochemical methods and electrochemical degradation are some of the chemical methods used in textile dyeing wastewater treatment (Holkar et al., 2016; Gosavi & Sharma, 2014).

Chemical oxidation is a technique used to oxidise wastewater pollutants such as dyes. The oxidising agents used are ozone and/or hydrogen peroxide because of their high oxidation potential. The two oxidising agents have been found to be effective in breaking down conjugated double bonds and complex aromatic rings present in dyes. Ozonation is reported to be a costly method due to the short half-life of ozone (Tehrani-Bagha et al., 2010; Miralles-Cuevas et al., 2016). Dye removal and toxicity reduction in textile wastewater have also been achieved through the use of photocatalytic oxidation on immobilised TiO_2 in the presence of solar irradiation and combined with electrochlorination (Ratna & Padhi, 2012). The application of powdered TiO_2 is however believed to increase solution turbidity in wastewater treatment, which interferes with the interaction of UV light and pollutants, causing a reduction in the photocatalytic potential of the system (Tijani et al., 2017). Electrochemical degradation such as electrochemical oxidation has been effective in decolourising dye effluents. Electrochemical oxidation consists of two electrodes, anode and cathode, connected to a power source. When energy is input in the system and an electrolyte is present, strong oxidising agents are formed (hydroxyl radicals) which degrade dyes. Similarly to most of the chemical methods, one major disadvantage of using a electrochemical oxidation method is its high initial cost of equipment and maintenance cost (Anglada et al., 2009; Singh et al., 2016). Chemical methods can be more effective when combined with each other.

2.5. Advanced oxidation processes

In the last two decades advanced oxidation processes have been the object of study for the purpose of mineralising pollutants that are difficult or impossible to treat using conventional treatment methods (Saharan et al., 2012).

Most of the dyes in the textile effluents are non-biodegradable and toxic (Ghaly et al., 2013), which makes them difficult to treat using conventional methods; however advanced oxidation processes (AOPs) show a high removal rate of dyes (Wang et al., 2011).

The mechanism of AOPs is the production of highly reactive OH radicals and their ability to destroy components that are not easily oxidised (Ghaly et al., 2013; Badmus et al., 2018). Hydroxyl radicals have a relative oxidation potential of 2.06. Hydroxyl radicals (^{o}OH) can be generated in many ways and AOPs are therefore classified based on the mechanism involved in generation OH radicals (Punzi, 2015). Some of the ways of generating OH radicals are through photolytic oxidation, Fenton oxidation, acoustic cavitation and hydrodynamic cavitation (Saharan et al., 2012). But the list is not exhaustive.

The mechanism of degradation of organic substances proceeds as follows (Stasinakis, 2008):

$R + HO^{o} \rightarrow ROH$ ..... *(Equation 0-1)*

$RH + HO^{o} \rightarrow R^{o} + H_2O$ ..... *(Equation 0-2)*

$R^{n} + HO^{o} \rightarrow R^{n-1} + {}^{o}OH$ ..... *(Equation 0-3)*

With R being the organic compound.

The mechanism above is as follows: In the first reaction, the generated OH radicals attack the organic substance followed by hydrogen abstraction of the organic substance; in the second and third reaction there is electron transfer (Ghaly et al., 2013; Tijani et al., 2014).

2.5.1. Photolytic chemical processes

These techniques can be classified into two main categories based on the phases of the constituents of a given process. There is homogeneous photolytic chemical process and heterogeneous photolytic chemical process. All these photolytic processes occur under irradiation. The homogeneous process involves the use of techniques such as ultraviolet (UV) by itself or a combination of O_3/H_2O_2/UV and the photo-Fenton process. The heterogeneous photolytic chemical process involves the use UV light with metal oxides as catalyst (Gosavi & Sharma, 2014).

2.5.1.1. UV

UV radiation by itself is known to cause discolouration of dyes and pigments through photolysis. In this case the dye absorbs photons which causes ionisation of dye molecules. The possible reactions of azo dye under UV irradiation are (Feng et al., 2006):

$R_1N=NR_2 \rightarrow R_1NH_2 + R_2NH_2$ ……..... *(Equation 0-4)*

$R_1N=NR_2 \rightarrow$ R + fragments. …….. *(Equation 0-5)*

R → Product ……. *(Equation 0-6)*

$R + O_2 \rightarrow RO_2$ …….. *(Equation 0-7)*

The use of UV light alone does not give a high degree of decolourisation. UV has also limitations such as high energy requirements which make it expensive. It has however been found that when used in combination with other AOPs, it has a greater efficiency in degrading dyes or other recalcitrant organic pollutants (Badmus et al., 2018).

2.5.1.2. $O_3/H_2O_2/UV$

The $O_3/H_2O_2/UV$ process is a versatile combined advanced oxidation technique that is highly efficient in decolourising dyes. This technology is used to degrade pollutants from heavily polluted wastewater. OH radicals are produced in this system through the decomposition of H_2O_2 in the presence of light. Dissolved ozone in water can also produce hydrogen peroxide and oxygen in the presence of UV radiation (Gosavi & Sharma, 2014; Raju et al., 2015). The equations below illustrate the reactions that possibly occur when OH radicals, H_2O_2 and O_2 are produced in the presence of UV light (Raju et al., 2015).

$O_3 + H_2O + h\nu \rightarrow H_2O_2 + O_2$ …… *(Equation 0-8)*

$H_2O_2 + h\nu \rightarrow 2\ {}^{o}OH$ …… *(Equation 0-9)*

$O_3 + H_2O_2 \rightarrow 2\ {}^{o}OH + 3O_2$ ……. *(Equation 0-10)*

$O + H_2O \rightarrow 2\ {}^{o}OH$ …… *(Equation 0-11)*

When investigating the $O_3/H_2O_2/UV$ process for decolourisation efficiency of Reactive Red 2 dye, Wu and Ng (Wu & Ng, 2007) obtained a COD removal of 97.6% at pH 10, 97.2% at pH 7 and 94.3% at pH 4. The $O_3/H_2O_2/UV$ process is no doubt an efficient process when it comes to degrading organic dyes (Badmus et al., 2018; Wu & Ng, 2007). The process however would be even more widely used if it was less chemical intensive (Lester et al., 2011).

2.5.1.3. Photo-Fenton

The photo-Fenton process is a combined advanced oxidation process that involves the use of H_2O_2 and UV with iron (Fe) used as a catalyst. When compared to the Fenton process, this method has the advantage of producing a higher amount of hydroxyl radicals.

This is believed to be due to the fact that in the Fenton process, ferric ions are accumulated through the system and the reaction does not proceed once all ferrous ions are consumed. In the photo-Fenton process, due to photo-reduction of ferric ions, ferrous ions are easily regenerated. The ferrous ions react with hydrogen peroxide generating OH radicals and ferric ions again (Ameta et al., 2018). Ameta et al. (2018) further reported that the photo-Fenton process is favourable in acidic conditions at around pH 3 due to the fact that carbonate and bicarbonate species are converted into carbonic acid under those conditions and that carbonic acid has low reactivity with OH radicals. Below are the equations that describe the reaction mechanisms of the photo-Fenton process as reported by Khandelwal and Ameta (2013):

$Fe_3^+ + H_2O + h\nu \rightarrow Fe_2^+ + {}^oOH + H^+$ ..... *(Equation 0-12)*

$Fe_3^+ + H_2O_2 + h\nu \rightarrow Fe_2^+ + {}^oO_2H + H^{+.}$ ..... *(Equation 0-13)*

$Fe_2^+ + H_2O_2 \rightarrow Fe_3^+ + {}^oOH + OH^-$ ..... *(Equation 0-14)*

${}^oOH + H_2O_2 \rightarrow {}^oO_2H + H_2O$ ..... *(Equation 0-15)*

$Fe_2^+ + {}^oOH \rightarrow Fe_3^+ + OH^-$ ..... *(Equation 0-16)*

$Fe_3^+ + {}^oO2H \rightarrow Fe_2^+ + O_2 + H^+$ ..... *(Equation 0-17)*

${}^oOH + {}^oOH \rightarrow H_2O$ ..... *(Equation 0-18)*

Dye + ${}^oOH \rightarrow$ Products ..... *(Equation 0-19)*

In the presence of UV light aqueous ferric ion reduces to ferrous ion with water dissociating into a proton and hydroxyl radical (Equation 2-12).

The ferric ions react with hydrogen peroxide under UV radiation to produce ${}^oO_2H$ radical, a proton and ferrous ion (Equation 2-13).

Ferrous ions react with hydrogen peroxide to give hydroxyl ions, hydroxyl radicals and ferric ions (Equation 2-14). Ferric ion reacts with O_2H radical to produce ferrous ion, oxygen molecule and a proton (Equation 2-17).

In the photo-Fenton system, the OH radicals produced may be consumed in 4 different ways such as:

- the reaction of OH radical with H_2O_2 to produce O_2H radical and water (Equation 2-15)
- the reaction of OH radical with ferrous ion to produce ferric ion and hydroxyl ion (Equation 2-16)
- the reaction of OH radical with another OH radical to produce H_2O_2 (Equation 2-18)
- the reaction of OH radical with dye or organic pollutant to produce CO_2, H_2O and inorganic ions or biodegradable compounds (Equation 2-19).

As stated above, the Photo-Fenton reaction allows for the regeneration of ferrous ions when they are reduced to ferric ions and that is what makes this method really advantageous, especially when it comes to industrial use as further separation of ferric ions is not necessary after wastewater treatment. The limitations of the photo-Fenton process are that it generates sludge and it is an energy-intensive process which makes it expensive (Tijani et al., 2017).

2.5.1.4. UV/TiO_2

UV/TiO_2 is a combined advanced oxidation process using a heterogeneous photocatalysis chemical process to treat dyestuff and organic pollutants in wastewater. Heterogeneous photocatalysts are commonly made of transition metal oxides and semiconductors.

The most used photocatalyst is TiO_2 (Tijani et al., 2017). Some other used photocatalysts include zinc oxide (ZnO) and strontium titanium trioxide ($SrTiO_3$) (Julkapli et al., 2014; Gosavi & Sharma, 2014).

This dye degradation mechanism consists of photon absorption by the photocatalyst, charge separation and the generation of active species. The active species are generated through the oxidation of water molecules by photogenerated holes. The main active species generated are OH radicals. Another mechanism of dye decolouration using UV/TiO_2 process is by self-sensitisation. In this mechanism, the dye molecule absorbs the light. From the excited dye molecule there is charge transfer to the conduction band of the semiconductor which results in the formation of an unstable dye cation radical. At the same time there is formation of an active specie on the semiconductor surface that attacks the destabilised molecule (Rochkind et al., 2015).

2.5.2. Non-photolytic chemical processes

The non-photolytic chemical processes are advanced oxidation processes that do not involve light (direct or indirect light) in the generation of hydroxyl radicals. Some of those techniques are ozonation, electrochemical process, Fenton process, and cavitation (Gosavi & Sharma, 2014).

2.5.2.1. Ozonation

Ozonation is a wastewater treatment process that uses ozone (O_3) to decolourise dye pollutants and reduce organic loads in wastewater. Ozone is a powerful oxidising agent and it has the advantage of not creating chemical sludge. Literature has shown that it can be used to break conjugated bonds from azo dyes which reduces the molecular weight of organic acids, thus promoting colour removal. Furthermore, ozonation increases the biodegradability of the polluting compounds (Shimizu et al., 2013). Ozone has a low solubility and is highly reactive. It is usually generated on-site through high-voltage corona discharge from dry air or pure oxygen.

Ozone can also be generated using a dielectric barrier discharge (DBD). It is a system that uses plasma in aqueous solution; plasma is defined as the fourth state of matter which can induce both physical and chemical processes (Tijani et al., 2017). The mechanism of colour removal and organic compounds reduction using ozonation consists of two pathways, namely direct reaction with ozone and indirect reaction with the radical species ^{o}OH and $^{o}O_2H$. Those radical species are formed through ozone decomposition of water. Both direct ozone oxidation and radical oxidation depend on the pH of the medium and the ozone dose. Ozone has proven to be effective in colour removal; however, when it comes to COD and TOD reduction, it is less effective (Shriram & Kanmani, 2014). With the latter, it can be said that ozone is more beneficial when coupled with other AOPs.

2.5.2.2. Electrochemical oxidation process

Among electrochemical methods, electrochemical oxidation is the most applicable method for dye degradation and textile wastewater treatment. It is a clean process that operates at low temperatures and that does not require an addition of reagents in most cases. In this method, the degradation of pollutants follows two mechanisms such as anodic oxidation and electrogeneration of oxidising agents in solution (Weng et al., 2013; Ghanbari & Moradi, 2016). Anodic oxidation involves the oxidation of organic pollutants using direct electrolysis or electrogenerated hydroxyl radicals on the anode surface. Electrogeneration of oxidising agents on the other hand involves the electrogeneration of active chlorine species and the electrogeneration of hydrogen peroxide. The active chlorine species are generated at anodes such as dimensionally stable anodes (DSA), boron-doped diamond (BDD), PbO_2 and Pt. Hydrogen peroxide is in turn generated at carbon-based cathodes. An electrolyte containing chloride ions is used for the electrogeneration of the active chlorine species while a chloride-free electrolyte is used for hydrogen peroxide electrogeneration (Ghanbari & Moradi, 2016). The electrochemical oxidation method has the disadvantage of requiring costs of maintenance for the electrodes due to sludge deposition on the electrode and for the passivation of anode.

2.5.2.3. Fenton process

The Fenton process is a catalytic reaction for the generation of hydroxyl radicals using hydrogen peroxide (H_2O_2) and ferrous ions as the homogeneous catalyst. The reaction is based on an electron transfer between H_2O_2 and ferrous ions. This method efficiently mineralises organic pollutants such as dyes. It is cost-effective and practically viable due to the fact that it operates at ambient pressure and temperature and it is easy to handle (Tuty et al., 2016).

Fenton process involves the lowering of pH, oxidation reaction, neutralisation and coagulation. A low pH of about 3 has proven to give better results when degrading organic compounds using the Fenton process.

Also, the acidic pH promotes the stability of H_2O_2 and ferrous ions (Nidheesh & Gandhimathi, 2013).

The following equations illustrate some of the reactions in the mechanism of degradation of organic contaminants (RH) using Fenton process with ferrous salts as catalysts (Neyens & Baeyens, 2002; Ma et al., 2005; Badmus et al., 2018):

$Fe^{2+} + H_2O_2 \rightarrow Fe^{3+} + HO^o + OH^-$ ……. *(Equation 0-20)*

$RH + HO^o \rightarrow R^o + H_2O$ …….. *(Equation 0-21)*

$Fe^{2+} + HO^o \rightarrow Fe^{3+} + OH^-$ ……. *(Equation 0-22)*

Ferrous ions can be regenerated into the system as shown in the equations 2-7 to 2-9 by the reaction of ferric ions with H_2O_2, hydroperoxyl radicals and organic radical intermediates (Neyens & Baeyens, 2002; Ma et al., 2005).

$Fe^{3+} + H_2O_2 \rightarrow Fe^{2+} + H^+ + HO_2{}^o$ ……. *(Equation 0-23)*

$Fe^{3+} + HO_2{}^o \rightarrow Fe^{2+} + O_2 + H^+$ ……. *(Equation 0-24)*

$Fe^{3+} + R^o \rightarrow Fe^{2+} + R^+$ …….. *(Equation 0-25)*

The conversion of ferric ions into ferrous ions is a slow reaction while the reaction of ferrous ions with H_2O_2 is a fast one which causes the accumulation of ferric ions in the system.

One of the main drawbacks of the Fenton process is the wastage of oxidants through radical scavenging by the reaction of OH radicals with H_2O_2 or/and reaction of OH radicals with $Fe_2{}^+$ as in the two equations below. Another drawback of the Fenton process is the generation of Fe sludge (Matavos-Aramyan & Moussavi, 2017).

$H_2O_2 + HO^o \rightarrow H_2O + HO_2{}^o$ …….. *(Equation 0-26)*

$Fe^{2+} + HO^o \rightarrow HO^- + Fe^{3+}$ …….. *(Equation 0-27)*

2.5.2.4. Cavitation

Cavitation is a phenomenon characterised by the presence of gas in a flow of fluid that is predominantly composed of the liquid phase. There are different types of cavitation based on how the phenomenon occurs (Terentiev et al., 2011). The most common are acoustic cavitation and hydrodynamic cavitation. The other forms are optic cavitation and particle cavitation.

Acoustic cavitation is defined as the formation, growth and collapse of pre-existing microbubbles under the influence of an ultrasonic field in the liquids. In acoustic cavitation the acoustic waves cause local pressure fluctuations in liquids.

An ultrasonic horn is often used to generate acoustic cavitation in a liquid medium (Kalumuck & Chahine, 2000; Ayanda et al., 2018). Hydrodynamic cavitation is bubble generation, growth and collapse due to an increase in velocity of moving liquids and a subsequent pressure drop below or equal to the vapour pressure of the liquid, and then an increase of the pressure again which causes the bubble formed during the pressure drop to collapse (Gogate & Thanekar, 2018; Warade et al., 2016). In hydrodynamic cavitation, the geometry of the system causes a velocity increase and pressure drop in the liquid flow. Hydrodynamic cavitation can be generated using mainly four different devices such as a rotor, a throttling valve, a venturi and an orifice plate.

The bubble collapse in cavitation systems is what causes the dissociation of water molecules, thus generating hydroxyl radicals which oxidise organic pollutants (Badmus et al., 2016; Dular, Griessler-bulc, Gutierrez-aguirre, et al., 2015). Wastewater treatment using cavitation is a simple process, and hydrodynamic cavitation is considered to be low maintenance and energy-efficient which makes it an attractive AOP. Hydrodynamic cavitation will be discussed further in Section 2.6.

2.6. Hydrodynamic cavitation

Hydrodynamic cavitation (HC) is reported to be an energy-efficient method of treating aqueous effluents and is a promising, inexpensive, and less polluting way of treatment since it does not usually introduce any new chemical into the process of treatment or result in sludge production because it is a physical phenomenon (Dular, Griessler-bulc, Gutierez, et al., 2015).

Brennen (1995) explored cavitation bubbles, and explained that bubble collapse in cavitation that occurs when cavitation bubbles grow bigger than their original size (small nucleus) gives rise to high velocities, high pressures and high temperatures, which cause noises and damage to material. The collapse starts when a bubble grows to maximum radius with partial pressure of gas. The maximum radius can grow to 100 times the original size. If for example the original gas pressure was 1 bar at the start of collapse, the partial pressure of gas will be 10^{-6} bar. Calculations made by Brennen show that during collapse there is not only potential for generation of high pressures and temperatures but also generation of shock waves and noise. Thermal effects in bubble collapse are of substantial importance due to the temperature gradients that occur in very little time.

Figure 2-1 provides a description of the hydrodynamic cavitation phenomenon occurring in a venturi.

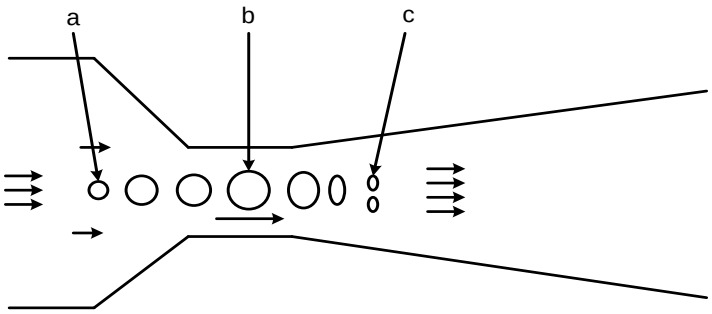

Figure 0-1: Hydrodynamic cavitation phenomenon through a venturi (Liu et al., 2019)

a) Bubble Inception and beginning of static pressure drop
b) Bubble growth and point where static pressure is equal to or smaller than the vapour pressure
c) Bubble collapse and static pressure recovery

2.6.1. Cavitation inception

Cavitation inception is a term used to describe the minimum conditions required to initiate cavitation. The likelihood of cavitation occurring in a flow regime can be estimated by calculating the cavitation number σ as in Equation 2-28, which is the ratio of forces collapsing cavities to those initiating their formation (Jyoti & Pandit, 2001).

$$\sigma = \frac{P_r - P_v}{\frac{1}{2}\rho V^2} \quad \text{..... (Equation 0-28)}$$

Where P_r is the recovery pressure; P_v is the vapour pressure of the liquid at the operating temperature of the liquid density; ρ is the density of the liquid and V is the velocity of the liquid at the orifice constriction (Jyoti & Pandit, 2001).

Cavitation normally occurs in flows with cavitation numbers that are below the cavitation inception number. The values of the cavitation inception number are typically between 1 to 2.5 for orifice flow in pipes. The value of the cavitation inception number decreases as the diameter of the orifice decreases and it increases as the sharpness of the orifice entrance increases. Therefore, the smaller the cavitation number, the higher is the cavitational intensity which means lower collapsing forces and greater initiating forces (Yan et al., 1988).

According to Boczkaja, Gągola and Przyjaznyb (2018), the geometry of a venturi tube as a cavitating device is highly important when it comes to cavitation inception. As the throat and divergent section of the venturi are responsible for the initial pressure recovery in the cavitation phenomenon, it is therefore crucial to pay special attention to the dimensions of the diameter and length of the throat as well the angle of the divergent section.

In a venturi tube, it is believed that cavitation inception occurs when the ratio of the outlet to inlet pressure is 0.8 (liquid critical pressure factor). A lower ratio will cause the linear speed of a liquid to be constant and independent of outlet pressure (Peng & Xiong, 2015; Ghassemi & Ashrafizadeh, 2015). Cavitation inception (bubble inception) is more often observed over rough surfaces rather than smooth surfaces (Ozcelik et al., 2014). Bubble inception and cavitation in a microchannel sidewall as reported by Ozcelik et al., (2014) were observed at the sidewalls of the microchannel which had a root-mean-square roughness of 100 nm based on atomic force microscopic images. On the top and bottom surfaces of the microchannel no bubble inception was observed, thus no cavitation. The top and bottom surfaces mean-root-square roughness was found to be 2.2 nm and 23 nm respectively on the basis of atomic force microscopic forces. In their study, Costa and Parkin (1975) found that polymer fluids appeared to delay cavitation inception when compared to pure water. They reported that the use of 20 ppm polymer fluid had an inception cavitation of 0.50, whereas 50 ppm polymer fluid had an inception cavitation of 0.39, with 100 ppm of polymer fluid having an inception cavitation of 0.41 and pure water had an inception cavitation of 0.73.

2.6.2. Cavitation growth and collapse

When using cavitation bubbles for cleaning, bubble implosion is indispensable. In cavitation, when a bubble forms it first grows, then collapses. The collapse of the bubble occurs because of the high pressure recovery in the vicinity of the bubbles. When conducting studies on cavitation of ship propellers Rayleigh found a mathematical expression of the collapse of a cavity (Wijngaarden, 2016):

$$R\ddot{R} + \frac{3}{2}(\dot{R})^2 = \frac{P(R)-P(\infty)}{\rho} \quad \text{..... (Equation 0-29)}$$

With R = radius of the bubble

ρ = density of the liquid

P = liquid pressure

$P(R)$ = liquid pressure at the interface

$P(\infty)$ = liquid pressure away from the bubble

$\dot{}$ = differentiation with respect to time

With R_o as initial radius $P(R) = 0$, (Equation 29) becomes:

$$R^2 = \frac{2P(\infty)}{3\rho}\left(\frac{R_0^3}{R^3} - 1\right) \quad \text{..... (Equation 0-30)}$$

In the final stage of collapse R_o is much larger than R and the bubble wall velocity u reaches the value:

$$u = [\frac{2P(\infty)}{3\rho}(\frac{R_0}{R})^3]^{1/2} \quad \text{..... (Equation 0-31)}$$

Wijngaarden (2016) also reported that cavitation collapse is responsible for the surface cleaning effect of cavitation. When a cavitation bubble collapses it emits shock waves and microjets in micro- and milliseconds. The shock waves and microjets cause surface cleaning. They generate concentrated pressures and shear and lift forces on the dirt particle and exert high impulsive loads on the layer of material to be removed. Another way of cleaning surfaces with cavitation is through the explosive growth of cavitation bubbles. This mechanism generates strong suction forces which can lift particles from the surfaces to be cleaned, sucking them towards the bubble. Fujikawa and Akamatsu (1980) found in their study that maximum temperatures and pressures of 6700K and 848 bar formed at the bubble centre and maximum temperature of 3400K at the interface. However, these temperatures existed for 2 fractions of a microsecond. After 2μs the interface temperature dropped to 300K.

2.6.3. Degradation of organic pollutants using hydrodynamic cavitation

According to Dindar (2016), there are three main factors that influence the intensity and efficiency of HC process and those are: the size and shape of the cavitating device, the characteristics of the liquid medium (viscosity, density, dissolved gas contents and surface tension), the amount of time the liquid takes to pass through the cavitating device, and interdependence between the temperature and pressure of the process.

According to Rajoriya et al. (2016), there are two mechanisms of degradation of pollutants by cavitation. They consist of thermal decomposition (pyrolysis) of pollutant molecules that are found inside the collapsing cavity and reaction of OH radicals with the pollutants. The highly reactive OH radicals are generated in the hydrodynamic cavitation system when the microbubbles collapse through the dissociation of water molecules. The OH radicals oxidise and mineralise the organic pollutants in wastewater (Saharan et al., 2012).

The following four equations illustrate the reactions that are likely to occur during oxidation of organic pollutant molecules using HC (Saharan et al., 2014):

$H_2O \rightarrow {}^{o}H + {}^{o}OH$ ..... *(Equation 0-32)*

${}^{o}H + {}^{o}H \rightarrow H_2$ ..... *(Equation 0-33)*

${}^{o}OH + {}^{o}OH \rightarrow H_2O_2$ ..... *(Equation 0-34)*

${}^{o}OH$ + Organic molecules $\rightarrow CO_2 + H_2O$ ..... *(Equation 0-35)*

2.6.4. Effect of inlet pressure upon the HC device efficiency

As mentioned above, cavitational intensity highly depends on the inlet pressure. There is an optimum pressure for a given solution to be treated using HC (Rajoriya et al., 2016). Gogate and Bhosale (2013) treated orange acid II dye with HC using an orifice plate as the cavitating device over a pressure range of 294.2 to 686.5 kPa, and found that the optimum pressure was 490.3 kPa with 23% decolouration at a pressure of 294.2 kPa, 34.2% decolouration at 490.3 kPa, and 25% decolouration at 686.5 kPa.

Mishra and Gogate (2010) treated rhodamine B dye using HC by varying inlet pressure and found an optimum inlet pressure of 486.4 kPa when using a venturi as cavitating device. The authors also found that at 587.7 kPa the extent of degradation was observed to decrease marginally.

2.6.5. Effect of initial pH of the solution

pH plays an important role in the degradation of pollutants using HC (Madhu et al., 2014). Depending on the pollutant being treated, the pH of the solution to be treated must be optimised in order to get the highest possible degradation in the shortest time (Rajoriya et al., 2016). Rajoriya and his colleagues state that the optimum pH differs from one solution to be treated to the next. The degradation of malachite green for instance was high (100% after 3 h) when the pH of the dye solution was at pH 11 (Madhu et al., 2014), while for reactive orange 4 dye the degradation was high when the dye solution pH was at pH 2, which gave a maximum degradation of 37.23% after 2 h (Ghaly et al., 2013). At pH 10 the degradation of reactive orange 4 dye was 4.6% (Ghaly et al., 2013). Acid red 88 dye could also be degraded at pH of 2 using HC with 92% degradation (Saharan et al., 2012).

2.6.6. Effect of operating temperature of the solution

Temperature is also an important parameter when using HC for the treatment of textile wastewater (Rajoriya et al., 2016). According to Wang et al. (2009), the degradation of rhodamine B using HC was investigated over a range of 30 to 60^{o}C and the highest degradation was recorded at 50^{o}C. The degradation of chitosan was also investigated and it was found that the extent of degradation increased from 54% to 89% when the temperature was increased from 30^{o}C to 70^{o}C (Wu et al., 2014). Many researchers agree that the maximum cavitation aggressiveness lies at 50 ^{o}C (Šarc et al., 2017).

2.6.7. Effect of geometry of HC device

Different researchers have shown that between the orifice plate and venturi design, the cavitating device that provides the highest dye degradation is the venturi, with the slit venturi providing a higher degradation compared to the circular venturi (Rajoriya et al., 2016; Gogate & Bhosale, 2013).

Saharan et al. (2013) have shown that the decolouration of Orange-G using slit venturi was 92% (at 3 bar and pH 2), while using a circular venturi a 76% decolouration was obtained at 5 bar and pH 2. When using an orifice plate only 45% decolouration was obtained at 5 bar and pH 2. However, Šarc et al.(2017) have found significant differences in cavitation outcomes despite the fact that very similar geometries were compared, and the same hydrodynamic conditions were used.

Figure 2-2 below illustrates orifice plates with different hole size diameter and hole number.

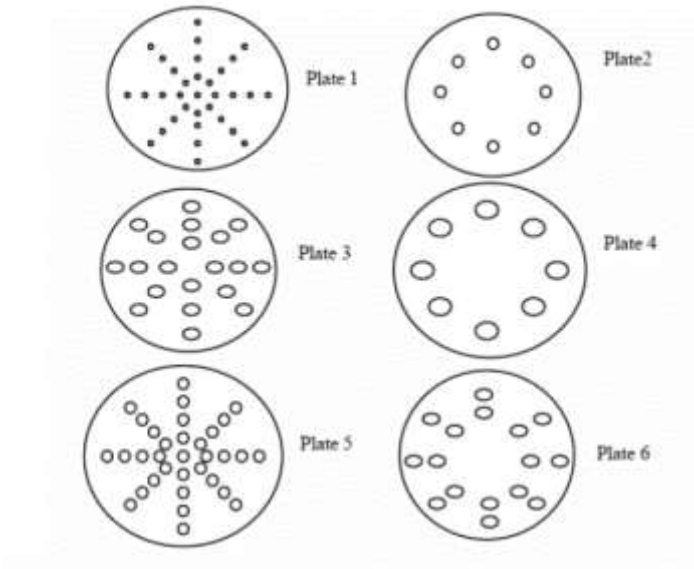

Figure 0-2: Multiple-hole orifice plates with different hole number and different hole size diameter (Dindar, 2016)

2.7. Hydrodynamic cavitation using a venturi

As far as venturis are concerned there are 2 types of venturis commonly used by researchers for generation of cavitation, namely the circular venturi and slit venturi. A circular venturi has a throat that is circular while a slit venturi has a throat that is rectangular. A venturi is made of a convergent-divergent passage. The cavitational intensity when using a venturi as cavitating reactor depends on geometrical parameters such as throat height-to-length ratios and divergent angle of the venturi.

The venturi has an advantage in creating high cavitation intensity (lower cavitation number) because it can generate a higher velocity at the throat for a given pressure drop across it. Cavities (cavitation bubbles) are created in the low pressure zone which is the throat. For a cavitation bubble to generate intense collapse forces, it needs to grow to a sufficiently large size and gather enough energy which it can release when it collapses. For a bubble to grow to a required size, its residence time in the low pressure zone (the throat) should be optimal.

Pandit et al. (2011) investigated slit venturi with different divergence angles from 5.5^{o} to 8.5^{o} and different slit height-to-length ratios from 1:0.5 to 1:3. Their results showed that a 1:1 slit height-to-length ratio gave the best results for cavitational intensity, while in terms of divergence angle, 5.5^{o} gave the best results. Dular et al. (2017) also investigated the performance of venturis with different geometrical parameters. The venturis used had the same convergence angle of 18^{o}, the same throat height-to-length ration of 1:1 and a throat cross sectional area of 10 x 10 mm^{2}. However, the divergence angles of the venturis were varied. The divergence angle degrees used were 4^{o}, 8^{o}, and 12^{o}. Two venturis of divergence angle 8^{o} were used, while one had a round continuous throat while the other had a sharp non-continuous throat. Results showed that venturis of 8^{o} divergence angle have longer cavity length (more bubbles that are agglomerated), with the non-continuous, sharply shaped venturi having the longest cavity length. It is believed that sharp venturis produce a larger pressure drop which causes the generation of longer cavity length.

Jain, Carpenter and Saharan (2014) investigated different operational and geometrical parameters of slit and circular venturis. The inlet pressure was investigated for both types of venturis and the pressures tested were of 101.325 kPa to 1013.25 kPa. Throat and slit height-to-length ratios from 1:0.5 to 1:3 were tested for both types of venturi. Also, the half divergence angles were tested for both types of venturi from 5.5^{o} to 8.5^{o}.

Jain and his colleagues showed that for a slit venturi the inlet pressure of 810.6 kPa, slit height-to-length ratio of 1:1 and divergence angle of 5.5^{o} gave the highest cavitational yields. For a circular venturi, an inlet pressure of 5 atm, throat height-to-length ratio of 1:1 and a divergence angle of 6.5^{o} gave the best cavitational yields. The circular venturi had a throat diameter of 2 mm and the slit venturi had a slit of 2 mm and a depth of 3.14 mm. These authors explained that the higher divergence angle did not give the best cavitation intensity because the boundary layer separation pressure recovered immediately in the downstream section, causing the cavities to collapse faster compared to lower divergence angles. The life of the cavity was thus reduced, which might have reduced the cavitation intensity.

2.8. Hydrodynamic cavitation using orifice plates

Orifice plates are circular plates with a hole or multiple holes. As stated above they are used to create a constriction in a piping system which has the potential of generating cavitation. Randhavane (2019) in his comparative study on 2 orifice plates with different geometrical parameters for the treatment of pesticide effluent found that orifice plate 1 with 17 1.5 mm holes performed better than orifice plate 2 with a single 2 mm hole. Orifice plate 1 achieved a 60% COD and 98% chlorpyrifos removal while orifice plate 2 achieved a 40% COD and 96% chlorpyrifos removal in 2 h.

Saharan, Rajoriya and Bargole (2017) conducted a study on the degradation of reactive blue 13 using cavitating devices with different configurations and different total flow area, with different throat perimeter to cross-sectional area ratio, as well as different throat shape and size. To investigate the different throat perimeter to cross-sectional area ratio, these authors used slit venturis and orifice plates with rectangular shaped holes. Of the orifice plates investigated, three had a cross-sectional throat area of 7.065 mm^2 while the other three had a cross-sectional throat area of 3.14 mm^2. The orifice plate with the higher throat cross-sectional area performed better than the others. In terms of orifice plate throat perimeters, it has been noticed that degradation increases up to an optimum value then upon reaching the optimum value the degradation starts decreasing slowly. For instance, for the orifice plates with a throat cross-sectional area of 7.065 mm^2, the highest degradation of reactive blue 13 was 44 % at a throat perimeter of 16.13 mm. When the throat perimeter of the orifice plate was increased to 29.28 mm the degradation slightly decreased to 42%. For the orifice plate with a 3.14 mm^2 throat cross-sectional area, the highest degradation of reactive blue obtained was 31% at a throat perimeter of 8.28 mm. When the throat perimeter was increased to 13.56 mm, the degradation decreased to 28%. A slit venturi and a circular venturi with the same throat cross-sectional area of 3.14 mm^2 were also tested and the slit venturi which had a throat perimeter of 8.28 mm achieved the best degradation of 47% while the circular venturi with 6.28 mm throat perimeter achieved a degradation of 32%. These results also showed that venturis of the same throat cross-sectional area as orifice plates performed better than the orifice plates. This is due to the fact that in a venturi the cavitation bubbles/cavities can grow bigger than in an orifice plate because of the divergent and convergent sections which allow them to generate higher cavitational intensity at their collapse.

Pandit and Sivakumar (2001) also investigated the use of orifice plates in degrading rhodamine B and they found that for orifice plates with more or less the same flow areas, the orifice plate with a greater number of holes and smaller hole diameter performed better which gave them a higher cavitational yield. A cavitational yield was defined in the authors' study as the ratio of the amount of rhodamine B degraded to energy supplied to the system.

For instance, for the degradation of rhodamine B their orifice plate of 33 holes of 1 mm hole diameter gave a cavitational yield of 3.20×10^{-8} g/J while their orifice plate of 8 holes of 2 mm hole diameter gave a cavitational yield of 1.70×10^{-8} g/J.

Table 2-2 below provides some of the results from previous studies that have been conducted on wastewater treatment using orifices plates and venturis. The pollutants treated were different dye solutions and raw textile wastewater. The table includes the type of pollutants and properties, the cavitating devices and parameters used, the percentage colour degradation and the treatment time.

Table 0-2: Wastewater treatment using orifice plates and venturis as cavitating devices

Cavitating device and their parameters	Pollutant	% colour degradation	Reference
Circular venturi with a convergent angle of 22.6°, a divergent angle of 6.4°, 2 mm throat diameter, and inlet pressure of 500 kPa	15 L solution of 22.62 ppm of Orange G at pH 2	76% in 2h	(Pandit et al., 2013)
Slit venturi with a width of 6 mm, height of 1.9 mm, length of 1.9 mm, a convergent angle of 23.5°, a divergent angle of 5.5° and inlet pressure of 300 kPa	15 L solution of 22.62 ppm of Orange G at pH 2	92% in 2h	(Pandit et al., 2013)
Orifice plate with 1 mm thickness, 2 mm hole diameter and inlet pressure of 5 bar	15 L solution of 22.62 ppm of Orange G at pH 2	45% in 2h	(Pandit et al., 2013)
Slit venturi with a width of 3.14 mm, height of 1 mm, length of 1 mm, a convergent angle of 23.5°, a divergent angle of 6.5° and inlet pressure of 500 kPa	6 L of Raw textile dyeing wastewater at pH 6.8	25% in 2h	(Rajoriya et al., 2018)
Slit venturi with a width of 3.14 mm, height of 1 mm, length of 1 mm, a convergent angle of 23.5°, a divergent angle of 6.5° and inlet pressure of 500 kPa	6 L solution of 10 ppm of rhodamine 6G at pH 10	32% in 2h	(Saharan et al., 2017a)
Circular venturi with a convergent angle of 22.6°, a divergent angle of 6.4°, 2 mm throat diameter, and inlet pressure of 500 kPa	6 L solution of 10 ppm of rhodamine 6G at pH 10	29.65 % in 2h	(Saharan et al., 2017a)
40 mm **orifice plate** with 33 holes of 1 mm diameter and inlet pressure of 206.8 kPa	50 L solution of 5-6 ppm of rhodamine B	~ 90% in 1h	(Pandit & Sivakumar, 2001)
40 mm **orifice plate** with 8 holes of 2 mm diameter and inlet pressure of 206.8 kPa	50 L solution of 5-6 ppm of rhodamine B	~ 45% in 1h	(Pandit & Sivakumar, 2001)

2.9. Characterisation techniques

The characterisation techniques used in this study are to determine the amount of OH radicals produced by the HC jet loop system and to determine the degree of decolouration in the simulated textile wastewater. This study is limited to two characterisation techniques namely spectrofluorometry and ultraviolet-visible spectrophotometry.

a. Ultraviolet-visible spectrophotometry

In this study, a spectrophotometer was used to determine the extent of decolouration of the simulated textile wastewater.

Ultraviolet-visible (UV-visible) spectrophotometry is an analytical technique that involves the measurement of the ultraviolet or visible radiation absorbed by a substance in a solution (Behera et al., 2012). The absorbance of a solution measured by a spectrophotometer can be related to the concentration of the absorbing species through the Beer-Lambert law by using a calibration curve. The Beer-Lambert law states that the absorbance of a solution is directly proportional to the concentration of the absorbing species in the solution and the path length. The Beer-Lambert law is represented by the following equation (Royal Society of Chemistry, 2009):

$$A = log_{10}\left(\frac{I_0}{I}\right) = \varepsilon CL,$$

with A being the absorbance; I_0 the intensity of incident light at a given wavelength; I is the transmitted intensity; L the path length through the sample; C the concentration of the absorbing species and ε the molar absorptivity. ε and L are both constants.

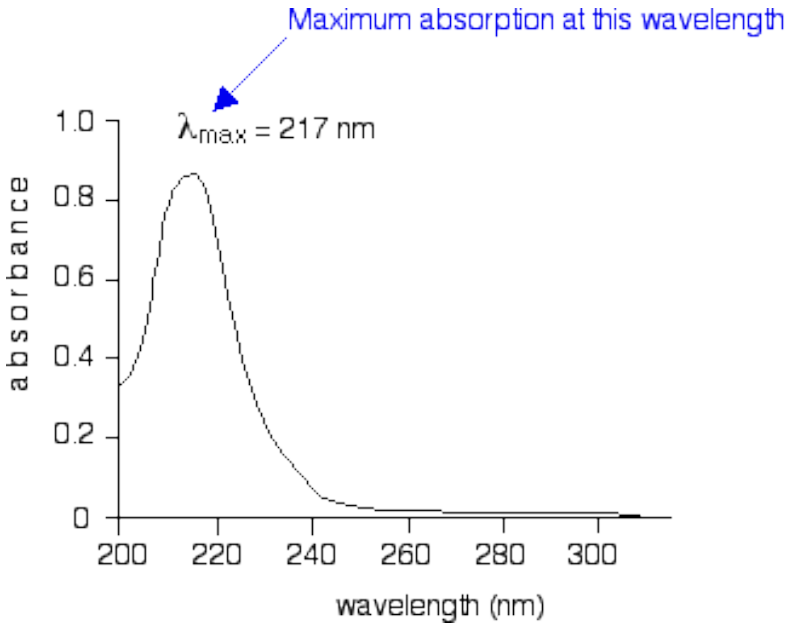

Figure 0-3: UV-visible absorption spectra of buta-1,3-diene (Clark, 2016)

b. Spectrofluorometry

To determine the amount of OH radicals produced a spectrofluorometer, was used. Spectrofluorometry is a characterisation technique that takes advantage of the fluorescence properties of compounds to determine information regarding their concentrations in a given sample. To analyse a given sample, it is excited at a certain wavelength using a light source, and the fluorescence emission of the sample can be observed at another wavelength. The latter can be a single wavelength, or a scan can be done by recording the intensity versus wavelength, also known as an emission spectra (Genovesi, 2015).

The fluorescence probing method for OH radical quantification is based on the formation of a fluorescent product after the reaction of the molecular probe with OH radicals. When the fluorescent product is excited at a specified wavelength, an emission of fluorescence occurs which is then recorded and translated in terms of concentration through a calibration curve. Compounds such as terephthalic acid (TA), sodium terephthalate (NaTA), coumarin, coumarin-3-carboxylic-acid (3 CCA) and ninhydrin have been successfully used as molecular probes in the quantification of OH radicals (Tryba et al., 2013; Manevich et al., 2019; TANG et al., 2006). Figure 2-4 below shows the reactions of molecular probes TA, coumarin and 3CCA with OH radicals which give fluorescence products. Figure 2-5 shows the fluorescence spectra as a function of treatment time.

The fluorescence intensity on figure 2-5 is that of 2-hydroxyterepthalic acid (HTA) which is related to the concentration of OH radicals in the system used to produce HTA from the reaction of TA and OH radicals. HTA is excited at a wavelength around 310 nm and emits at a wavelength around 425 nm.

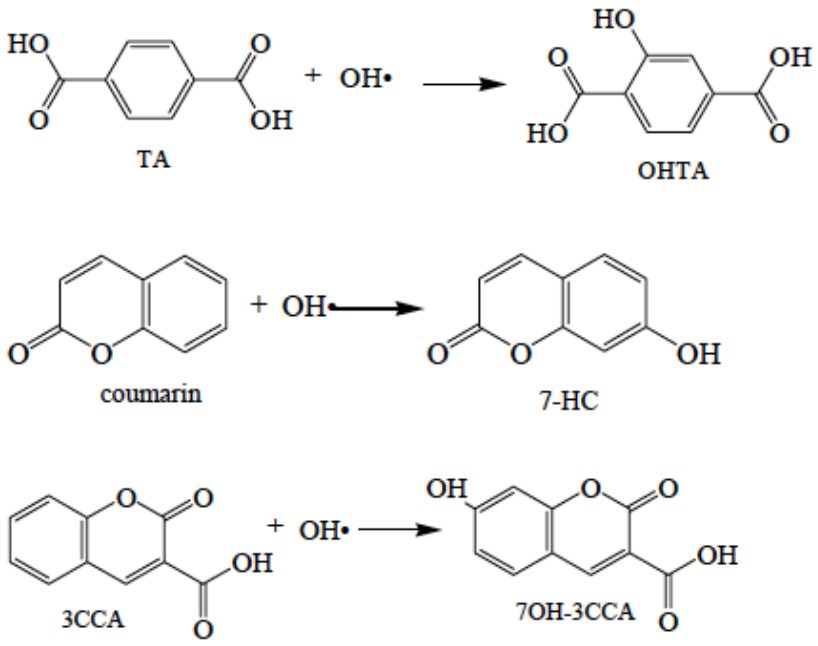

Figure 0-4: Reactions of molecular probes with OH radicals (Ortiz et al., 2015)

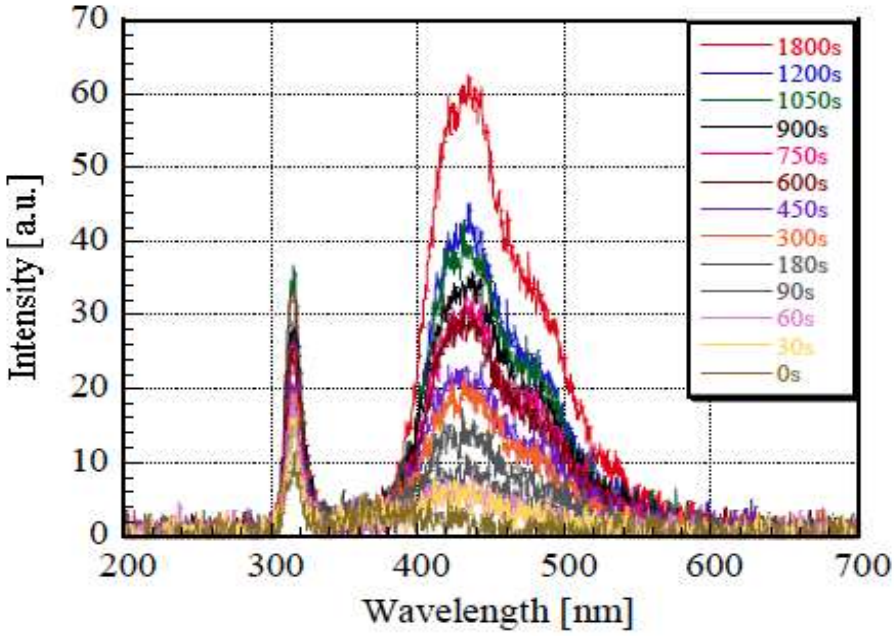

Figure 0-5: Fluorescence spectra of aqueous TA solutions irradiated by underwater discharge (Kanazawa & Kawano, 2013)

2.10. Gaps in the literature concerning the use of HC in wastewater treatment

Studies that have been conducted on HC systems as wastewater treatment techniques have shown that these systems have the potential to treat wastewater like those containing dyes that are not easily biodegradable (Badmus et al., 2018; Badmus et al., 2019). When using HC systems however, it has been found that there is a need to optimise the systems which is why more studies need to be conducted in terms of optimisation of certain parameters of the HC systems, and also more investigations need to be done on the combination of different cavitating devices (Šarc et al., 2017; Sun et al., 2020). These parameters include the types of cavitating devices used in HC systems, the sizes of the cavitating devices, the temperature of the medium, the inlet pressure, the surface roughness of the flow tract, and the flow velocity (Šarc et al., 2017; Sun et al., 2020).

Due to the insufficiency of data in the published research related to the topic aforementioned, this study focused on the use of different types and sizes of cavitating devices, the combination of different cavitating devices and the use of different inlet pressures.

2.11. Chapter summary

Chapter 2 gives a summary of available literature pertaining to this study. The first section of this chapter contains the characteristics of textile wastewater emanating from different operations of textile industry. This section also contains the impact of textile wastewater on the environment. The second section gives a description of the different methods used in textile wastewater treatment. This is followed by a third section that gives a detailed description of how HC is used as a textile wastewater treatment technique. The fourth section talks about the characterization techniques used in this study and lastly the fifth section identifies gaps found in the research reported to date relevant to the current study.

CHAPTER 3: RESEARCH DESIGN AND METHODOLOGY

Introduction

This chapter provides a description of how the study was conducted, the materials, chemicals and equipment used. The analytical procedure used is also found in this chapter.

3.1. Study outline

The schematic below shows how this study was carried out. It was mainly divided into 3 stages. The first stage consisted of the designing and construction of the HC jet loop system, the second stage consisted of experiments to optimise the HC jet loop system while the third stage consisted of experiments using optimised conditions.

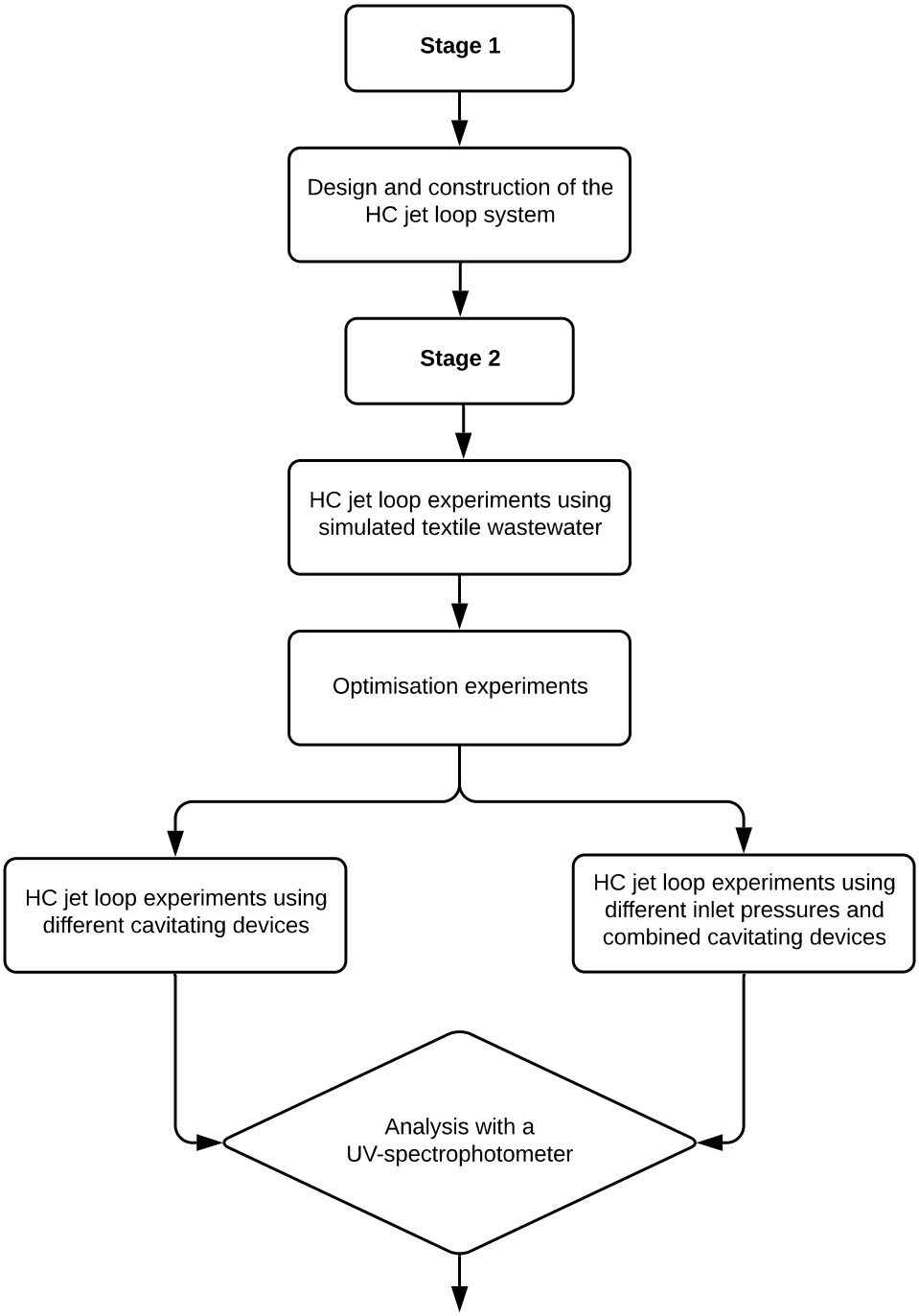
Stage 1
Design and construction of the HC jet loop system
Stage 2
HC jet loop experiments using simulated textile wastewater
Optimisation experiments
HC jet loop experiments using different cavitating devices
HC jet loop experiments using different inlet pressures and combined cavitating devices
Analysis with a UV-spectrophotometer

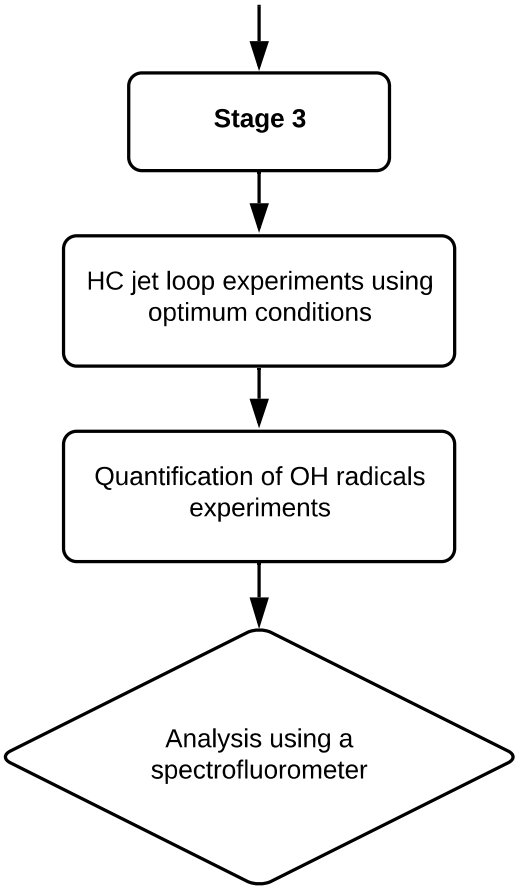

Figure 0-1: Study outline

3.2. Materials and chemical reagents

The table below provides a description of the chemical reagents used in this study and their supplier

Table 0-1: List of chemical reagents used in this study

Reagents	Purity	Supplier
Terephthalic acid (TA)	98%	Sigma-Aldrich
Hydroxyterephthalic (HTA)	97%	Sigma-Aldrich
Sodium hydroxide	98%	Kimix
Hydrochloric acid	37%	Sigma-Aldrich
Orange II sodium salt (OR2)	≥ 85%	Sigma-Aldrich

3.3. Equipment used

The following section gives information on equipment used to conduct this research. It provides a list of all the equipment used as well as pictorial and graphic representations.

Table 0-2: List of equipment used in this study

Equipment	Use
HC jet loop system	To generate OH radicals
Spectrofluorometer	To determine the OH radicals produced
UV-spectrophotometer	To determine the COD removal
Benchtop scale	To weigh different reagents used
Portable pH meter	To determine the pH of solutions used

3.3.1. Description and Illustration of the HC jet loop system and the cavitating devices used

Figures 3-2 and 3-5 give a pictorial and graphical representation of the HC jet loop system. The system consists of a tank, a pump, a cavitation device slot in which an orifice plate can be placed, a venturi, or a combination of an orifice plate and a venturi, or 2 orifice plates. In addition to that the HC jet loop system also has pressure and temperature gauges mounted on it. Figures 3-4 and 3-5 provide pictures of the orifice plate and venturi installed in the HC jet loop system.

Figure 0-2: Set-up of the HC Jet loop system

Figure 0-3: An orifice plate and its slot in the HC Jet loop system

Figure 0-4: A part of the HC Jet loop system containing the venturi

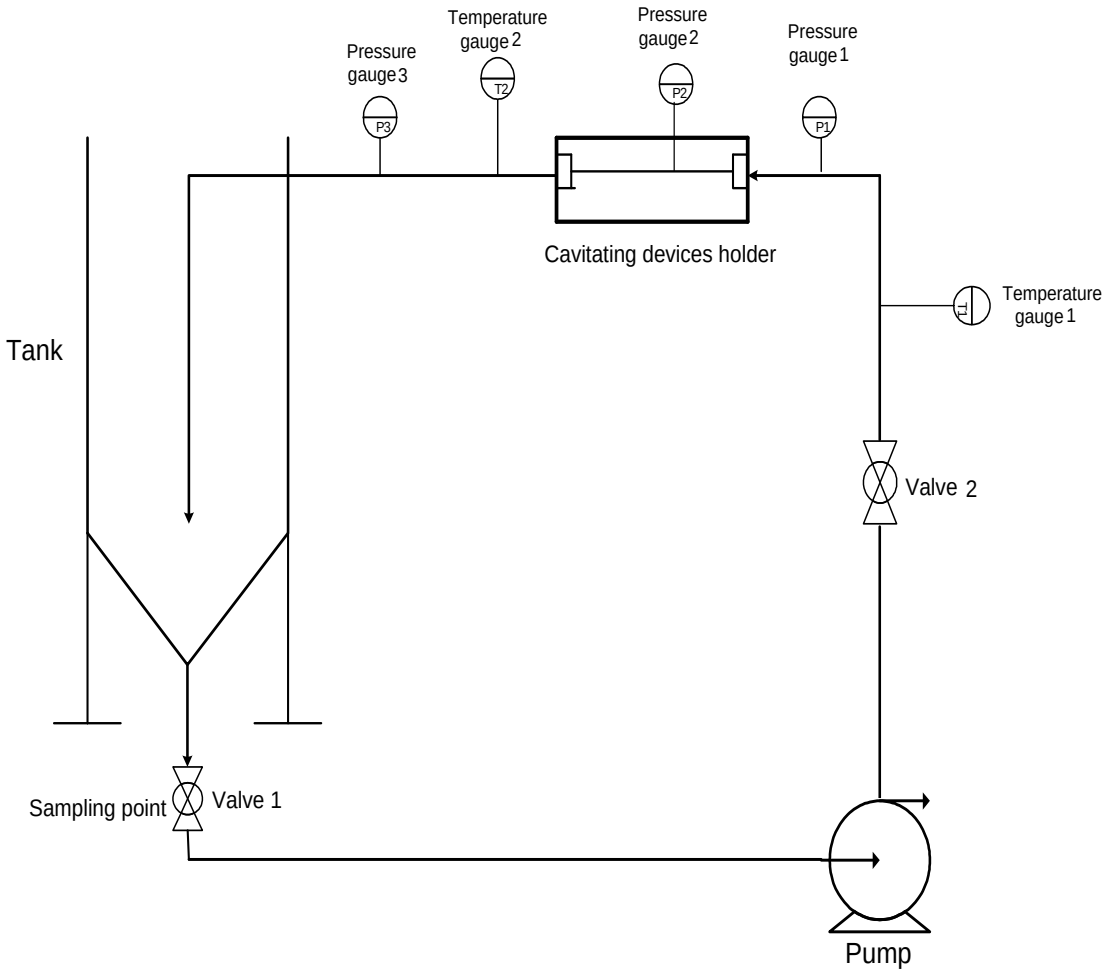

Figure 0-5: PFD of the HC jet loop system

In the HC jet loop system, the design of the cavitating device is of high importance as it is responsible for the generation of the free radicals that degrade the pollutants in wastewater. Figure 3-6, 3-7, 3-8 and 3-9 show designs and configurations of the venturi and orifice plates used in the HC jet loop system.

Figure 3-6 and 3-7 show the circular venturi used and its dimensions. The circular venturi has a 13 degree convergence angle and a 3 degree divergence angle. The throat diameter is 10 mm and its length is also 10 mm. The venturi is made of Afrimide 6G nylon material.

Figure 3-8 and 3-9 show 5 different types of orifice plates with same plate diameter and thickness of 25 mm and 3 mm respectively, but different hole diameter sizes on the plates. All the orifice plates are made of stainless steel grade 316.

Figure 0-6: Venturi

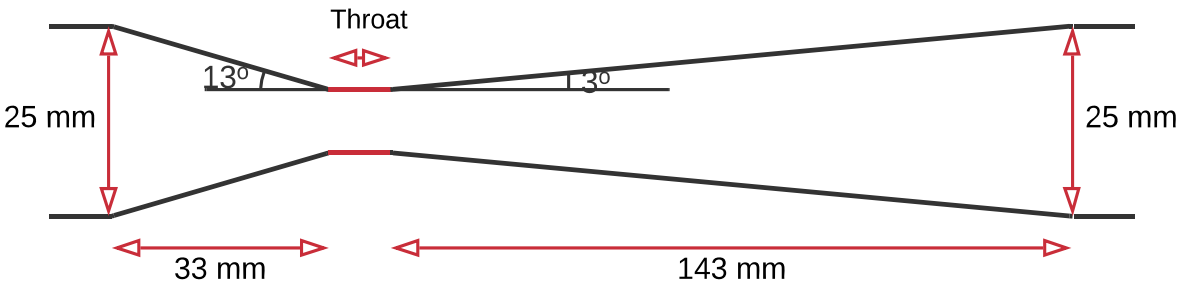

Dimensions of the throat

Diameter of the throat = 10 mm and length of the throat = 10 mm

Figure 0-7: Graphical representation of the circular venturi

Figure 0-8: Orifice plates

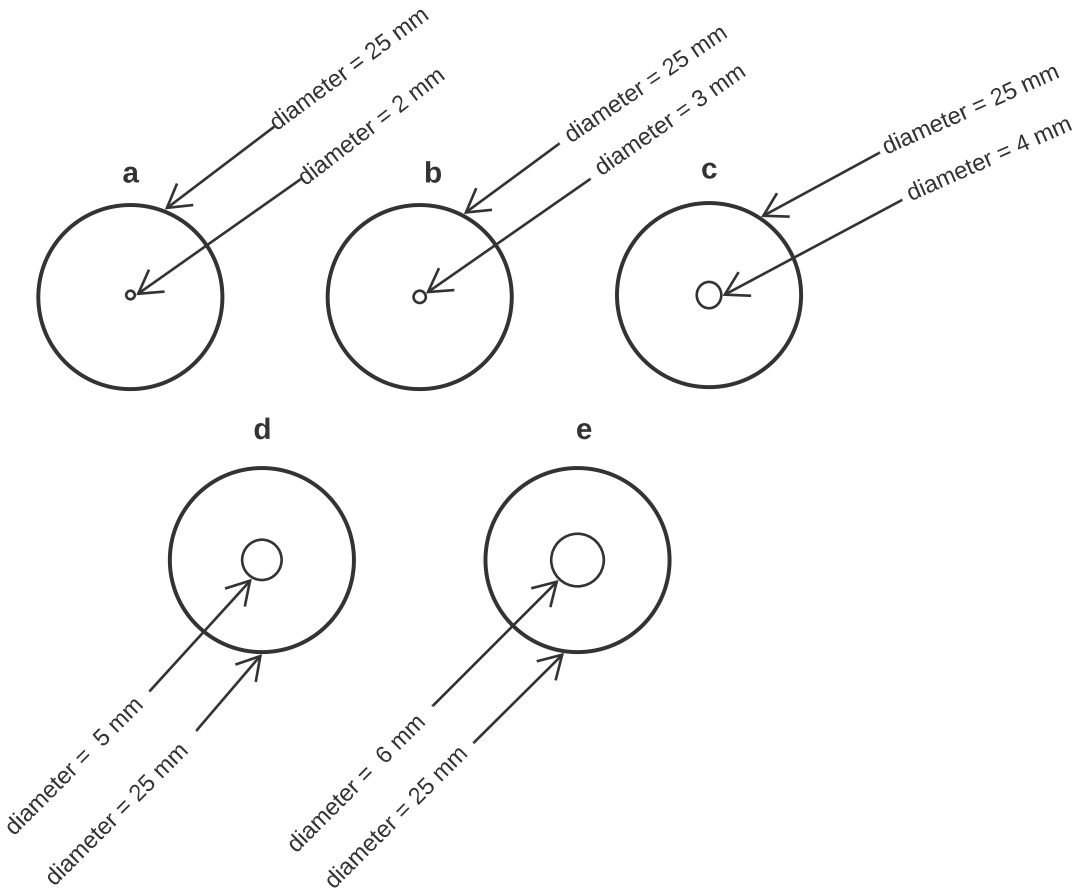

Figure 0-9: Graphical representation of the orifice plates

a) 25 mm orifice plate diameter with 1 hole of 2 mm diameter
b) 25 mm orifice plate diameter with 1 hole of 3 mm diameter
c) 25 mm orifice plate diameter with 1 hole of 4 mm diameter
d) 25 mm orifice plate diameter with 1 hole of 5 mm diameter
e) 25 mm orifice plate diameter with 1 hole of 6 mm diameter
The thickness of all the orifice plates is 3 mm

3.4. Experimental procedure

In the HC jet loop system experiments, two types of experiments divided into three batches were performed. One type was to determine how efficient the system was in treating simulated textile wastewater and the other type was to determine how many OH radicals were produced by the system.

For the first type of experiments, OR2 dye solution was used and treated in the HC Jet Loop system using different orifice plates and a venturi. Five different types of orifice plates, one venturi and a combination of venturi and orifice plate arranged in series were tested in the HC jet loop to determine which cavitating device was more effective in decolourising the dye solution and if a combination of cavitating devices was more effective than each cavitating device alone. For each experiment the solution was run in the HC jet loop system for 10 min and samples were collected every 2 min. After finding the best performing cavitating devices, inlet pressures were varied to determine at what pressure decolouration of OR2 dye solution was most favourable.

For the second set of experiments, a TA solution was used in the HC jet loop system to quantify the OH radicals produced by the HC jet loop system at optimum design and operating conditions. When TA reacts with OH radicals, HTA is produced. The concentration of HTA solution produced is equivalent to the OH radicals produced in the HC jet loop system (Barati et al., 2006). Therefore, for the quantification of OH radicals generated by the HC jet loop system, a solution of TA was used and run into the jet loop system for 10 min. For each experiment, a 2 μM TA solution was used. 10 L of 2 μM TA solution was run into the HC jet loop system for 10 min.

Tables 3-3, 3-4 and 3-5 below illustrate all the experiments that were performed.

Table 0-3: 1st batch: Colour decolouration of OR2 dye solution for cavitating devices optimisation

Time (min)	Set
10	2 mm orifice plate (O.P.) 3 mm orifice plate (O.P.) 4 mm orifice plate (O.P.) 5 mm orifice plate (O.P.) 6 mm orifice plate (O.P.) 10 mm venturi (V.)
Total samples/set	108

Table 0-4: 2nd batch: Colour decolouration of OR2 dye solution for pressure optimisation

Pressure (kPa)	1st set	2nd set	3rd set
200 300 400	3 runs with O.P.	3 runs with V.	3 runs with O.P. + V.
Total samples/set	18	18	18

Table 0-5: 3rd batch: OH radicals quantification at optimum conditions

Time (min)	1st set	2nd set	3rd set
10	2 runs with O.P.	2 runs with V.	2 runs with O.P + V.
Total samples/set	12	12	12

a. First batch

The first batch of experiments was to determine the extent of decolouration that can be achieved using different cavitating devices in the HC Jet Loop system. 10 L of 20 ppm OR2 dye solution was treated in the HC jet loop system for each experiment. In this batch of experiments the five orifice plates and one venturi designed were tested. All the experiments run in the HC jet loop system were triplicated. They were run for 10 min and the samples were collected every 2 min. The inlet pressure for this batch of experiments was 300 KPa.

b. Second batch

The second batch of experiments was to look at what pressure between 200 kPa, 300 kPa and 400 kPa was more favourable for decolourising OR2 dye solution in the HC jet loop system. In this batch there were three sets of experiments, with the first set involving the use of best performing orifice plate found in the first batch; the second set was to use the venturi in the HC jet loop system at different inlet pressures; and the third set involved the use of the optimum orifice plate and venturi in decolouration of the OR2 dye solution. The dye solution was 20 ppm concentration and 10 L volume, and it was run for 10 min in the HC jet loop system for all the experiments. Samples were taken every 2 min. All the experiments in this batch were also triplicated.

c. Third batch

In the third batch of experiments a TA solution was run into the HC Jet Loop system for 10 min and samples were taken every 2 min. The TA solution used for each experiment had a concentration of 2μM and a volume of 10 L. Three sets of experiments were performed in this batch. The first set was aimed at determining the amount of OH radicals generated by the HC jet loop system equipped with the best performing orifice plate, and the second set was to determine the OH radicals generated when using the venturi. The third set was to determine the OH radical production of the HC jet loop system using a combination of the best performing orifice plate and a venturi. All the experiments in this batch were duplicated and the inlet pressure used was the optimum inlet pressure found in the second batch

3.5. Analytical techniques

3.5.1. UV-spectrophotometry

In this study, a spectrophotometer was used to determine the extent of decolouration of OR2 dye solution in the collected samples.

Spectrophotometry uses photometers to quantitively analyse molecules based on the amount of light absorbed by coloured compounds. It basically is a quantitative measurement of the reflection or transmission properties of a material as a function of wavelength. For this study, to determine the absorbance of the different samples of treated OR2 dye solution, a UV-wavelength was set at 483 nm on the spectrophotometer, which is the wavelength peak of OR2 salt (Sigma-Aldrich, 2017). The absorbance of a solution is directly proportional to its concentration.

Figure 0-10: UV-spectrophotometer used to determine decolouration of dye

3.5.2. Spectrofluorometry

For the quantification of OH radicals a spectrofluorometer was used. A spectrofluorometer is an instrument used to measure the fluorescence intensity of fluorescent compounds. The fluorescence intensity of a given compound is observed at the compound-defined excitation wavelength and at the compound-defined emission wavelength (Genovesi, 2015).
For this study, the fluorescence intensity of HTA produced into the HC jet loop system by the reaction between TA and OH radicals will be determined. The emission of HTA absorbs at a wavelength of 425 nm and HTA excites at a wavelength of 310 nm (Badmus et al., 2016). The fluorescence intensity of HTA recorded is directly proportional to the concentration of HTA produced in the HC jet loop system, which gives a measure of the amount of OH radicals generated by the HC jet loop system (Barati et al., 2006).

3.5.3. Calibration curve for OR2 dye concentration measurement using a UV-spectrophotometer

For this calibration, six solutions of OR2 dye at different concentrations were prepared. The concentrations were 1 ppm, 2 ppm, 4 ppm, 6 ppm, 8 ppm and 10 ppm. The absorbance of the 6 OR2 dye solutions was therefore determined using a spectrophotometer. A calibration curve of absorbance versus OR2 dye concentration used was therefore plotted which allowed the determination of the slope of the curve. The latter was used to calculate the concentration of OR2 dye left in the OR2 dye solution treated using the HC jet loop system after measuring the absorbance of the samples taken.

Table 0-6: Absorbance measurement of different OR2 dye solution concentrations

OR2 dye solution concentration (ppm)	Absorbance
0	0
1	0.0874
2	0.1455
4	0.2789
6	0.4082
8	0.5446
10	0.6848

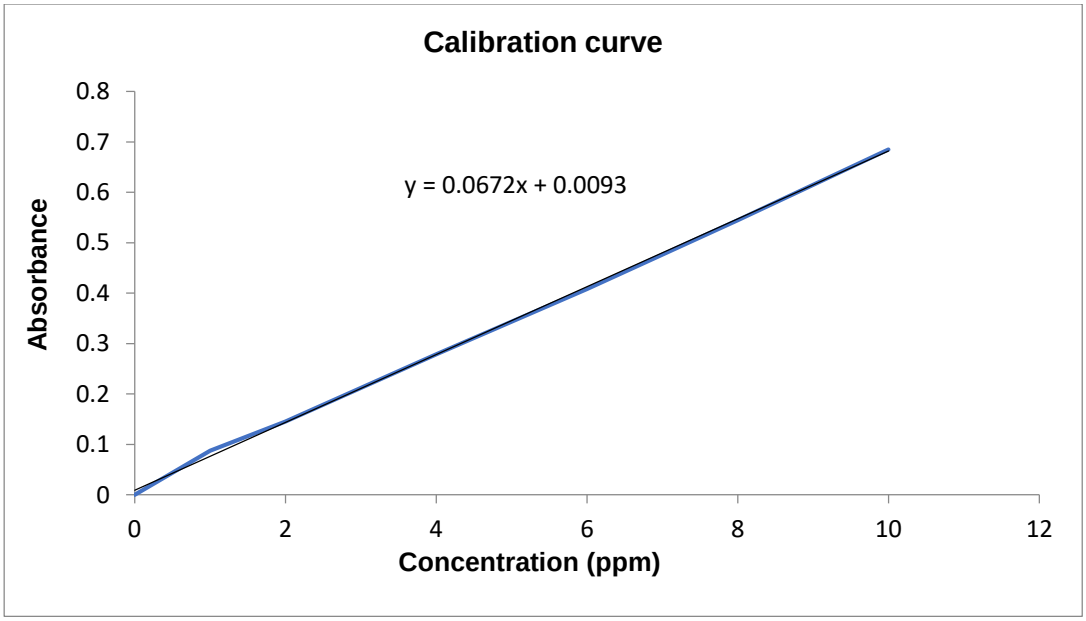

Figure 0-11: Calibration curve for OR2 dye concentration measurement

3.5.4. Calibration curve for HTA concentration measurement using a spectrofluorometer

For calibration, six solutions of HTA at different concentrations were prepared. The concentrations were 0.2 ppm, 0.4 ppm, 0.6 ppm, 0.8 ppm and 1 ppm. The fluorescence intensity of the 6 HTA solutions was therefore determined using a spectrofluorometer. A calibration curve of HTA fluorescence intensity versus HTA concentration was therefore plotted, which allowed the determination of the slope. The latter was used to calculate the concentration of HTA solution generated by the HC jet loop system which in turn could be related to the concentration of OH radicals produced by the HC jet loop system.

Table 0-7: Fluorescence intensity measurements for different HTA solution concentration

HTA Concentration (ppm)	HTA fluorescence intensity
0	0
0.2	477820
0.4	1014010
0.6	2049300
0.8	3030417
1	3821140

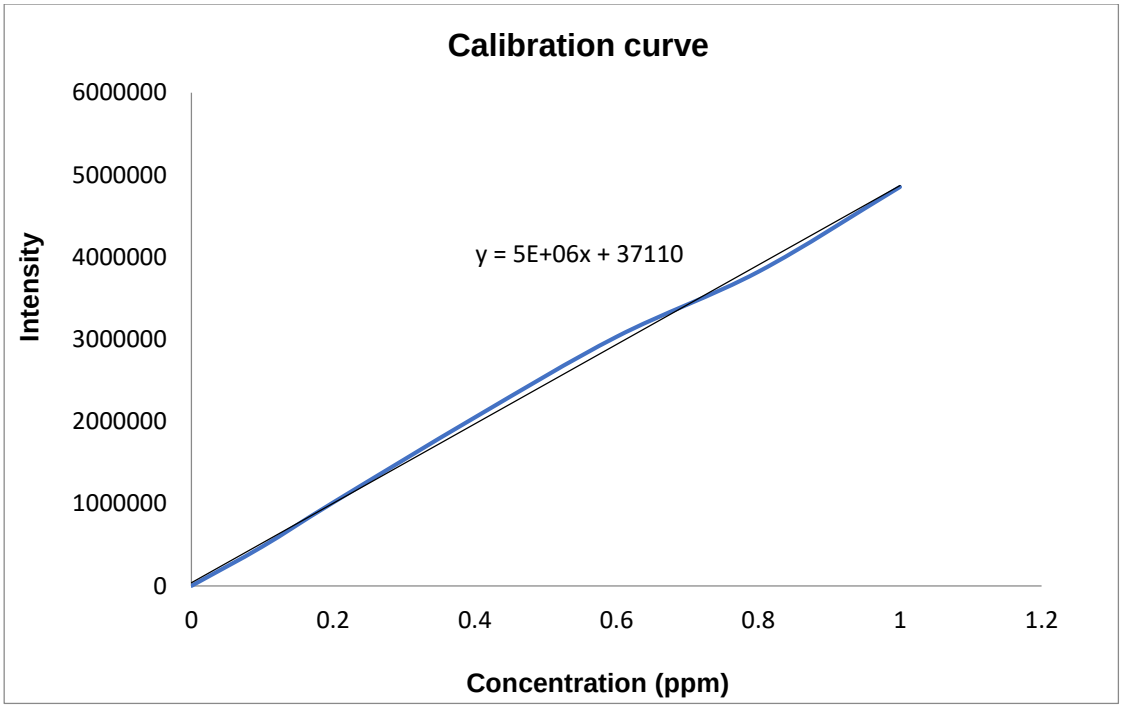

Figure 0-12: Calibration curve for HTA concentration measurement

3.6. Chapter summary

This chapter covers all the materials, chemicals and equipment used in this study. It also gives a detailed description of how the experiments were performed as well as the analytical techniques used in the study.

In the first set of experiments, the cavitating devices performance were investigated; in the second set of experiments, the inlet pressure and the combination of cavitating devices were investigated; and in the last of experiments the quantification of OH radicals generated in the HC jet loop system was investigated.

The analytical techniques used in this study were UV-spectrophotometry and the spectrofluorometry.

CHAPTER 4: RESULTS AND DISCUSSION

Introduction

This chapter describes and discusses the results of the HC jet loop system experiments. There are three main sections in this chapter. The first section will cover the optimisation of the cavitating devices used in the HC jet loop system for the decolouration of OR2 dye. The second section considers the optimisation of inlet pressure and combination of cavitating devices in the HC jet loop system for the decolouration of OR2 dye, while the third section provides the findings of the quantification of OH radicals generated by the HC jet loop using orifice plate, venturi and a combination of orifice plate and venturi at the optimum conditions.

4.1. The HC jet loop system set-up and operation

This study started with the design of the HC jet loop piping as well as the design of the orifice plates and venturi. The HC jet loop system and the cavitating devices were then constructed and commissioned. After commissioning, the newly designed HC jet loop system started operating. The system was equipped with a tank that could treat 80 L of wastewater. However, 10 L was used in this study. The HC jet loop system was also equipped with a pump connected to a control box that could be used to change the inlet pressure as desired. With regard to the cavitating devices, the HC jet loop system was set up such that the cavitating devices could be mounted along the piping system and could be easily changed as needed. In Chapter 3, figure 3-2 to figure 3-5 provide a pictorial and graphical description of the HC jet loop system set-up. To operate the system, the wastewater was introduced in the tank of the HC jet loop system which was then followed by switching on the system. After switching on the system, the wastewater passed through the pump and from the pump into the cavitating device, either the orifice plate, venturi, or a combination of the two, depending on which device was being investigated. After the cavitating device, the wastewater went back into the tank and a new cycle started until the system was switched off (which happened when the desired results were obtained or when the time set was reached). To monitor the pressure and temperature, there were gauges installed along the piping system as shown in figures 3-2 and 3-5.

4.2. Optimisation of cavitating devices for the decolouration of OR2 dye using the HC jet loop system.

The optimisation of cavitating devices was performed using six cavitating devices, including five orifice plates and a venturi. In this batch of experiments, each cavitating device was used on its own. The orifice plates had whole diameter sizes of 2 mm, 3 mm, 4 mm, 5 mm and 6 mm while the venturi had a throat diameter of 10 mm. A full description of the sizes of the cavitating devices is given in Section 3.3.1. Each experiment in this batch of experiments had a duration of 10 min with a start temperature of approximately 25°C. Samples were collected every 2 min. A detailed experimental procedure of how this set of experiment was done is provided in Section 3.4. To determine the percent decolouration of OR2 dye, the UV-spectrophotometry technique was used as described in Sections 3.5.1 and 3.5.3.

The results obtained when varying the cavitating devices in the HC jet loop system and when using the HC jet loop system without any cavitating device to decolourise OR2 are shown in Figure 4-1. The 6O, 5O, 4O, 3O and 2O in Figure 4-1 stand for orifice plates having 6 mm hole diameter, 5 mm hole diameter, 4 mm hole diameter, 3 mm hole diameter and 2 mm hole diameter respectively.

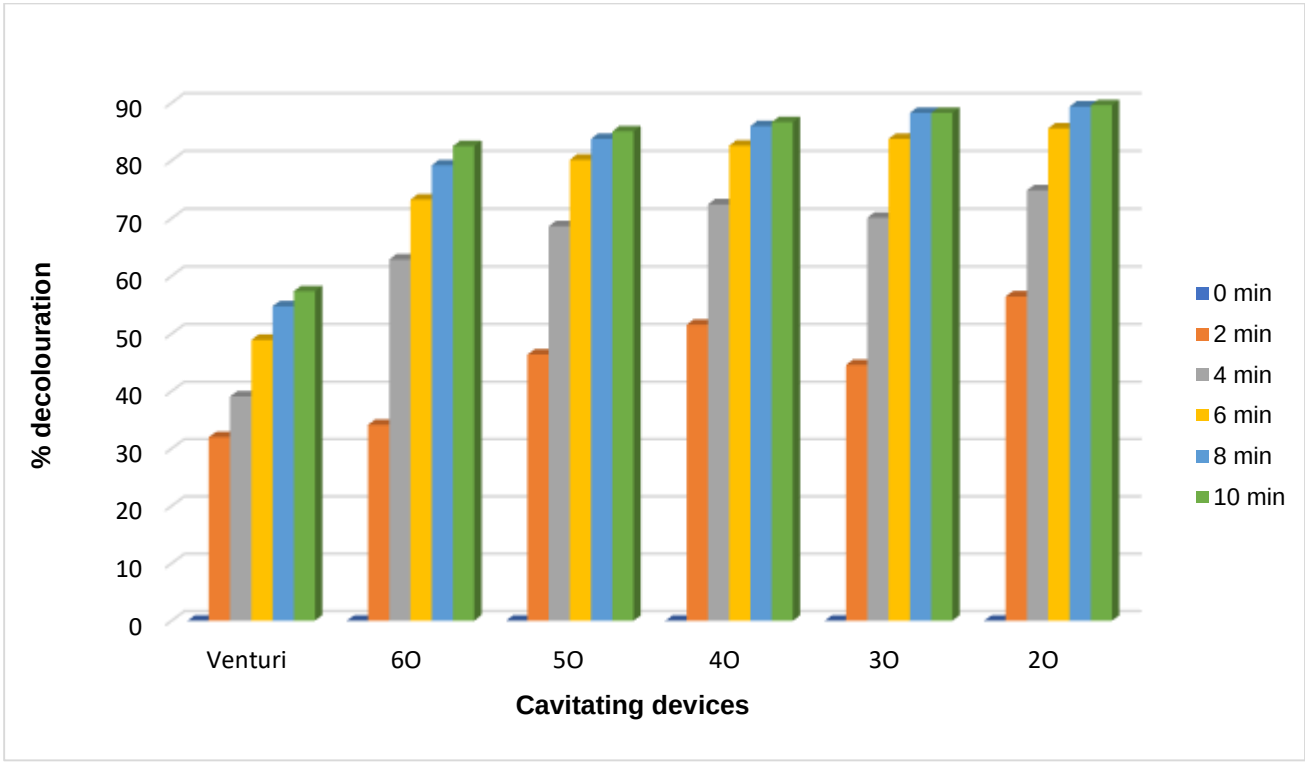

Figure 0-1: Effect of different cavitating devices on the decolouration OR2 in the HC jet loop system (Fixed conditions: OR2 concentration 20 ppm, solution pH 2.31, solution volume 10 L, sampling interval of 2 min for 10 min experiment run, inlet pressure 300 kPa, starting temperature 25°C)

Looking at Figure 4-1, it can be observed that among all the cavitating devices used, the best performing cavitating device was the orifice plate with a 2 mm hole diameter. As the hole diameters of the orifice plates increased, the percent decolouration of OR2 decreased. With a 2 mm hole diameter orifice plate, the percentage decolouration achieved after 10 min was 89.60%, while using the orifice plate having a 6 mm hole diameter achieved a decolouration of 82.52%. For the 3 mm, 4 mm and 5 mm orifice plates, the percentage colour decolouration after 10 min was 88.25%, 86.68% and 85.05% respectively. Using the circular venturi which had a 10 mm throat diameter, a decolouration of 57.45% was achieved after 10 min. Compared to the orifice plates the venturi performed poorly, and this trend was observed after 2 min as can be seen in Figure 4-1. In Section 2.8 of this study, it was noticed that normally the venturi performed better than the orifice plates when it came to decolourising dyes. The results obtained in Figure 4-1 did not follow that trend. This could be due to the fact that the venturi used in this study had a big throat diameter which possibly did not allow a high pressure drop, thus not allowing the generation of a lot of cavitation bubbles necessary to allow a higher generation of OH radicals which would result in a lower decolouration of OR2. OH radicals are believed to be generated when the cavitation bubbles formed in the throat collapse as they leave a low pressure zone (the throat) to a high pressure zone (Warade et al., 2016).

When comparing the performance of the different orifice plates used for decolouration in this study, it can be noticed that there was no significant difference between them. This could be due to the fact that the difference between the hole diameter of the orifice plates was not significant. Looking at the decolouration of OR2 dye as time passed, it can be seen that the highest decolouration for all the orifice plates was achieved in the first 4 min of the experiment, and from 4 min to 10 min the decolouration was not significant. For the venturi the biggest decolouration was achieved in the first 6 min of the experiment. This shows that in the current design of the HC jet loop system, the orifice plates decolourised the OR2 dye at a faster rate compared to the venturi.

From the analysis of the results presented in Figure 4-1, it can be concluded that incremental optimisation was possible, and small adjustments in the hole size improved the decolouration of OR2 easily for the orifice plates. For the venturi, it was not so easy to adjust the throat diameter which is why the size of the throat could not be reduced to optimise it. Therefore, the orifice plate with a 2 mm hole diameter was found to be the optimum orifice plate among those tested in this study, and that it also is the best cavitating device compared to the current design of the venturi.

4.3. Optimisation of inlet pressure and combination of cavitating devices in the HC jet loop system for the decolouration of OR2 dye

In this set of experiments, the OR2 dye was decolourised using the venturi, the orifice plate (2 mm hole diameter) and the combination of the venturi and orifice plate (2 mm hole diameter) in the HC jet loop system at inlet pressures of 200 kPa, 300 kPa and 400 kPa. Figures 4-2, 4-3 and 4-4 show the results obtained after 10 min time on stream for each inlet pressure using the venturi, the orifice plate and their combination. For the combination of the orifice plate and venturi experiment, the cavitating devices were mounted in series with the orifice plate coming first, followed by the venturi.

Similarly to the first set of experiments mentioned in Section 4.2, the concentration of OR2 dye was 20 ppm, the pH of the solution was 2.33, and the starting temperature was 25^{o}C.

Section 2.7 shows that the decolouration of dyes using hydrodynamic cavitation was highly dependent on inlet pressure. The best percent dye decolouration was found to be at inlet pressures between 400 kPa and 500 kPa.

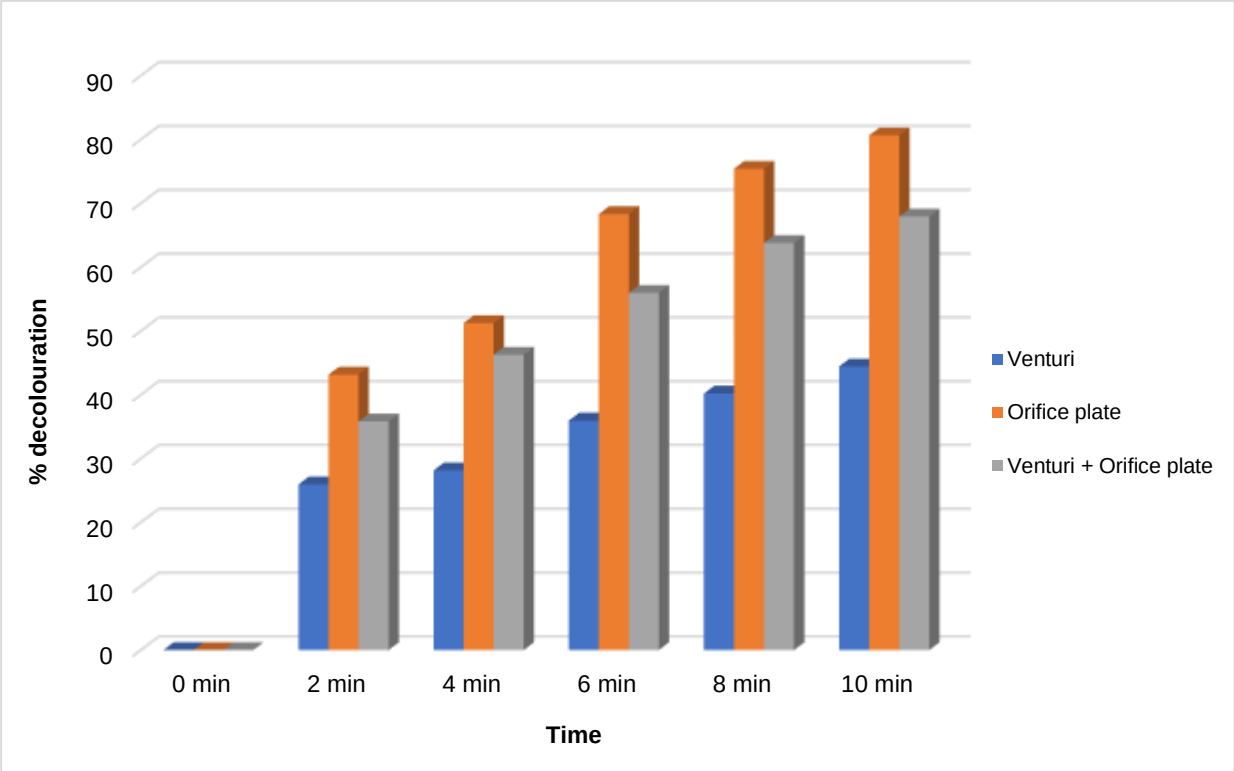

Figure 0-2: Effect of use of a venturi, an orifice plate and combination of venturi and orifice plate for the decolouration of OR2 in the HC jet loop system (Fixed conditions: 2 mm hole diameter orifice plate, OR2 concentration 20 ppm, solution pH 2.34, solution volume 10 L, sampling interval of 2 min for 10 min experiment run, inlet pressure 200 kPa, starting temperature 25^{o}C)

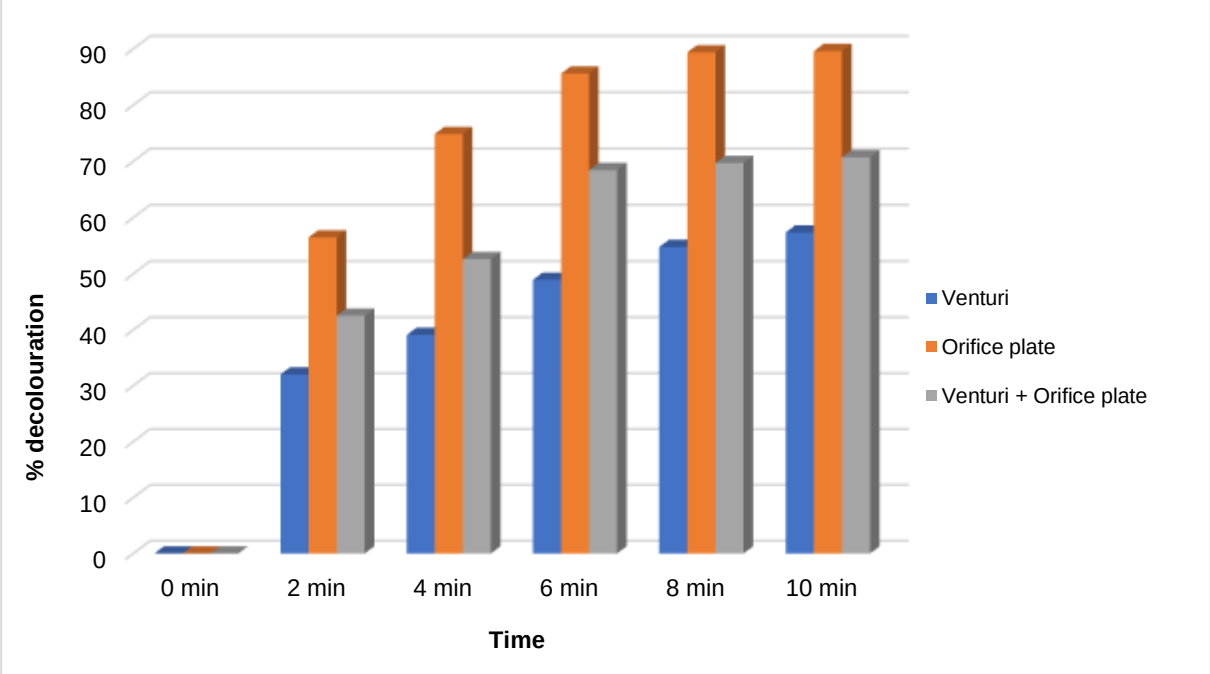

Figure 0-3: Effect of use of a venturi, an orifice plate and combination of venturi and orifice plate for the decolouration of OR2 in the HC jet loop system (Fixed conditions: 2 mm hole diameter orifice plate, OR2 concentration 20 ppm, solution pH 2.33, solution volume 10 L, sampling interval of 2 min for 10 min experiment run, inlet pressure 300 kPa, starting temperature 25ºC)

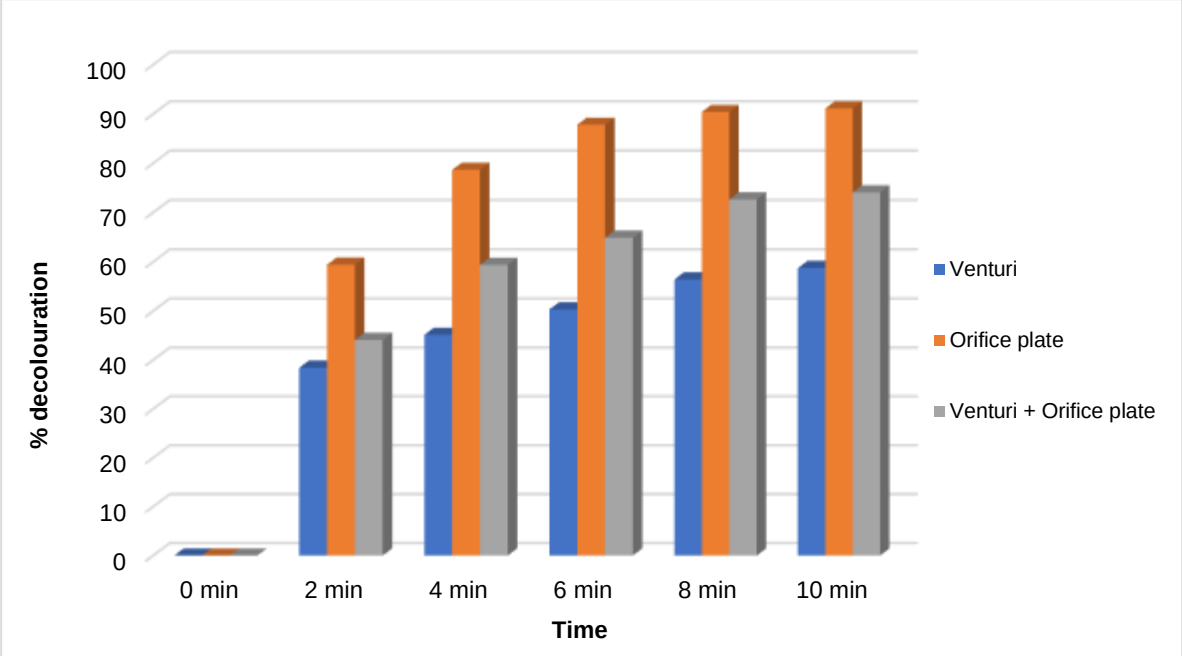

Figure 0-4: Effect of use of a venturi, an orifice plate and combination of venturi and orifice plate for the decolouration of OR2 in the HC jet loop system (Fixed conditions: 2 mm hole diameter orifice plate, OR2 concentration 20 ppm, solution pH 2.33, solution volume 10 L, sampling interval of 2 min for 10 min experiment run, inlet pressure 400 kPa, starting temperature 25ºC)

Figure 0-5: From left to right 0 min: 10 min samples collected when decolourising 10 L of 20 ppm OR2 in the HC jet loop system for 10 min using a 2 mm hole diameter orifice plate and 400 kPa inlet pressure

It was observed (Figures 4-2, 4-3 and 4-4) that for all the different pressures used, the orifice plate (2mm hole diameter) alone performed better compared to the venturi or the combination of venturi and orifice plate (mounted in series). For the inlet pressure of 400 kPa, the decolouration of OR2 after 10 min was 91.11% when using orifice plate alone, 74.08% when using the combination of venturi and orifice plate, while it was 58.73% when using the venturi alone. For an inlet pressure of 300 kPa, the decolouration of OR2 after 10 min of experiment was found to be 89.60% when using the orifice plate alone, 57.35% when using the venturi alone and 70.71% when using a combination of orifice plate and venturi. For the 200 kPa inlet pressure, the decolouration was 80.66% when using the orifice plate alone, 67.93% when using the combination of orifice plate and venturi and 44.44% when using the venturi alone. The poor performance of the combination of the orifice plate and venturi compared to that of the orifice plate alone could be explained by the fact that when the OR2 solution passed through the orifice plate then went through the venturi from the orifice plate, the solution did not have enough time from the pressure drop to fully recover, which did not allow for all the bubbles that were believed to have formed through the passing in the orifice plate to collapse.

When the fluid entered the venturi, then went into its throat, bubbles were formed again; however, the pressure drop in the venturi and the fluid velocity were not as high as in the orifice plate as the throat of the venturi was bigger compared to the hole of the orifice plate. This could then mean that the bubbles formed were not as big as those generated in the orifice plate, as a sufficient pressure drop is required for the bubbles to form and grow (Kuldeep et al., 2014). When the bubbles in the throat of the venturi did not grow up to a certain size, as the pressure recovered, the bubble collapse would not generate intense collapse pressure in the venturi. And Saharan et al. (2012) reported that it is during the bubble collapse phase that production of OH radicals occurs through the dissociation of water molecules. Less intense bubble collapse pressure might then lead to lower production of OH radicals. The OH radicals generated when using an orifice plate alone is therefore believed to be higher than that obtained using a combination of the cavitation devices due to the growth of their formed bubbles being higher, which permits higher cavitational intensity.

Looking at the performance of the HC jet loop system at the various inlet pressures investigated, it can be seen that the highest decolouration of OR2 among the inlet pressures used was obtained at 400 kPa. This finding correlates with the observations made by Badmus et al. (2019) and those made by Gogate & Bhosale (2013) and Mishra & Gogate (2010) that the best performance in decolouration of dyes using hydrodynamic cavitation was found between 400 kPa and 500 kPa. Among the inlet pressures tested in the current investigation, 200 kPa performed the poorest. As presented in Section 2.6 explaining cavitation inception, a low cavitation number leads to greater cavitational intensity and compared to the other inlet pressures, 200 kPa provides the highest cavitation number, which in turn leads to a smaller cavitational intensity.

In conclusion, it can be said that a 2 mm orifice plate and an inlet pressure of 400 kPa were found to be respectively the optimum design and operating conditions in decolourising OR2 dye using the current HC jet loop design compared to a circular venturi with 10 mm throat diameter and compared to the combination of the orifice plate and circular venturi mounted in series.

4.4. Effect of Cavitation number and temperature change in the HC jet loop system when using different inlet pressures

Temperature is one of the factors that influences the performance of hydrodynamic cavitation systems in the decolouration of dyes. Table 4-1 below depicts the temperature change when using inlet pressures of 200 kPa, 300 kPa or 400 kPa.

The temperature was monitored for a 10 min run and it was recorded every 2 min. The starting temperature for all the runs was 25ºC. Table 4-2 shows the cavitation numbers obtained when different inlet pressures were used in the HC jet loop system containing a 2 mm hole diameter orifice plate. The cavitation number was calculated using Equation (2-28) found in Section 2.6.1 of this thesis.

Table 0-1: Temperature change in the HC jet loop system when using the orifice plate with a 2 mm hole diameter at inlet pressure of 200 kPa, 300 kPa or 400 kPa for a run of 10 min

Time (min)	Temperature at 200 kPa (ºC)	Temperature at 300 kPa (ºC)	Temperature at 400 kPa (ºC)
0 min	25	25	25
2 min	28	28	29
4 min	30	30	35
6 min	32	33	39
8 min	34	35	43
10 min	35	37	46

Table 0-2: Cavitation number at inlet pressures of 200 kPa, 300 kPa or 400 kPa using an orifice plate with 2 mm hole diameter in the HC jet loop system

Orifice plate diameter	Inlet pressure	Volumetric flowrate	Velocity at the orifice	Cavitation number
2 mm	400 kPa	0.1078 L/s	34.4 m/s	0.166
2 mm	300 kPa	0.0810 L/s	25.80 m/s	0.295
2 mm	200 kPa	0.0729 L/s	23.14 m/s	0.367

In Table 4-1 it can be seen that the temperature increased more rapidly when a higher inlet pressure was used. According to Section 4.2, it was observed that the inlet pressure of 400 kPa allowed for a higher extent of decolouration of OR2. The fact that this corresponds to a higher temperature increase with the highest temperature being 46ºC after 10 min of experiment,

corresponds with what has been reported by Dular et al., (2017) that maximum cavitation aggressiveness lies at 50^{o}C.

According to Yan et al. (1988), the cavitation number decreases as the orifice hole diameter decreases. In table 4-2 above it can be seen that the cavitation number decreased as the inlet pressure increased though the orifice plate diameter was kept constant. This can be explained by the fact that as the inlet pressure increased the velocity of the fluid at the throat of the orifice plate increased and similarly when there was a decrease in the orifice plate diameter there was an increase of fluid velocity at the throat.
Rajoriya et al. (2016) has reported that when degrading rhodamine dye, a cavitation number ranging between 0.1 and 0.2 provided better results. Looking at the cavitation numbers obtained in this study and comparing it with results obtained in Figure 4-4, it can be seen that a 0.166 cavitation number provided the best results when decolourising OR2.

4.5. Quantification of OH radicals generated by the HC jet loop using orifice plate, venturi and a combination of orifice plate and venturi at optimum conditions.

As seen in Sections 2.5.2.4 and 2.6.3 of this study, OH radical generation is believed to be one of the main factors in pollutant destruction in hydrodynamic cavitation systems. Below in Tables 4-3, 4-4 and 4-5 are the concentrations in ppm of the OH radicals produced by the HC jet loop system when using the 2mm hole diameter orifice plate, the venturi and a combination of the venturi and 2 mm hole diameter orifice plate. The experiments were run in the jet loop for 10 min, samples collected every 2 min and the inlet pressure used was of 400 kPa for all the experiments. To determine the concentration of OH radicals produced, the terephthalic acid dosimetry method as described in Sections 3.5.2 and 3.5.4 was used.

Table 0-3: Concentration of OH radicals produced by the HC jet loop system in 10 min using a 2 mm hole diameter orifice plate

Orifice plate					
Time (min)	**Sample**	**Absorbance 1**	**Absorbance 2**	**Absorbance**	**Concentration (ppm)**
0	TO0	0	0	0	0
2	TO1	60269000	60731000	121000000	24.2
4	TO2	70843220	71156780	142000000	28.4
6	TO3	76109800	75890200	152000000	30.4
8	TO4	78508000	78992000	157500000	31.5
10	TO5	80940000	80560000	161500000	32.3

Table 0-4: Concentration of OH radicals produced by the HC jet loop system in 10 min using a venturi

Venturi					
Time (min)	**Sample**	**Absorbance 1**	**Absorbance 2**	**Absorbance**	**Concentration (ppm)**
0	TV0	0	0	0	0
2	TV1	38626600	38873400	77500000	15.5
4	TV2	45314400	46185600	91500000	18.3
6	TV3	50175800	50824200	101000000	20.2
8	TV4	57500000	57000000	114500000	22.9
10	TV5	60661000	60839000	121500000	24.3

Table 0-5: Concentration of OH radicals produced by the HC jet loop system in 10 min using a combination of a 2 mmm hole diameter orifice plate and a venturi

Orifice plate + Venturi					
Time (min)	**Sample**	**Absorbance 1**	**Absorbance 2**	**Absorbance**	**Concentration (ppm)**
0	TOV0	0	0	0	0
2	TOV1	45148000	45352000	90500000	18.1
4	TOV2	54826400	54673600	109500000	21.9
6	TOV3	58288000	58712000	117000000	23.4
8	TOV4	64250000	64250000	128500000	25.7
10	TOV5	68125040	67874960	136000000	27.2

The amount of OH radicals generated in the HC jet loop system increased with time as can be seen in Tables 4-3, 4-4, and 4-5. The highest generation of OH radicals across the different cavitating devices can be observed using a 2 mm hole diameter orifice plate in the HC jet loop system. This finding could also be expected when looking at the results from Figure 4-4.

The concentration of OH radicals generated after 10 min was 32.3 ppm using the 2 mm hole diameter orifice plate. When using the venturi in the HC jet loop system, the lowest amount of OH radicals was generated over time and its concentration was 24.3 ppm after 10 min time on stream. The combination of orifice plate and venturi mounted in series allowed a generation of 27.2 ppm of OH radicals in the HC jet loop system, which was intermediate.

Looking at the results obtained from the quantification of OH radicals, it can be seen that the size of the constriction of a cavitating device matters significantly. This is because a 2 mm hole diameter orifice plate performed better in decolourising OR2 dye using the HC jet loop system compared to the venturi with a 10 mm throat diameter. This is despite that fact that researchers such as Saharan et al. (2013) and Mishra & Gogate (2010) have found that venturis perform better than orifice plates when using them as cavitating devices in the decolouration of dyes. However the venturis used had much smaller throat diameter (2 mm) compared to the one used in this study.

For this study, a 10 mm throat size venturi was chosen as it was easier to construct compared to a smaller diameter venturi such as a 2 mm throat diameter. Also, there are many instances in literature where a venturi with a 2 mm throat diameter has been used to decolourise dyes while a 10 mm throat diameter venturi has not been used for that purpose, which made it interesting to see what results could be obtained using a bigger throat diameter venturi.

4.6. Chapter summary

The performance of cavitating devices in the HC jet loop system for the decolouration of OR2 dye, the effect of inlet pressures, and the combination of different cavitating devices were investigated in this chapter. Along those investigations, the OH radicals generated by the HC jet loop system were determined. The cavitation number and the temperature change overtime in the HC jet loop system were noted.

It was found that of the cavitating devices investigated, the 2 mm hole diameter orifice plate performed better compared to all the cavitating devices used, including the 10 mm throat diameter venturi. It can be noted that the 2 mm hole diameter orifice plate had the smallest hole diameter, as the other orifice plates had 3 mm, 4 mm, 5 mm and 6 mm hole diameters.

The observations made showed that the use of the 2 mm hole diameter orifice plate helped to achieve 89.60% decolouration of OR2 dye in the HC jet loop system. When using the 10 mm throat diameter venturi, only a 57.45% decolouration of OR2 dye was achieved. It was also noted that even the orifice plate which had a 6 mm hole diameter performed significantly better than the 10 mm throat diameter venturi. The 6 mm hole diameter orifice plate had an OR2 dye percent decolouration of 82.52%. In this batch of experiments performed to determine the best performing cavitating device, the inlet pressure used was 300 kPa.

When determining which inlet pressure performed better in the HC jet loop system, it was found that 400 kPa performs better compared to 200 kPa and 300 kPa. Previous studies have shown that the operating and design conditions allowing for lower cavitation number in hydrodynamic cavitation systems provide better performance of the cavitating devices. In this study it was found that the lowest cavitation number was obtained at 400 kPa. This explains why 400 kPa performed better compared to 300 kPa and 200 kPa. The cavitation numbers found were 0.166, 0.295 and 0.367 at inlet pressures 400 kPa, 300 kPa and 200 kPa respectively.

When it came to the combination of the orifice plate and venturi, it was found in this study that the orifice plate alone performed better than the combination of venturi and orifice plate. However, the combination of the cavitating devices performed better than the venturi alone.

Regarding temperature change, it was observed that at 400 kPa the temperature increase was highest, with the temperature after 10 min on stream being 46^{o}C after a starting temperature of 25^{o}C. The highest temperature recorded for 200 kPa and 300 kPa was 35^{o}C and 37^{o}C respectively. The increase in temperature as the pressure increased is understandable because when the pressure of the fluid increases there is also an increase in the fluid kinetic energy, thus increasing its thermal energy which leads to the fluid temperature increase.

With regard to the quantification of OH radicals during each experimental run, it was observed that the highest amount of OH radicals was generated in the HC jet loop system when using a 2 mm hole diameter orifice plate. The lowest amount of OH radicals was generated in the HC jet loop system when using a 10 mm throat diameter venturi. 32.3 ppm of OH radicals were generated after 10 min when using the 2 mm hole diameter orifice plate and only 24.3 ppm of OH radicals were generated when using a 10 mm throat diameter venturi over the same time period. The highest OH radicals were generated when using the 2 mm orifice plate because of the small hole diameter. In hydrodynamic cavitation systems, OH radicals are produced through the dissociation of water molecules when cavitation bubbles collapse. Further, the intensity of the bubble collapse is dependent on the size of the cavitation bubble, while the degree of the intensity of the bubble collapse may affect OH radical generation. For the cavitation bubbles to form and grow, there needs to be a sufficient pressure drop, which occurs when a fluid passes through the constriction of a cavitating device. The 2 mm hole diameter orifice plate is believed to have allowed for a better pressure drop for the cavitation bubbles to form and grow compared to the other cavitating devices or to the combination of cavitating devices.

CHAPTER 5: MATERIAL AND ENERGY BALANCES

Introduction

As noted in its title, Chapter 5 presents the material and energy balances around the HC jet loop system.

The material balance was performed on the overall HC jet loop system while the energy balance was performed around the pump of the HC jet loop system.

5.1. Material balance around the HC jet loop system

Material or mass balance is an application of conservation of mass to the analysis of physical systems. By conservation of mass, the mass that enters a system must either leave the system or accumulate within the system (Himmelblau & Riggs, 2013).

Mathematically, the mass balance for a system without a chemical reaction is as follows (Fogler, 2005):

Input = Output + Accumulation …… (Equation 0-1)

When there is no chemical reaction, the amount of any chemical species flowing in and out will be the same.
However, where there is a chemical reaction, generation and consumption of chemical species need to be taken into account. The equation that represents mass balance for a system with a chemical reaction is as follows (Fogler, 2005):

Input + Generation = Output + Accumulation + Consumption …… (Equation 0-2)

In a system involving a chemical reaction, the generation and consumption of chemical species depend on the rate of the chemical reaction, which is the rate at which reactants are consumed or products are generated. For a reaction A→B for instance, a mole balance on specie A, which enters, leaves, reacts and accumulates in a system with volume V, is represented by the equation below (Fogler, 2005),

$$F_{A0} - F_A + \int_0^V r_A dV = \frac{dN_A}{dt} \quad (mole\ balance\ equation) \ldots\ldots\ldots\ldots \textit{(Equation 0-3)}$$

Where,

F_{A0} is the rate of flow of A into the system

F_A is the rate of flow of A out of the system

$\int_0^V r_A dV$ is the rate of generation of A by chemical reaction within the system

$\frac{dN_A}{dt}$ is the rate of accumulation of A within the system

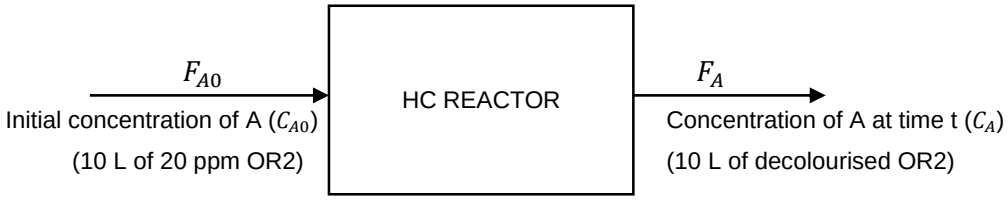

Figure 0-1: BFD of material balance around the HC jet loop system

In the experiments done in this study, 10 L of 20 ppm of OR2 dye solution were put into the HC jet loop system and 10 L of decolourised OR2 dye solution were collected from the HC jet loop after 10 min.

The mole balance equation changes its form based on the type of reactor used for a given chemical reaction.

For a batch reactor, which is the case of the HC jet loop system, there is no inflow or outflow of reactants or products while the reaction is being carried out (Fogler, 2005). This means that $F_{A0} - F_A = 0$. Therefore, the mole balance can be represented as follows:

$$\frac{dN_A}{dt} = \int_0^V r_A\, dV \ldots\ldots\ldots\ldots \textit{(Equation 0-4)}$$

If the reaction mixture is perfectly mixed in such a way there is no variation in the rate of reaction throughout the reactor volume, the mole balance equation becomes (Fogler, 2005),

$$\frac{dN_A}{dt} = r_A dV \rightarrow \textit{with the rate of reaction } r_A = \frac{dC_A}{dt} \ldots\ldots\ldots\ldots \textit{(Equation 0-5)}$$

In algebraic form the rate of reaction equation will be:

$$-r_A = kC_A^n, \ldots\ldots\ldots\ldots \textit{(Equation 0-6)}$$

with k being the reaction rate constant, C_A being the concentration of A and n the order of reaction.

The rate of reaction equation could also be written in differential form as below,

$$-\frac{dC_A}{dt} = kC_A^n \quad \text{..... (Equation 0-7)}$$

To determine the order of reaction in a batch reactor, different methods can be used such as the integral method, the differential method, non-linear regression method, etc.

In this study, the integral method will be used to determine the order of the reaction occurring in the HC jet loop system. Using the integral method, a reaction order is guessed, and the differential equation is integrated. If the order guessed is correct, the appropriate plot of concentration versus time data should be linear.

For a zero order of reaction, the plot of the concentration of reactant (C_A) versus time (t) should be linear. For a first order of reaction, the plot of the natural log of ($\frac{C_{A0}}{C_A}$) versus time (t) should be linear. C_{A0} is the initial concentration of A and C_A is the concentration of A at time (t).

For a second order of reaction, the plot of $\frac{1}{C_A}$ versus time (t) should be linear.

To determine the order of the reaction in the HC jet loop system, the results presented in Section 4.2, which were obtained from the results of the experiments of decolouration of OR2 using the venturi, the 2 mm hole diameter orifice plate and a combination of orifice plate and venturi at different inlet pressures were used. The specific results used were those obtained when investigating 400 kPa inlet pressure as it was found to be the optimum pressure. Figures 5-2, 5-3 and 5-4 below represent the plots of the results for determination of order of reaction.

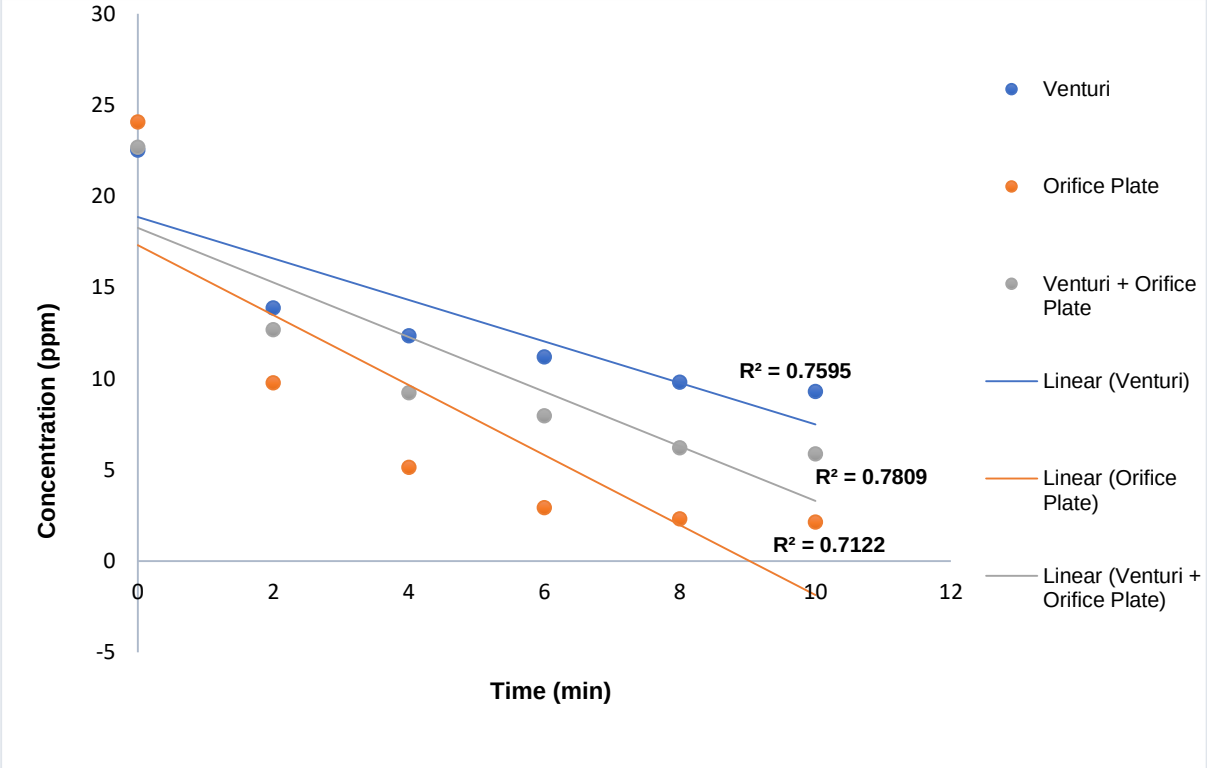

Figure 0-2: Zero order of reaction plot

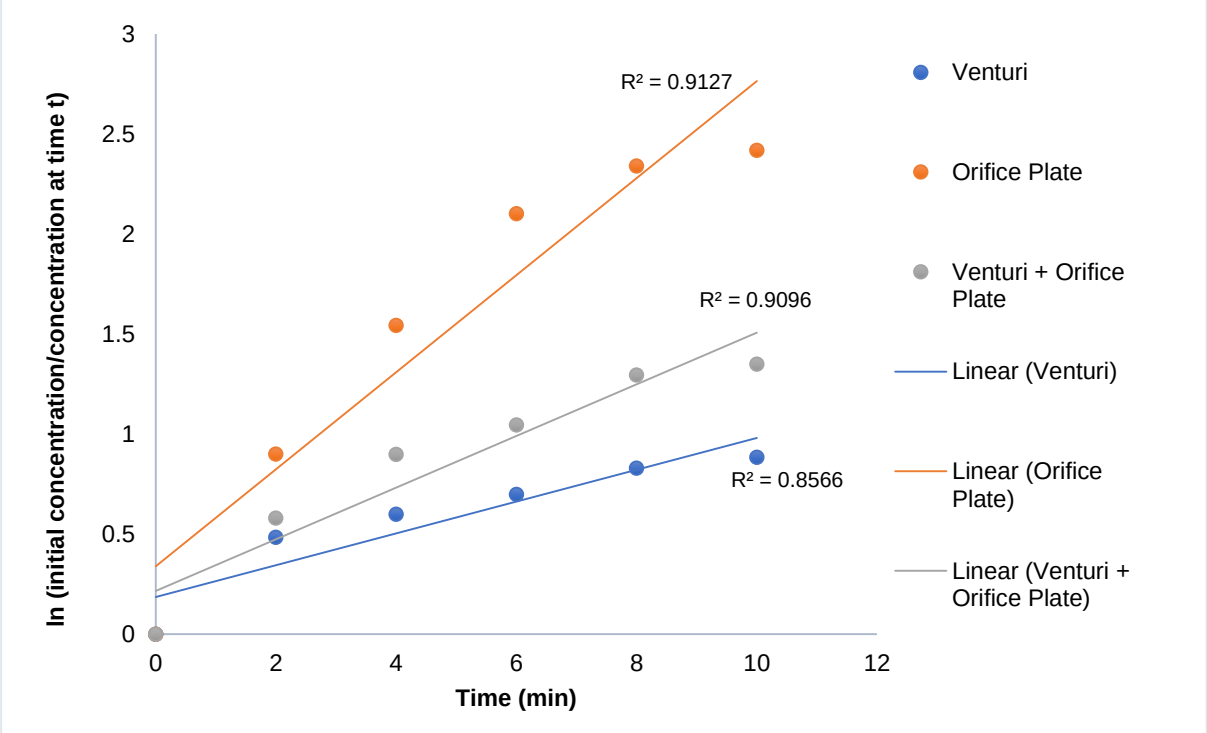

Figure 0-3: First order of reaction plot

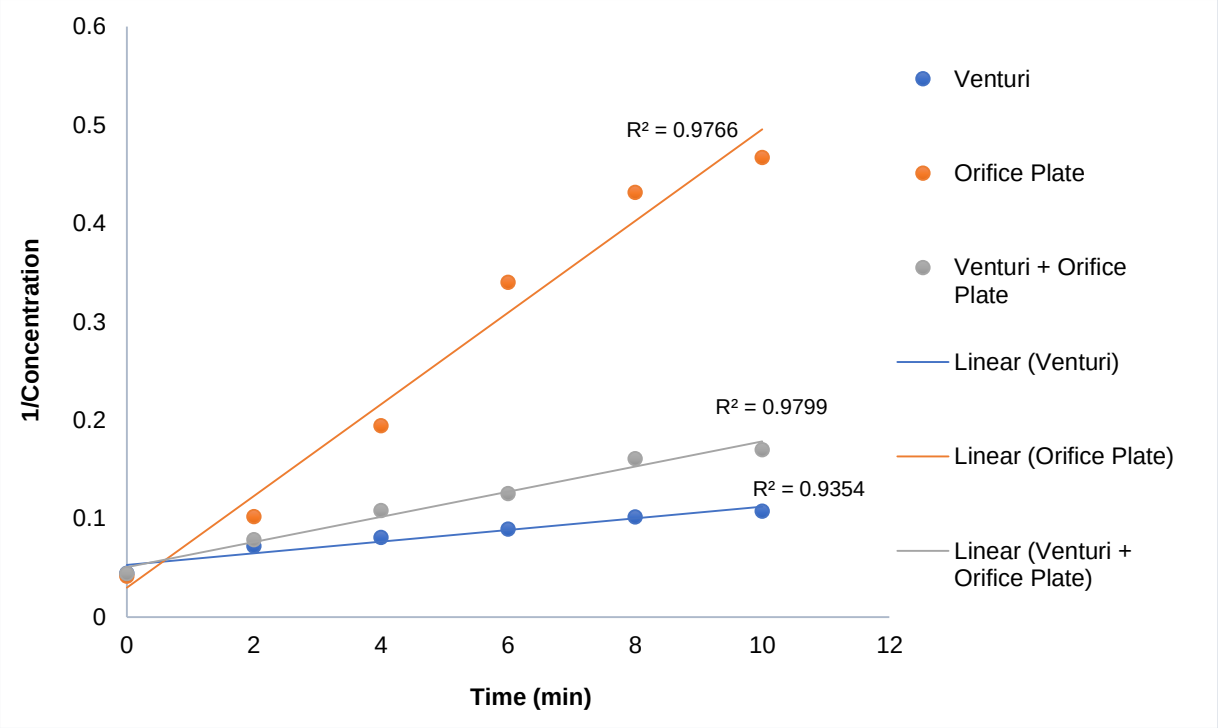

Figure 0-4: Second order of reaction plot

When comparing Figures 5-2, 5-3 and 5-4, it can be seen that the figure that provides a more linear plot of concentration data and time is Figure 5-4. The R^2 values in each figure also show that when fitted to a straight line, Figure 5-4 represents the data that are closest to the fitted straight line. This is because in Figure 5-4, R^2 values are 0.9766, 0.9799 and 0.9354 for the orifice plate, the combination of the orifice plate and venturi, and for the venturi respectively. For Figures 5-3 and 5-2, the R^2 values are smaller than those in Figure 5-4. This means that the order of reaction of decolouration of OR2 dye in the current HC jet loop system is second order as it is the plot represented by Figure 5-4. Therefore, the rate of reaction order for the reaction in the HC jet loop system is given by the equation below:

$$-r_{OR2} = k[OR2]^2 \quad \text{..... } \textit{(Equation 0-8)}$$

In their studies, Badmus (2019) and Wang et al. (2009) have found that dye decolouration follows a pseudo first-order kinetic when using hydrodynamic cavitation. Badmus's experimental run was for 1 hour and the hydrodynamic cavitation system that he used was equipped with 2 orifice plates mounted in parallel with a venturi in series with the 2 paralleled orifice plates. Both the venturi and orifice plates had 4 mm throat and hole size diameter. For Wang and his colleagues, their experiments were for 1h and 30 min and they used a swirling jet cavitation reactor.

A pseudo first-order reaction is a second order reaction that behaves like a first order reaction due to the increase of the concentration of one of the reactants (the reactant is in excess) (Tinoco Jr. et al., 1995). In the case of the experiments in the current study, it could be that the reaction remained a second order reaction because the experiments performed using the current design of the HC jet loop system were not long (10 min run time), which did not allow a large generation of OH radicals, thus resulting in a second order reaction instead of a pseudo first order reaction.

5.2. Energy balance around the HC Jet loop system

To determine the energy consumption of the HC jet loop system when decolourising OR2 dye, an energy balance needs to be performed around the pump. The energy balance expresses the law of conservation of energy while the material balance expresses the law of conservation of material as seen in Section 5.1.

The general energy balance is given by the following equation (Himmelblau & Riggs, 2013):

$$\frac{\Delta E}{\Delta t} = F_{in}E_{in} - F_{out}E_{out} + Q - W \quad \text{..... (Equation 0-9)}$$

With $\frac{\Delta E}{\Delta t}$ representing the accumulation of energy in the system

$F_{in}E_{in}$ representing the transfer of energy into the system through the system boundary

$F_{out}E_{out}$ representing the transfer of energy out of the system through the system boundary

Q representing the energy generation within the system

W representing the energy consumption within the system

There are 3 different forms of energy in a system:

- Kinetic energy (E_k) which is due to the movement of a mass from one place to another
- Potential energy (E_p) which is due to the position of a mass in a gravitational field
- Internal energy (U) includes all other types of energy in the system such as vibrational and rotational energy in chemical bonds

The total energy E is equal to the sum of the 3 forms of energy;

$$E = E_K + E_p + U \quad \text{..... (Equation 0-10)}$$

Where $E_K = \frac{v^2}{2}$; with v being the velocity of the mass and $E_p = z\,g$; with z being the relative height from a reference plane and g being gravitational acceleration. U is derived from the enthalpy equation represented by $H = U + PV$; with H being the enthalpy, P being the pressure and V being the volume (Geankoplis, 1993b)

For a steady-state system the overall energy balance equation would be:

$$H_2 - H_1 + \frac{1}{2\propto}({v_2}^2 - {v_1}^2) + g\,(z_2 - z_1) = Q - Ws \quad \text{..... (Equation 0-11)}$$

where, Q represents heat and W_s represents Work (Geankoplis, 1993b)

Energy balance calculations

Below is Figure 5-5, which represents the system around the pump on which the energy balance was conducted.

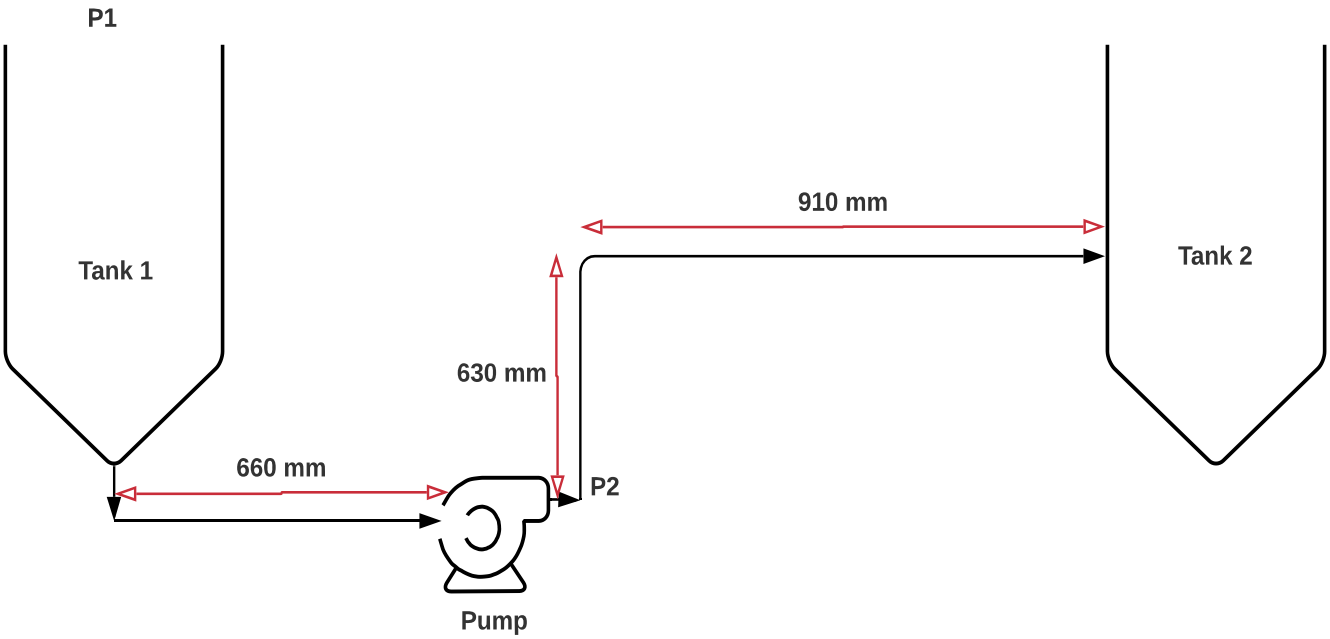

Figure 0-5: PFD of the system around the pump

Tank 2 shown in Figure 5-5 was not there in the actual experimental process as the jet loop was a water circulating system, therefore one tank was used, but for ease of calculations tank 2 was added.

For the energy balance calculations, the following assumptions were made:

Assumptions:

1. z_1 = 0 because position 1 is the reference elevation
2. P_1 = atmospheric pressure because tank 1 is open to the atmosphere and P_2 = 400000 Pa at tank Tank 2 due to the pressure of the pump.
3. No phase change and no chemical reactions
4. At point 1 the velocity v_1 is negligible hence v_1 = 0
5. The density of the fluid is constant because it is an incompressible fluid.
6. The density of the fluid is taken to be 1000 kg/m^3, which is that of water since the amount of OR2 salt was too small to change the density of the fluid in a significant way.
7. Steady flow in the pipe since the system is at steady state
8. Existence of surface friction losses in the pipes
9. The friction losses were due to valves, fittings, contraction and expansion of the pipe and are assumed to be negligible including those due to venturi and orifice plates.
10. Viscosity of water is used since the amount of OR2 dye is small enough to be insignificant when it comes to changing the viscosity of the fluid in the pipe
11. The material of the pipes are stainless steel

Table 5-1 below illustrates the parameters used in energy balance calculations around the pump:

Table 0-1: Energy balance calculation parameters

Density ρ = 1000 kg/m^3
Discharge pressure P_2 = 400000 Pa
Height Z_2 = 0.63 m
Inner diameter D = 0.025 m
Length L = 2.2 m
Specific heat capacity c_p= 4.2 kJ/kg^{o}C
Suction pressure P_1 = 101325 Pa
Viscosity μ = 0.001 Pa. s
Volumetric flow rate $\dot{V}$= 0.0001078 m^3/s (when using a 2mm hole diameter orifice plate in the HC jet loop system)

The pumping head which is the distance up to which the fluid can be lifted using the pump of this system can be calculated using Equation 5-12 (Geankoplis, 1993b):

$H_D = (Z_2 - Z_1) + \frac{v_2^2 - v_1^2}{2 \propto g} + \frac{P_{2-} P_1}{\rho\, g} + H_L$ *(in m) ……. (Equation 0-12)*

where:

- $\propto$ = kinetic energy correction factor (no units)
- ${v_2}^2$ - ${v_1}^2$ = change in velocity (in m^2/s^2); where v_1 is the velocity of the fluid before it enters the pump and v_2 is the velocity of the fluid after it enters the pump.
- z_2 - z_1 = change in elevation (in m)
- g = gravitational acceleration (in m/s^2)
- H_L = Head loss (in m)
- ρ = density (in Kg/m^3)
- $P_2 - P_1$ = Change in Pressure (in Pa)

To determine the pumping head H_D the area inside the pipe, the velocity of the fluid inside the pipe, the Reynold number, the friction factor and the head loss were calculated below.
From the pumping head H_D, the fluid power was calculated.

Area of the pipe calculation

$$\mathrm{A} = \frac{\pi \mathrm{d}^2}{4} = \frac{\pi(0.025)^2}{4} = 4.91 \times 10^{-4}\, m^2$$

Velocity of the fluid calculation

$$v = \frac{\dot{\mathrm{V}}}{\mathrm{A}} = \frac{0.0001078}{4.91 \times 10^{-4}} = 0.220\ \mathrm{m/s}$$

Reynold number calculation

$$\mathrm{R}e = \frac{\rho v D}{\mu} = \frac{1000 \times 0.220 \times 0.025}{0.001} = 5500$$

The flow was turbulent because the $\mathrm{R}e$ found was greater than 4100 (Geankoplis, 1993a).

Friction factor calculation

Stainless steel absolute roughness is $\varepsilon = 3 \times 10^{-5}$ m

The relative roughness $\in$ is given by:

$\in = \frac{\varepsilon}{D}$ (Geankoplis, 1993a)

$$\epsilon = \frac{3 \times 10^{-5}}{0.025} = 1.2 \times 10^{-3}$$

Using the Moody chart, the Darcy friction factor f was found to be 0.033.

Head loss calculation

$H_L = \mathrm{f} \times \frac{\mathrm{L}}{\mathrm{D}} \times \frac{v^2}{2\mathrm{g}}$ (Geankoplis, 1993a)

$$H_L = 0.033 \times \frac{2.20}{0.025} \times \frac{0.220^2}{2 \times 9.81} = 0.00716\, m$$

Pumping head calculation

$\propto = 1$ for turbulent flow

$$H_D = (Z_2 - Z_1) + \frac{v_2^2 - v_1^2}{2 \propto g} + \frac{P_2 - P_1}{\rho\, g} + H_L$$

$$\mathrm{H_D} = (0.63 - 0) + \frac{0.220^2 - 0^2}{2 \times 1 \times 9.81} + \frac{400000 - 101325}{1000 \times 9.81} + 0.00716 = 31.09 \text{ m}$$

Fluid power calculation

$$\mathrm{Power_{Fluid}} = \dot{V} \times \rho \times \mathrm{H_D} \times \mathrm{g}$$

$$\mathrm{Power_{Fluid}} = 0.0001078 \times 1000 \times 31.09 \times 9.81 = 32.88 \text{ W}$$

The power imparted by the pump to the fluid in the decolouration of OR2 dye was found to be 32.88 W at a flow rate of 0.0001078 m^3/s and an inlet pressure of 400 kPa. This means that for an almost complete decolouration (91.11%) of 10L of OR2 in 10 min, the energy used per m^3 of OR2 is shown in the calculation below:

$$32.88 \text{ W} \times \frac{1 \text{ kW}}{1000 \text{ W}} \times 10 \text{ min} \times \frac{1\text{h}}{60 \text{ min}} \times \frac{1}{10 \text{ L}} \times \frac{1000 \text{ L}}{\text{m}^3} = 0.548 \text{ kWh/m}^3.$$

Therefore, the energy consumed per m^3 by the HC jet loop system is 0.548 kWh/m^3. Compared to other AOPs such as UV, this is a lower consumption of energy. For instance, Yen (2016) used UV/H_2O_2 to decolourise textile wastewater and he reported that his energy consumption for decolourisation was 1.73 kWh/m^3, which is a bit more than triple the amount of the energy consumed by the HC jet loop system.

5.3. Chapter summary

In this chapter the material balance on the HC jet loop system and an energy balance around the pump of the system were performed. The material balance has shown that the amount of solution that goes into the system is the same as that which comes out of the system. However, the chemical composition is different as there is a reaction occurring within the system whereby the dye solution that is put into the HC jet loop is decolourised. The determination of the order of the reaction has shown that it is a 2^{nd} order reaction. For the energy balance around the HC jet loop system, the results found showed that the energy consumed by the HC jet loop system for the decolouration of 10 L of 20 ppm of OR2 dye solution was 0.548 kWh/m^3 at a flow rate of 0.0001078 m^3/s and an inlet pressure of 400 kPa.

CHAPTER 6: COSTING

Introduction

When planning to build any chemical plant, its cost is always very crucial as it will determine whether the project is viable or not. In this chapter, the costing of setting up an HC jet loop system for wastewater treatment is estimated. The chapter considers the capital investment costs as well as the operating cost.

6.1. Capital investment costs

When setting up a chemical plant, there is capital investment needed which involves the cost related to the construction of a new plant or the modification of an existing plant and costs incurred to start operating the newly constructed or modified plant (Turton et al., 2009).
There is a fixed capital investment which is the amount needed for a plant to be ready for start-up. It includes the design stage, purchasing equipment, piping, instrumentation, and installation costs.
The other type of capital investment required is the working capital. This is the amount required to start up the plant. Depending on what type of plant is being built, the working capital can vary from 5% to 30% of the fixed capital (Turton et al., 2009).
To estimate the capital cost needed for a plant, the methods used can be classified into two main categories based on the amount of design detail at hand and the decision that needs to be made. There is the rapid capital cost estimating method and there is the factorial method of cost estimation (Sinnott, 2005).

The rapid capital cost estimate is mostly used when decisions regarding alternate plant designs are still being made. It does not require a lot of details. For rapid cost estimate, historical costs which are costs of previous, similar projects can be used. Another method used in rapid cost estimate is step counting. It is based on the premise that the capital cost is determined by a number of significant processing steps in the overall process. Factors such as material of construction, yield, operating pressure and temperature are also included in the estimate.

The factorial method is a cost estimate that can be used for more accurate capital investment estimates compared to rapid capital cost estimate. There are mainly two types of factorial methods: the Lang factor method and the detailed factorial estimates method. In the Lang factor

method, the fixed capital cost is given as a function of the total purchase equipment cost. This estimate is given by the equation below (Sinnott, 2005):

$$C_f = f_L C_e \quad \text{..... (Equation 0-1)}$$

With C_f being the fixed capital cost

C_e being the total delivered cost of all the major equipment items

f_L being the Lang factor which depends on the type of process.

The Lang factor is equal to 3.1 for solids processing plants, equal to 3.6 for fluids-solids processing plants, or equal to 4.7 for fluids processing plants.

In a detailed factorial estimate method, the cost factors that are compounded into the Lang factor are considered individually (Sinnott, 2005). Some of the direct costs incurred in the construction of a plant, in addition to the cost of equipment, are:

1. Equipment erection including foundations and minor structural work
2. Piping, including insulation and painting
3. Electrical, power, lighting.
4. Instruments, local and control room
5. Process buildings and structures
6. Ancillary buildings, offices, laboratory buildings, workshops
7. Storage, raw materials and finished product
8. Utilities (service), provision of plant for steam, water, air, firefighting services (if not costed separately)
9. Site and site preparation

In addition to direct cost of purchase and installation of equipment, the capital cost of a project will include the indirect cost such as design and engineering costs, contractor's fees and contingency allowances.

In this study, the detailed factorial estimate method will be used to estimate the capital cost.

- **Capital investment cost calculations**

The steps used to estimate capital cost using the detailed factorial estimate method are as follows (Towler & Sinnott, 2008):

1. Identify if it is a whole new plant being built or if it is an extension
2. Determine the purchase cost of equipment (PCE)
3. Determine the physical plant cost (PPC). Below is the equation for PPC calculation:

$$PPC = PCE \times (1 + f_1 + \cdots + f_9) \quad \text{..... (Equation 0-2)}$$

with f_1 to f_9 being the different factors for the direct costs.

4. Determine the fixed capital cost (FCI). The FCI is given by the equation below.

$$FCI = PPC \times (1 + f_{10} + f_{11} + f_{12}) \quad \text{..... (Equation 0-3)}$$

with f_{10} to f_{12} being the factors for the indirect costs

5. Determine the working capital cost which is 5% to 30% of the fixed capital cost.
6. Finally, determine the total capital cost which is the sum of the fixed capital cost and the working capital.

Table 6-1 below provides the factors (f_1 to f_{12}) used for the approximate estimation of the physical plant cost (PPC) and the fixed capital cost (FCI). It includes direct costs and indirect costs factors.

Table 0-1: Factors used for the estimation of the fixed capital cost (Towler & Sinnott, 2008)

Item	Process type		
	Fluids	Fluids-solids	Solids
1. Major equipment, total purchase cost	PCE	PCE	PCE
f_1 Equipment erection	0.40	0.45	0.50
f_2 Piping	0.70	0.45	0.20
f_3 Instrumentation	0.20	0.15	0.10
f_4 Electrical	0.10	0.10	0.10
f_5 Buildings, process	0.15	0.10	0.05
f_6 Utilities	0.50	0.45	0.25
f_7 Storage	0.15	0.20	0.25
f_8 Site development	0.05	0.05	0.05
f_9 Ancillary buildings	0.15	0.20	0.30
2. Total physical plant cost (PPC)			
PPC = PCE $(1 + f_1 + \cdots + f_9)$			
= PCE ×	3.40	3.15	2.80
f_{10} Design and Engineering	0.30	0.25	0.20
f_{11} Contractor's fees	0.05	0.05	0.05
f_{12} Contingency	0.10	0.10	0.10
Fixed capital = PPC $(1 + f_{10} + f_{11} + f_{12})$			
= PPC ×	1.45	1.40	1.35

Assumptions for capital cost estimation:

- The working capital cost is 30% of the fixed capital cost
- The plant is an extension of an existing plant. This means that not all direct costs will be counted for in the estimation as they are already existent.

- **PCE calculation**

The main equipment used in the hydrodynamic cavitation jet loop system are a jacketed vessel and a pump. The vessel is jacketed to ensure that temperature can be controlled. The actual cost of each component of the equipment is found in Table 6-2 below.

Table 0-2: Equipment cost

Equipment	Capacity	Cost	Source
Jacketed vessel	500 L	R 18 436.50	(Alibaba, 2020)
Centrifugal Pump	1.1 kW, 220 V	R 6 455.00	(Ecodepot, 2020)
PCE	R 18 436.50 + R 6 455.00 = **R 24 891.50**		

- **PPC calculation**

Apart from the cost of the main equipment, to determine the physical plant cost (PPC), the other direct costs must be added to the PCE. The other direct costs are:

- Equipment erection f_1
- Piping f_2
- Instrumentation f_3
- Electrical f_4

Since the building of this plant was assumed to be an extension of an existing plant, there is no need to add all the direct costs listed in Table 6-1.

PPC = PCE $(1 + f_1 + f_2 + f_3 + f_4)$

PPC = R 24 891.50 (1 + 0.40 + 0.70 + 0.20 + 0.10) = **R 59 739.60**

- **Fixed capital cost**

To determine the fixed capital cost, the indirect costs must be added to the PPC. The indirect costs for this HC jet loop system are:

- Design and Engineering f_{10}
- Contractor's fees f_{11}

Therefore, the fixed capital cost is equal to PPC $(1 + f_{10} + f_{11})$

Fixed capital cost = R 59 739.60 (1+ 0.30 + 0.05) = **R 80 648.46**

- **Working capital cost**

The working capital cost = 0.3 (R 80 648.46) = **R 24 194.54**

- **Total capital cost**

The total capital cost = fixed capital cost + working capital
The total capital cost = R 80 648.46 + R 24 194.54 = **R 104 843.00**

6.2. Operating costs

The operating costs, also known as the cost of production, can be divided between fixed operating costs and variable operating costs. The fixed operating costs consist of maintenance (labour and materials), operating labour, laboratory costs, supervision, plant overheads, capital charges, rates, insurance, license fees and royalty payments (Sinnott, 2005).
Variable costs consist of raw materials, miscellaneous operating materials, utilities, shipping and packaging. The fixed and variable operating costs are the direct cost of treating wastewater.

Apart from the direct costs of treating wastewater, there are a company's general operating expenses such as general overheads, research and development costs, sales expenses and reserves. These are about 20% to 30% of the direct production costs at the site (Sinnott, 2005).

In this study, considering that it was assumed above that the HC jet loop system being built is an extension to an existing plant, the main operating costs would be the raw materials and utilities. The raw materials required to start operating the HC jet loop system were the wastewater to be treated, hydrochloric acid and sodium hydroxide to adjust the pH of the wastewater to be treated and the wastewater treated as required.
The utilities needed to start operating the HC jet loop system were the cooling water and electricity.

In Table 6-3 below are the costs of the raw materials and utilities.

Table 0-3: Raw materials and utilities costs

Raw Materials and Utilities	Cost	Source
Wastewater	Free	N/A
Hydrochloric acid	R 1920.37/2.5 L	(Merck, 2020a)
Sodium hydroxide	R 808.97/kg	(Merck, 2020b)
Cooling water	R 31.41/kL	(Water and Sanitation department, 2019)
Electricity	R 0.52/kWh	(The National Energy Regulator of South Africa, 2019)

When using the HC jet loop system at a flowrate of 0.0001078 m^3/s and an inlet pressure of 400 kPa, the cost of electricity would be $0.548\frac{kWh}{m^3} \times R\frac{0.52}{kWh} = R\ 0.285/m^3$

Assuming a treatment of 100 L of dye contaminated wastewater, the cost of electricity would be R 0.0285

For cooling water, it can be assumed that the amount needed for 100 L of dye contaminated wastewater would be 50 L of cooling water which would cost R 1.5705

For Sodium hydroxide (NaOH), assuming the use of 1g of NaOH in 100 L of dye contaminated wastewater, the cost would be R 0.809

For hydrochloric acid (HCl), assuming the use of 30 mL of in 100 L of dye contaminated wastewater, the cost would be R 23.04

The total cost of operating costs in the treatment of 100 L of dye contaminated wastewater in the HC jet loop system would be R 0.0285 + R 1.5705 + R 0.809 + R 23.04 = R 25.448

For a treatment of 500 L of dye contaminated wastewater the approximate estimate of operating costs would be R 25.448 x 5 = **R 127.24**

6.3. Chapter summary

The cost of having the HC jet loop system equipped with a 500 L tank, a 1.1 kW centrifugal pump, a venturi, and/or orifice plate(s) installed as an extension on an existing plant has been estimated in this chapter. The estimation method used was the detailed factorial method; it helped to estimate the capital investment cost using cost factors of the direct cost of construction of the plant. The total capital investment cost was estimated to be around R 104 843.00. The operating costs were also given in table 6-3. As the HC jet loop system was assumed to be an addition to an existing system, the fixed operating costs such as labour costs were not added to the operating costs. The main operating costs used for the estimate were raw materials and utilities. Therefore, the operating costs of treatment of 500 L of dye contaminated wastewater using the HC jet loop system at a flowrate of 0.0001078 m^3/s and an inlet pressure of 400 kPa, were approximated to be R 127.24.

CHAPTER 7: CONCLUSIONS AND RECOMMENDATIONS

Introduction

In this chapter, the main findings of this study, as well as conclusions and recommendations for future work are presented. The main findings and conclusions were drawn from the results obtained from the completion of the objectives set out in Chapter 1 Section 1.4.

7.1. Main findings of this study and conclusions

The aim of this study was to design an HC jet loop system with a view to improving its performance in the treatment of textile wastewater. In the newly designed HC jet loop system, six different cavitating devices were designed and tested. Five of the cavitating devices were orifice plates with different hole diameters, and one was a circular venturi. The hole diameter of the orifice plates were 2 mm, 3 mm, 4 mm, 5 mm and 6 mm respectively. The venturi had a throat diameter of 10 mm. In addition to the cavitating devices, different inlet pressures were also investigated in the HC jet loop system, namely 200 kPa, 300 kPa and 400 kPa.
This study started with the design and construction of the HC jet loop system. Upon completion of the construction of the system, its performance was investigated using the five set objectives in Chapter 1. The outcomes from the fulfilment of those objectives are presented and discussed in details in Chapter 4.

The first objective was to determine which orifice plate among various types of orifice plates with different hole diameters was more effective in treating simulated textile wastewater using the hydrodynamic cavitation jet loop system. To achieve this objective, the performance of each orifice plate was tested in the HC jet loop system. Each experiment in the HC jet loop system lasted 10 min and samples were collected every 2 min. 10 L of OR2 dye solution was used in the experiments and its colour degradation determined the performance of each orifice plate. The OR2 dye solution used initially had a 20 ppm concentration and a pH of 2.31 as it has been noticed in previous research on HC that the optimum pH for the colour degradation of dye solution using HC is an acidic pH (Badmus et al., 2019). The inlet pressure in these experiments was 300 kPa. The results obtained showed that the 2 mm hole diameter orifice plate was more efficient in decolourising dye solution using hydrodynamic cavitation compared to the other orifice plates tested. The percentage dye degradation using the 2 mm orifice plate diameter was 89.60%, while the percentage dye degradation using 3 mm, 4 mm, 5 mm and 6 mm was 88.25%, 86.68%, 85.05%, and 82.52% respectively. The results led to the conclusion that an

orifice plate with a smaller single hole diameter performs better than orifice plates with bigger single hole diameters. This correlates with what has been reported by Aris et al. (2016) and Pandit & Sivakumar (2001). Aris and his colleagues found that their orifice plate with a 0.8 mm hole diameter generated more Iodine, which was equivalent to OH radical production in their system. The other orifice plates that they tested had 0.9 mm and 1 mm hole diameter respectively. Pandit & Sivakumar investigated the use of 1 mm, 2 mm, 3 mm, and 5 mm hole diameter orifice plates and they found that the 1 mm hole diameter orifice plate provided the best results in decolouration of rhodamine B.

The second objective was to combine the venturi and the orifice plate to determine the effectiveness of simulated textile wastewater treatment using the two types of cavitating devices simultaneously in the hydrodynamic cavitation jet loop system. The designed venturi that was used had a 10 mm throat diameter. Similarly to the orifice plate experiments, the venturi and combination of cavitating devices experiments were also all run for 10 min. The simulated textile wastewater used was also 10 L of OR2 dye solution with a 20 ppm initial concentration. First an experiment with the venturi alone was performed in the HC jet loop system. This was in order to compare the performance of the venturi alone with that of the orifice plates alone. This experiment was carried out at an inlet pressure of 300 kPa and the OR2 dye solution had a pH of 2.31. The percent dye decolouration obtained using the venturi after 10 min of run time was 57.35%. This was the lowest percent degradation compared to all the orifice plates. This is thought to be due to the fact that the throat diameter of the venturi was bigger than the hole diameter of all the orifice plates. When combining the most efficient orifice plate (2 mm hole diameter) and the venturi in the HC jet loop system, the percent degradation of OR2 dye solution obtained was 70.71% when using an inlet pressure of 300 kPa and a dye solution pH of 2.33. The combination of the 2 cavitating devices performed better than the venturi alone. However, the orifice plate alone still provided better results compared to the combination of the orifice plate and venturi. This is probably due to the fact that when the OR2 solution passes through the orifice plate then immediately goes through the venturi, the amount of OH radicals generated is smaller than when the OR2 solution passes through the 2 mm hole diameter orifice plate alone. This is probably due to the high pressure drop in the orifice plate which allows for formation of more cavitation bubbles compared to those formed when using the designed venturi. In the combination of cavitating devices, as the OR2 solution goes through the orifice plate first, all the bubbles formed through the orifice plate are believed to not have enough time to collapse as the fluid flows then through the venturi. In the venturi, bubbles are formed again through the throat, but in lower numbers compared to those formed in the orifice plate, and as they exit the throat of the venturi, the pressure recovers.

As the pressure recovers, the bubbles collapse. It is from the bubble collapse that the OH radicals are formed by splitting of the water molecules. Though some studies, such as Mishra & Gogate (2010), have shown that a 2 mm throat diameter venturi performs better than a 2 mm orifice plate when decolourising rhodamine B, the current study found that when the venturi has a bigger throat diameter, it does not perform better or as well as an orifice plate that has a smaller hole diameter.

The third objective was to determine at what inlet pressure the hydrodynamic cavitation jet loop is more effective in treating simulated textile wastewater. In these experiments, three inlet pressures were investigated such as 200 kPa, 300 kPa and 400 kPa. The venturi, the 2 mm hole diameter orifice plate, and a combination of the venturi and orifice plate were all tested in the HC jet loop at the different inlet pressures. The OR2 dye solution was used for each experiment and like the previous experiments, the same duration of experiment, the same volume and the same pH were also used. The results obtained showed that for each cavitating device and for the combination of the cavitating devices, the inlet pressure of 400 kPa was found to be the optimum pressure for dye decolouration using the designed HC jet loop system. Yan et al. (1988) has reported that a low cavitation number allows for greater cavitational intensity, which implies a higher production of cavitation bubbles and thus a higher chance of OH radical production. Further, a higher inlet pressure provides a low cavitation number. This explains why the 400 kPa inlet pressure provided better results for dye degradation compared to 200 kPa and 300 kPa inlet pressures. This finding correlates with what other studies comparing inlet pressures in HC systems have found, namely that the optimum inlet pressure are between 400 kPa and 500 kPa.

The fourth objective was to determine the concentration of OH radicals produced by the hydrodynamic cavitation jet loop system when applying the optimum operating conditions and the optimum design conditions. In the experiments carried out to accomplish this objective, 10 L terephthalic acid (TA) having a 2μM concentration was used in the HC jet loop system. The TA solution was run in the HC jet loop system for 10 min and the samples were taken every 2 min. The amount of OH radicals generated by the jet loop system was determined by relating the hydroxyterephthalic acid (HTA) produced by the HC jet loop system using a spectrofluorometer. HTA is produced through the reaction of TA and OH radicals. The results showed that in 10 min, 32.3 ppm of OH radicals were produced by the HC jet loop system using the orifice plate (2 mm hole diameter), 24.3 ppm of OH radicals were produced using the venturi and 27.2 ppm were produced by the HC jet loop system using a combination of the venturi and orifice plate (2 mm hole diameter). All the experiments towards the fulfilment of this objective were done using the optimum inlet pressure (400 kPa).

The findings of these experiments lead to the conclusion that the current design of the HC jet loop system shows excellent performance when it comes to the generation of OH radicals and that the optimum operating and design conditions are an inlet pressure of 400 kPa and a 2 mm hole diameter orifice plate respectively. When compared to the system used by Badmus (2019), the current design of the HC jet loop system generated almost 3 times more OH radicals in a shorter period of time. Badmus reported a generation of 11.29 ppm in 1h.

The fifth objective was to determine the energy consumption and cost of using the hydrodynamic cavitation jet loop system for the treatment of simulated textile wastewater when applying the optimum operating conditions and optimum design conditions. The energy consumption of the HC jet loop system was calculated using the Bernoulli equation. It was found that energy consumed by the HC jet loop system for the decolouration of OR2 dye was 0.548 kWh/m^3 at a flow rate of 0.0001078 m^3/s and an inlet pressure of 400 kPa. When comparing with AOPs such as UV, the HC jet loop system does consume less energy, as Yen (2016) has reported that the energy consumed by the UV in a UV/H2O2 is 1.73 kWh/m^3. To determine the cost of using the HC jet loop system, the capital investment and the operating costs were estimated. In the process of estimating those costs, it was assumed that the HC jet loop system is an extension of an existing plant. It was estimated that the capital investment cost for a plant with a capacity of treating 500 L of wastewater would be R 104 843.00. The operating cost of treatment of 500 L of dye contaminated wastewater using the HC jet loop system at a flowrate of 0.0001078 m^3/s and an inlet pressure of 400 kPa was estimated to be R 127.24 (when only considering raw materials and utilities as the estimation considered the HC jet loop system to be an extension to an existing plant).

In brief, this study has shown that the use of HC jet loop system in the treatment of textile dye contaminated wastewater is an effective, simple, inexpensive and energy-efficient method. It is a system that is simple to construct, easy to operate and has low maintenance requirements. No chemical addition into the system is required as the decolouration of the azo dye used has proved to be rapid.

7.2. Recommendations for future work

Recommendations for future work are for work that was not within the scope of this study but are likely to be helpful in advancing knowledge on the use of hydrodynamic cavitation as a wastewater treatment method using orifice plates and venturi as cavitating devices.

The findings of this study have brought to light ideas for more research that needs to be done on the HC jet loop system.

In conducting this study, it was noticed that most of the 20 ppm OR2 dye solution decolourised in 10 min; it would be worth investigating how long it would take to decolourise higher concentrations of dye using the HC jet loop system.

Regarding the operating temperature, it was noted that the temperature continued to increase with the highest temperature reached in 10 min of run time, being 46^{o}C with an initial temperature of 25^{o}C. It would be important to consider what would be the effect of controlling the temperature by keeping it constant and by investigating different temperatures.

In Section 4.2 of this study, it was observed that the venturi performed poorly as a cavitating device compared to the other cavitating devices. It would be interesting to investigate how a venturi with a smaller throat diameter such as 2 mm will perform compared to the 2 mm hole diameter orifice plate when using the current design of the HC jet loop system, as other researchers have found that a small diameter venturi performs better.

Regarding orifice plates, it would be helpful to see what the performance of orifice plates with multiple holes would be compared to the orifice plates with single holes.

The combination in series of orifice plate and venturi in the current research was found to perform poorly compared to the use of an orifice plate alone. It would also be worth considering what would be the results of a combination of cavitating devices mounted in parallel and compare them to the results of those mounted in series.

In this study, only dye solution was used in the HC jet loop system and it would be important to know with future research how efficient the system would be in the treatment of other types of wastewater.

Future research should also look at determining if free radicals other than OH radicals such as ozone and hydrogen peroxide are generated in the designed HC jet loop system.

REFERENCES

Ahmed, A.M. 2007. *Removal of colour and organic pollutants from textile wastewater using integrated biological and Advanced Oxidation Process*. Universiti Putra Malaysia.

Alibaba. 2020. Jacketed stainless steel Bright Beer Tank 500L for Sale for the storage of beer. *Alibaba*. https://www.alibaba.com/product-detail/Jacketed-stainless-steel-Bright-Beer-Tank_60835034063.html?spm=a2700.7735675.normalList.14.5e517ca2T7Xuov&s=p 20 May 2020.

Ameta, R., Chohadia, A.K., Jain, A. & Punjabi, P.B. 2018. Fenton and Photo-Fenton Processes. In S. Ameta & R. Ameta, eds. *Advanced Oxidation Processes for wastewater treatment*. Mumbai: Academic Press: 49–87.

Anglada, A., Urtiaga, A. & Ortiz, I. 2009. Contributions of electrochemical oxidation to waste-water treatment : fundamentals. *Chemical Technology and Biotechnology*, 84(12): 1747–1755.

Anjum, M., Miandad, R., Waqas, M., Gehany, F. & Barakat, M.A. 2016. Remediation of wastewater using various nano-materials. *Arabian Journal of Chemistry*, 12(8): 4897–4919. http://dx.doi.org/10.1016/j.arabjc.2016.10.004.

Aris, A., Jusoh, M.N.H. & Talib, J. 2016. Hydrodynamic cavitation using double orifice-plates for the generation of hydroxyl radicals. *Jurnal Teknologi*, 78(11): 41–47.

Ayanda, O.S., Nelana, S.M., Petrik, L.F. & Naidoo, E.B. 2018. Kinetic Study of Ultrasound Degradation of 2 , 2-Bis (4-hydroxyphenyl) propane Assisted by nFe / TiO 2 Composite. *Journal of Advanced Oxidation Technologies*, 21(1): 1–8.

Babu, B.R., Parande, A.K., Raghu, S. & Kumar, T.P. 2007. Cotton Textile Processing : Waste Generation and Effluent Treatment. *The Journal of Cotton Science*, 11(3): 141–153.

Badmus, K.O. 2019. *Treatment of persistent organic pollutants in wastewater with combined advanced oxidation*. University of the Western Cape. https://etd.uwc.ac.za/handle/11394/6785.

Badmus, K.O., Irakoze, N., Adeniyi, O.R. & Petrik, L. 2019. Synergistic Advance Fenton Oxidation and Hydrodynamic Cavitation treatment of persistent organic dyes in textile wastewater. *Journal of Environmental Chemical Engineering*, 8(2): 103521. https://doi.org/10.1016/j.jece.2019.103521.

Badmus, K.O., Tijani, J.O., Eze, C.P., Fatoba, O.O. & Petrik, L.F. 2016. Quantification of Radicals Generated in a Sonicator. *Analytical and Bioanalytical Chemistry Research*, 3(1): 139–147.

Badmus, K.O., Tijani, J.O., Massima, E. & Petrik, L. 2018. Treatment of persistent organic pollutants in wastewater using hydrodynamic cavitation in synergy with advanced oxidation process. *Environmental Science and Pollution Research*, 25(8): 7299–7314.

Barati, A.H., Mokhtari, M., Mozdarani, H., Bathaei, S.Z. & Hassan, Z.M. 2006. Free hydroxyl

radical dosimetry by using 1 MHz low level ultrasound waves. *Iran Journal Radiation Research*, 3(4): 163–169.

Beck, S. & Collins, R. 2008. Moody diagram. *Wikimedia*. https://commons.wikimedia.org/wiki/File:Moody_diagram.jpg 22 June 2020.

Behera, S., Ghanty, S., Ahmad, F., Santra, S. & Banerjee, S. 2012. UV-Visible Spectrophotometric Method Development and Validation of Assay of Paracetamol Tablet Formulation. *Journal of Analytical & Bioanalytical Techniques*, 3(6): 151–156.

Bhatia, D., Sharma, N.R., Singh, J. & Kanwar, R.S. 2017. Biological methods for textile dye removal from wastewater : A Review. *Critical Reviews in Environmental Science and Technology*, 47(19): 1836–1876.

Bisschops, I. & Spanjers, H. 2003. Literature review on textile wastewater characterisation. *Environmental Technology*, 24: 1399–1411.

Boczkaja, G., Gągola, M. & Przyjaznyb, A. 2018. Wastewater treatment by means of advanced oxidation processes based on cavitation – A review. *Chemical Engineering Journal*, 338: 599–627.

Brennen, C.E. 1995. *Cavitation and Bubble Dynamics*. Oxford: Oxford University Press.

Buthelezi, S.P., Olaniran, A.O. & Pillay, B. 2012. Textile dye removal from wastewater effluents using bioflocculants produced by indigenous bacterial isolates. *Molecules*, 17(12): 14260–14274.

Carmen, Z. & Daniela, S. 2012. Textile Organic Dyes – Characteristics , Polluting Effects and Separation / Elimination Procedures from Industrial Effluents – A Critical Overview. In T. Puzyn & A. Mostrag-Szlichtyng, eds. *Organic Pollutants Ten Years After the Stockholm Convention - Environmental and Analytical Update*. InTech: 482.

Chequer, D., Maria, F., Augusto, G., Oliveira, R. De, Raquel, E., Ferraz, A., Cardoso, J.C., Valnice, M., Zanoni, B. & Oliveira, D.P. De. 2013. Textile Dyes : Dyeing Process and Environmental Impact M. Gunay, ed. *IntechOpen*: 151–176.

Clark, J. 2016. UV-visible absorption spectra. *Chemguide*. https://www.chemguide.co.uk/analysis/uvvisible/theory.html#:~:text=That's easy - but unfortunately UV,the lower the wavelength is. 1 April 2019.

Cloete, T.E., Gerber, A. & Maritz, L. V. 2010. *A first order inventory of water use and effluent production by SA industrial, mining and electricity generation sectors*. Pretoria. http://webcache.googleusercontent.com/search?q=cache:Fa8lP76Q6HcJ:www.wrc.org.za/wp-content/uploads/mdocs/1547.pdf+&cd=1&hl=en&ct=clnk&gl=za.

Costa, A.J. & Parkin, B.R. 1975. Cavitation Inception - A Selective Review. *Journal of Ship Research*, 19(4): 193–205.

Crini, G. & Lichtfouse, E. 2019. Advantages and disadvantages of techniques used for wastewater treatment. *Environmental Chemistry Letters*, 17(1): 145–155. https://doi.org/10.1007/s10311-018-0785-9.

Deng, Y. & Zhao, R. 2015. Advanced Oxidation Processes (AOPs) in Wastewater Treatment. *Current Pollution Reports*, 1(3): 167–176.

Dindar, E. 2016. An Overview of the Application of Hydrodynamic Cavitation for the Intensification of Wastewater Treatment Applications : A Review. *Innovative Energy and Research*, 5(1): 1–7.

Dular, M., Griessler-bulc, T., Gutierez, I., Heath, E., Kosjek, T., Klemenčič, A.K., Oder, M., Petkovšek, M., Ravnikar, M., Šarc, A., Širok, B., Zupanc, M., Žitnik, M. & Kompare, B. 2015. Use of hydrodynamic cavitation in (waste)water treatment. *Ultrasonics sonochemistry*, 29: 577–588.

Dular, M., Griessler-bulc, T., Gutierrez-aguirre, I., Heath, E., Kosjek, T., Klemenčič, A.K., Oder, M., Petkovšek, M., Rački, N., Ravnikar, M., Šarc, A., Širok, B., Zupanc, M., Žitnik, M. & Kompare, B. 2015. Use of hydrodynamic cavitation in (waste) water treatment. *Ultrasonics Sonochemistry*, 29: 577–588.

Ecodepot. 2020. EBARA Cast Iron Centrifugal Pump CMA 150 M (1.1kW, 220V). *Ecodepot*.

Feng, X., Zhu, S. & Hou, H. 2006. Investigation of 207 nm UV radiation for degradation of organic dye in water. *Water SA*, 32(1): 43–48.

Ferrari, A. 2017. Fluid dynamics of acoustic and hydrodynamic cavitation in hydraulic power systems. *Royal Society Publishing*, 473(2199): 345–376.

Fogler, H.S. 2005. *Elements of chemical reaction engineering*. 4th ed. Massachussets: Prentice Hall.

Galán, J., Rodríguez, A., Gómez, J.M., Allen, S.J. & Walker, G.M. 2013. Reactive dye adsorption onto a novel mesoporous carbon. *Chemical Engineering Journal*, 219: 62–68.

Garlick, K. 1986. A brief review of the history of sizing and resizing practices. *The Book and Paper group Annual*. http://cool.conservation-us.org/coolaic/sg/bpg/annual/v05/bp05-11.html 6 October 2017.

Geankoplis, C.J. 1993a. *Transport-Processes-and-Unit-Operations*. 3rd ed. New Jersey: Prentice Hall.

Geankoplis, C.J. 1993b. Transport Processes and Unit Operations. : 921.

Genovesi, L. 2015. Spectrofluorometers: Tools for Measuring Fluorescence Signature. *Labcompare*.

Ghaly, A.E., Ananthashankar, R., Alhattab, M. & Ramakrishnan, V.V. 2013. Production, Characterization and Treatment of Textile Effluents: A Critical Review. *Journal of Chemical Engineering & Process Technology*, 05(01): 1–19.

Ghanbari, F. & Moradi, M. 2016. Electrooxidation Processes for Dye Degradation and Colored Wastewater Treatment. In *Advanced Nanomaterials for Wastewater Remediation*. London: CRC Press: 61–108.

Ghassemi, H. & Ashrafizadeh, S.M. 2015. Experimental and numerical investigation on the

performance of small-sized cavitating venturis. *Flow Measurement and Instrumentation*, 42: 6–15.

Gogate, P. & Thanekar, P. 2018. Application of Hydrodynamic Cavitation Reactors for Treatment of Wastewater Containing Organic Pollutants : Intensification Using Hybrid Approaches. *Fluids*, 3(4): 98–121.

Gogate, P.R. & Bhosale, G.S. 2013. Comparison of effectiveness of acoustic and hydrodynamic cavitation in combined treatment schemes for degradation of dye wastewaters. *Chemical Engineering and Processing: Process Intensification*, 71: 59–69. http://dx.doi.org/10.1016/j.cep.2013.03.001.

Gosavi, V.D. & Sharma, S. 2014. A General Review on Various Treatment Methods for Textile Wastewater. *Journal of Environmental Science, Computer Science and Engineering & Technology*, 3(1): 29–39.

Himmelblau, D.M. & Riggs, J.B. 2013. *basic principles and calculations in chemical engineering by himmelblau.pdf*. 5th ed. New Jersey: Prentice Hall.

Holkar, C.R., Jadhav, A.J., Pinjari, D. V, Mahamuni, N.M. & Pandit, A.B. 2016. A critical review on textile wastewater treatments : Possible approaches. *Journal of Environmental Management*, 182: 351–366. http://dx.doi.org/10.1016/j.jenvman.2016.07.090.

Imtiazuddin, S.M., Mumtaz, M. & Mallick, K.A. 2012. Pollutants of Wastewater Characteristics in Textile Industries. In *Journal of Basic & Applied Sciences*. 554–556.

De Jager, D. 2013. *Membrane bioreactor application within the South African textile industry : pilot to full-scale*. Cape Peninsula University of Technology. http://hdl.handle.net/20.500.11838/926.

Jain, T., Carpenter, J. & Saharan, V.K. 2014. CFD Analysis and Optimization of Circular and Slit Venturi for Cavitational Activity. *Journal of Material Science and Mechanical Engineering (JMSME)*, 1(1): 28–33.

Julkapli, N.M., Bagheri, S., Bee, S. & Hamid, A. 2014. Recent Advances in Heterogeneous Photocatalytic Decolorization of Synthetic Dyes. *The Scientific World Journal*, 2014.

Jyoti, K.K. & Pandit, A.B. 2001. Water disinfection by acoustic and hydrodynamic cavitation. *Biochemical Engineering Journal*, 7(March 2000): 201–212.

Kalumuck, K.M. & Chahine, L.G. 2000. The use of cavitating jets to oxidize organic compounds in water. *The journal of Fluids Engineering*, 122(3).

Kanazawa, S. & Kawano, H. 2013. Application of chemical dosimetry to hydroxyl radical measurement during underwater discharge. *Journal of Physics: Conference Series*, 418.

Kant, R. 2012. Textile dyeing industry an environmental hazard. *Scientific Research Publishing*, 4(1): 22–26.

Khan, S. & Malik, A. 2014. Environmental and Health Effects of Textile Industry Wastewater. In A. Malik, E. Grohmann, & R. Akhtar, eds. *Environmental Deterioration and Human Health*. Dordrecht: Springer: 55–71.

Khandelwal, D.H. & Ameta, R. 2013. Use of Photo-Fenton Reagent in the Degradation of Basic Yellow 2 in Aqueous Medium. *Research Journal of Recent Sciences*, 2(1): 39–43.

Lester, Y., Avisar, D., Gozlan, I. & Mamane, H. 2011. Removal of pharmaceuticals using combination of UV / H 2 O 2 / O 3 advanced oxidation process. *Water Science & Technology*, 64(11): 2230–2238.

Liang, C., Sun, S., Li, F., Ong, Y. & Chung, T. 2014. Treatment of highly concentrated wastewater containing multiple synthetic dyes by a combined process of coagulation / flocculation and nanofiltration. *Journal of Membrane Science*, 469: 306–315. http://dx.doi.org/10.1016/j.memsci.2014.06.057.

Liu, Y., Nie, Y., Lu, X., Zhang, X., He, H., Pan, F., Zhou, L., Liu, X., Ji, X. & Zhang, S. 2019. Cascade utilization of lignocellulosic biomass to high-value products. *Royal Society of Chemistry*, (21): 3499–3535.

Ma, J., Song, W., Chen, C., Ma, W., Zhao, J. & Tang, Y. 2005. Fenton Degradation of Organic Compounds Promoted by Dyes under Visible Irradiation. *Environmental Science and Technology*, 39(15): 5810–5815.

Madhu, G.M., Thomas, A., Deepak, S., Preetham, H.S. & Rajanandam, K.S. 2014. Escalation of degradation of malachite green and Methyl violet using hydrodynamic cavitations using different orifice geometry. *International Journal of Environmental Sciences*, 5(3): 644–651.

Manevich, Y., Held, K.D. & Biaglow, J.E. 2019. Coumarin-3-Carboxylic Acid as a Detector for Hydroxyl Radicals Generated Chemically and by Gamma Radiation. *Radiation research*, 148(6): 580–591.

Masupha, T.M. 2007. *Water Management at a textile industry : a case study in Lesotho*. University of Pretoria.

Matavos-Aramyan, S. & Moussavi, M. 2017. Advances in Fenton and Fenton Based Oxidation Processes for Industrial Effluent Contaminants Control - A Review. *International Journal of Environmental Sciences and Natural Resources*, 2(4).

Mecholic. 2018. Application, Advantages and Disadvantages of Cavitation. *Mecholic for Mechanical Engineering*. https://www.mecholic.com/2018/06/application-advantages-cavitation.html 4 July 2018.

Meng, X., Liu, G., Zhou, J. & Fu, Q.S. 2014. Effects of redox mediators on azo dye decolorization by Shewanella algae under saline conditions. *Bioresource Technology*, 151: 63–68. http://dx.doi.org/10.1016/j.biortech.2013.09.131.

Merck. 2020a. Hydrochloric acid. *Merck*. https://www.sigmaaldrich.com/catalog/search?term=Hydrochloric+acid&interface=All&N=0&mode=match partialmax&lang=en&region=ZA&focus=product 20 May 2020.

Merck. 2020b. Sodium hydroxide. *Merck*. https://www.sigmaaldrich.com/catalog/search?term=Sodium+hydroxide&interface=Product Name&N=0+&mode=mode matchpartialmax&lang=en&region=ZA&focus=productN=0 220003048 219853286

219853145 20 May 2020.

Miralles-Cuevas, S., Ollera, I., Agüerab, A., Llorcac, M., Pérezb, J.A.S. & Malatoa, S. 2016. Combination of nanofiltration and ozonation for the remediation of real municipal wastewater effluents: Acute and chronic toxicity assessment. *Journal of Hazardous Materials*, 323(Part A): 442–451. http://dx.doi.org/10.1016/j.jhazmat.2016.03.013.

Mishra, K.P. & Gogate, P.R. 2010. Intensification of degradation of Rhodamine B using hydrodynamic cavitation in the presence of additives. *Separation and Purification Technology*, 75(3): 385–391. http://dx.doi.org/10.1016/j.seppur.2010.09.008.

Neyens, E. & Baeyens, J. 2002. A review of classic Fenton ' s peroxidation as an advanced oxidation technique. *Journal of Hazardous Materials*, 98: 33–50.

Nidheesh, P.V. & Gandhimathi, R. 2013. Degradation of dyes from aqueous solution by Fenton processes : a review. *Environmental Science and Pollution Research*, 20(4): 2099–2132.

Ortiz, I., Fernández-castro, P., Vallejo, M., Fresnedo, M. & Román, S. 2015. Insight on the fundamentals of advanced oxidation processes . Role and review of the determination methods of reactive oxygen species. *Chemical Technology and Biotechnology*, 90(5): 796–820.

Ozcelik, A., Ahmed, D., Xie, Y., Nama, N., Qu, Z., Nawaz, A.A. & Huang, T.J. 2014. An Acoustofluidic Micromixer via Bubble Inception and Cavitation from Microchannel Sidewalls. *Analytical Chemistry*, 86: 5083−5088.

Pandit, A.B., Bashir, T.A., Soni, A.G. & Mahulkar, A. V. 2011. The CFD driven optimisation of a modified venturi for cavitational activity. *THE CANADIAN JOURNAL OF CHEMICAL ENGINEERING*, 89: 28–33.

Pandit, A.B., Saharan, V.K., Rizwani, M.A. & Malani, A.A. 2013. Effect of geometry of hydrodynamically cavitating device on degradation of orange-G. *Ultrasonics Sonochemistry*, 20(1): 345–353. http://dx.doi.org/10.1016/j.ultsonch.2012.08.011.

Pandit, A.B. & Sivakumar, M. 2001. Wastewater treatment : a novel energy efficient hydrodynamic cavitational technique. *Ultrasonics Sonochemistry*, 9: 123–131.

Peng, F. & Xiong, Y. 2015. Optimization of cavitation venturi tube design for pico and nano bubbles generation. *International Journal of Mining Science and Technology*, 25: 523–529. http://dx.doi.org/10.1016/j.ijmst.2015.05.002.

Peralta, E., Roa, G., Hernandez-Servin, J.A., Romero, R., Balderas, P. & Natividad, R. 2014. Hydroxyl Radicals quantification by UV spectrophotometry. *Electrochimica Acta*, 129: 137–141. http://dx.doi.org/10.1016/j.electacta.2014.02.047.

Petrie, B. 2016. Real reason behind South Africa's water crisis. *Plumbing online*. http://www.plumbingafrica.co.za/index.php/environment/1880-real-reasons-behind-south-africa-s-water-crisis 17 August 2017.

Punzi, M. 2015. *Treatment of textile wastewater by combining biological processes and advanced oxidation*. PhD Thesis, Lund University.

Rajoriya, S., Bargole, S., George, S. & Saharan, V.K. 2018. Treatment of textile dyeing industry effluent using hydrodynamic cavitation in combination with advanced oxidation reagents. *Journal of Hazardous Materials*, 344: 1109–1115. http://dx.doi.org/10.1016/j.jhazmat.2017.12.005.

Rajoriya, S., Carpenter, J., Saharan, V.K. & Pandit, A.B. 2016. Hydrodynamic cavitation : An advanced oxidation process for the degradation of bio- refractory pollutants. *Reviews in chemical engineering*, 32(4): 379–411.

Raju, G.B., Keerthi, R., Latha, S.S. & Prabhakar, S. 2015. Degradation of dyes by UV / Ozone / Hydrogen peroxide and electrooxidation techniques. *Water Practice & Technology*, 6(2).

Randhavane, S.B. 2019. Comparing geometric parameters in treatment of pesticide effluent with hydrodynamic cavitation process. *Environmental Engineering Research*, 24(2): 318–323.

Ratna & Padhi, B.S. 2012. Pollution due to synthetic dyes toxicity & carcinogenicity studies and remediation. *International Journal of Environmental Sciences*, 3(3): 940–955.

Robinson, T., Mcmullan, G., Marchant, R. & Nigam, P. 2001. Remediation of dyes in textile effluent : a critical review on current treatment technologies with a proposed alternative. *Bioresource technology*, 77: 247–255.

Rochkind, M., Pasternak, S. & Paz, Y. 2015. Using Dyes for Evaluating Photocatalytic Properties: A Critical Review. *Molecules*, 20: 88–110.

Le Roux, K. 2017. South Africa water shortage is huge risk to businesses and economy. *CapeTalk*. https://www.702.co.za/articles/240440/south-africa-s-water-shortage-is-huge-risk-to-business-and-the-economy 17 August 2017.

Roy, K., Carpenter, J. & Saharan, V.K. 2014. Study of Cavity dynamics in a Hydrodynamic Cavitation Reactor. *Energy Technology & Ecological Concerns: A Contemporary Approach*: 37–43.

Royal Society of Chemistry. 2009. Ultraviolet - Visible Spectroscopy (UV). *Advancing the Chemical sciences*. http://www.rsc.org/learn-chemistry/content/filerepository/CMP/00/001/304/UV-Vis_Student resource pack_ENGLISH.pdf 1 April 2019.

Saharan, V.K., Pandit, A.B., Satish Kumar, P.S. & Anandan, S. 2012. Hydrodynamic cavitation as an advanced oxidation technique for the degradation of Acid Red 88 dye. *Industrial and Engineering Chemistry Research*, 51(4): 1981–1989.

Saharan, V.K., Pinjari, D.V., Gogate, P.R. & Pandit, A.B. 2014. *Advanced Oxidation Technologies for wastewater Treatment: An Overview, Publisher: Butterworth-Heinemann, Editors: Vivek V. Ranade Vinay M. Bhandari, pp.141-191*. V. V. Ranade & V. M. Bhandari, eds. Butterworth-Heinemann.

Saharan, V.K., Rajoriya, S. & Bargole, S. 2017a. Degradation of a cationic dye (Rhodamine 6G) using hydrodynamic cavitation coupled with other oxidative agents: reaction mechanism and pathway. *Ultrasonics Sonochemistry*, 34: 183–194.

http://dx.doi.org/10.1016/j.ultsonch.2016.05.028.

Saharan, V.K., Rajoriya, S. & Bargole, S. 2017b. Degradation of reactive blue 13 using hydrodynamic cavitation: Effect of geometrical parameters and different oxidizing additives. *Ultrasonics Sonochemistry*, 37: 192–202. http://dx.doi.org/10.1016/j.ultsonch.2017.01.005.

Saharan, V.K., Rizwani, M.A., Malani, A.A. & Pandit, A.B. 2013. Effect of geometry of hydrodynamically cavitating device on degradation of orange-G. *Ultrasonics Sonochemistry*, 20(1): 345–353. http://dx.doi.org/10.1016/j.ultsonch.2012.08.011.

Šarc, A., Stepišnik-Perdih, T., Petkovšek, M. & Dular, M. 2017. The issue of cavitation number value in studies of water treatment by hydrodynamic cavitation. *Ultrasonics Sonochemistry*, 34: 51–59.

Savin, I. & Butnaru, R. 2008. Wastewater characteristics in textile finishing mills. *Environmental Engineering and Management Journal*, 7(6): 859–864.

Shimizu, A., Takuma, Y., Kato, S. & Yamasaki, A. 2013. Degradation kinetics of azo dye by ozonation in water. *The Journal of the Faculty of Science and Technology, Seikei University*, 50(2): 1–4.

Shriram, B. & Kanmani, S. 2014. Ozonation of Textile Dyeing Wastewater - A Review. *Journal of the Institution of Public Health Engineers, India*, 15(3): 46–50.

Sigma-Aldrich. 2017. *Orange II sodium salt: Product Specification*. http://www.sigmaaldrich.com/catalog/product/aldrich/195235?lang=en&region=DK 6 October 2017.

Singh, S., Lo, S.L., Srivastav, V.C. & Hiwarkar, A.D. 2016. Comparative study of electrochemical oxidation for dye degradation: Parametric optimization and mechanism identification. *Biochemical Pharmacology*, 4(3): 2911–2921. http://dx.doi.org/10.1016/j.jece.2016.05.036.

Sinnott, R.K. 2005. *Chemical Engineering Design*. 4th ed. Oxford: Elsevier Butterworth-Heinemann.

Skosana, G.G. 2015. *Viability, from a quality perspective on the reuse of wastewater effluents in the Southern Gauteng region, South Africa*.

Stasinakis, A.S. 2008. Use of selected advanced oxidation processes (AOPs) for wastewater treatment – A mini review. *Global Nest Journal*, 10(3): 376–385.

Sun, X., Liu, J., Ji, L., Wang, G., Zhao, S., Yong, J. & Chen, S. 2020. A review on hydrodynamic cavitation disinfection : The current state of knowledge. *Science of the Total Environment*, 737(1 October 2020): 139606–139628.

TANG, B., GAO, J.J., XU, K.H., HU, J.X. & HUANG, H. 2006. Determination of Trace Hydroxyl Radicals by Flow Injection Spectrofluorometry and Its Analytical Application. *Journal of Agricultural and Food Chemistry*, 54: 7968–7972.

Tao, Y., Cai, J., Liu, B., Huai, X. & Guo, Z. 2016. Application of Hydrodynamic Cavitation to

Wastewater Treatment. *Chemical Engineering & Technology*, 39(8): 1363–1376.

Tehrani-bagha, A.R., Mahmoodi, N.M. & Menger, F.M. 2010. Degradation of a persistent organic dye from colored textile wastewater by ozonation. *Desalination*, 260(1–3): 34–38. http://dx.doi.org/10.1016/j.desal.2010.05.004.

Teodosiu, C. & Petronela, M.C. 2007. Removal of Persistent Organic Pollutants from Textile Wastewater by Membrane Processes. *Environmental engineering and Management*, 6(3): 175–187.

Terán, R., César, J., Ajaz, M., Hwan, S., Silvério, S. & Han, J. 2016. Hydrodynamic cavitation-assisted alkaline pretreatment as a new approach for sugarcane bagasse biorefineries. *Bioresource technology*, 214: 609–614.

Terentiev, A.G., Kirschner, I.N., Uhlman, J.S., Terentiev, A.G., Kirschner, I.N. & Uhlman, J.S. 2011. *The hydrodynamics of cavitating flows*. New Jersey: Backbone Publishing Company.

The National Energy Regulator of South Africa. 2019. *Nersa approved tariffs*. Cape Town.

Tijani, J.O., Fatoba, O.O., Madzivire, G. & Petrik, L.F. 2014. A Review of Combined Advanced Oxidation Technologies for the Removal of Organic Pollutants from Water. *Water Air & Soil Pollution*, 225(2102): 1–30.

Tijani, J.O., Mouele, M.E.S., Tottito, T.C., Fatoba, O.O. & Petrik, L.F. 2017. Degradation of 2-Nitrophenol by Dielectric Barrier Discharge System : The Influence of Carbon Doped TiO 2 Photocatalyst Supported on Stainless Steel Mesh. *Plasma Chemistry and Plasma Processing*, 37(5): 1343–1373.

Tinoco Jr., I., Sauer, K. & Wang, J.C. 1995. *Physical chemistry: principles and applications in biological sciences*. 3rd ed. New Jersey: Prentice Hall.

Towler, G. & Sinnott, R. 2008. *Chemical Engineering Design: Principles, Practice and Economics of Plant and Process Design*. New York: Elsevier Inc.

Tryba, B., Bubacz, K., Kusiak-Nejman, E. & Morawski, A.W. 2013. Investigation of OH radicals formation on the surface of TiO2/N photocatalyst at the presence of terephthalic acid solution . Estimation of optimal conditions. *Journal of Photochemistry & Photobiology, A: Chemistry*, 261: 7–11. http://dx.doi.org/10.1016/j.jphotochem.2013.04.003.

Turton, R., Bailie, R.C., Whiting, W.B., Shaeiwitz, J.A. & Bhattacharyya, D. 2009. *Analysis, Synthesis, and Design of Chemical Processes*. Third Edit. Massachussets: Pearson Education, Inc.

Tuty, E.A., Yourdan, W.A. & Mermaliandi, F. 2016. Degradation of reactive red 2 by Fenton and Photo-Fenton oxidation processes. *ARPN Journal of Engineering and Applied Sciences*, 11(8): 5227–5231.

UNU-WIDER. 2016. *Potential Impacts of Climate Change on national water supply in South Africa*. Helsinki.

Visual Encyclopedia of Chemical Engineering. 2020. Adsorbers. *College of Engineering, Chemical Engineering, University of Michigan*. http://encyclopedia.che.engin.umich.edu/Pages/SeparationsChemical/Adsorbers/Adsorbers.html 11 June 2020.

Wang, X.-K., Zhang, S.-Y. & Li, S.-P. 2009. Decolorization of Reactive Brilliant Red K-2BP in Aqueous Solution by Using Hydrodynamic Cavitation. *Environmental Engineering Science*, 26(1).

Wang, X., Wang, J., Guo, P., Guo, W. & Wang, C. 2009. Degradation of Rhodamine B in aqueous solution by using swirling jet-induced cavitation combined with H2O2. *Journal of Hazardous Materials*, 169(1–3): 486–491.

Wang, Z., Xue, M., Huang, K. & Liu, Z. 2011. Textile Dyeing Wastewater Treatment. In *Advances in treating Textile Effluent*. IntechOpen: 91–116.

Warade, A.R., Gaikwad, R.W., Sapkal, R.S. & Sapkal, V.S. 2016. Review on Wastewater Treatment by Hydrodynamic Cavitation. *IOSR Journal of Environmental Science, Toxicology and Food Technology*, 10(12): 67–72.

Water and Sanitation department. 2019. *Water and sanitation tarrifs*. Cape Town.

Weng, M., Zhou, Z. & Zhang, Q. 2013. Electrochemical Degradation of Typical Dyeing Wastewater in Aqueous Solution : Performance and Mechanism. *International Journal of Electrochemical Science*, 8: 290–296.

Wijngaarden, L. Van. 2016. Mechanics of collapsing cavitation bubbles. *Ultrasonics Sonochemistry*, 29: 524–527. http://dx.doi.org/10.1016/j.ultsonch.2015.04.006.

Wu, C. & Ng, H. 2007. Degradation of C . I . Reactive Red 2 (RR2) using ozone-based systems : Comparisons of decolorization efficiency and power consumption. *Journal of Hazardous Materials*, 152(2008): 120–127.

Wu, Y., Huang, Y., Zhou, Y., Ren, X. & Yang, F. 2014. Degradation of chitosan by swirling cavitation. *Innovative Food Science and Emerging Technologies*, 23: 188–193.

Yan, Y., Thorpe, R.B. & Pandit, A.B. 1988. Cavitation noise and its suppression by air in orifice flow. In *The International Symposium on Flow Induced Vibration and Noise*. Chicago: American Society of Mechanical Engineers: 25–40.

Yen, H.Y. 2016. Energy consumption of treating textile wastewater for in-factory reuse by H 2 O 2 / UV process. *Desalination and Water Treatment*, 57(23).

APPENDICES

Appendix A: Decolouration of OR2 and OH radicals quantification readings

Table A 1: Absorbance measurements and percent decolouration of OR2 using the 10 mm throat diameter venturi in the HC jet loop system at an inlet pressure of 300 kPa

Time (min)	Sample	Abs 1	Abs 2	Abs 3	Abs	% Decolouration
0	VO0	1.509	1.5067	1.5057	1.50713333	0
2	VO1	1.0248	1.0249	1.0243	1.02466667	32.0122086
4	VO2	0.9181	0.9181	0.9181	0.9181	39.0830274
6	VO3	0.7697	0.7701	0.7692	0.76966667	48.9317468
8	VO4	0.6814	0.6822	0.682	0.68186667	54.757376
10	VO5	0.643	0.6433	0.6422	0.64283333	57.3472818

Table A 2: Absorbance measurements and percent decolouration of OR2 using 6 mm hole diameter orifice plate in the HC jet loop system at an inlet pressure of 300 kPa

Time (min)	Sample	Abs 1	Abs 2	Abs 3	Abs	% Decolouration
0	6O0	1.2873	1.2883	1.2869	1.2875	0
2	6O1	0.8511	0.846	0.8461	0.84773333	34.1566343
4	6O2	0.4781	0.4782	0.4784	0.47823333	62.8556634
6	6O3	0.3443	0.3442	0.3439	0.34413333	73.2711974
8	6O4	0.2677	0.2681	0.2678	0.26786667	79.194822
10	6O5	0.2256	0.2248	0.2248	0.22506667	82.5190939

Table A 3: Absorbance measurements and percent decolouration of OR2 using 5 mm hole diameter orifice plate in the HC jet loop system at an inlet pressure of 300 kPa

Time (min)	Sample	Abs 1	Abs 2	Abs 3	Abs	% Decolouration
0	5O0	1.3215	1.3218	1.321	1.32143333	0
2	5O1	0.7091	0.708	0.7083	0.70846667	46.3864995
4	5O2	0.4145	0.4149	0.4148	0.41473333	68.6148879
6	5O3	0.2631	0.262	0.2619	0.26233333	80.1478193
8	5O4	0.2145	0.2146	0.2147	0.2146	83.7600585
10	5O5	0.1973	0.1976	0.1976	0.1975	85.0541079

Table A 4: Absorbance measurements and percent decolouration of OR2 using 4 mm hole diameter orifice plate in the HC jet loop system at an inlet pressure of 300 kPa

Time (min)	Sample	Abs 1	Abs 2	Abs 3	Abs	% Decolouration
0	4O0	1.5341	1.5339	1.5332	1.53373333	0
2	4O1	0.7438	0.7431	0.7425	0.74313333	51.5474224
4	4O2	0.4228	0.4233	0.4235	0.4232	72.4071981
6	4O3	0.2669	0.2672	0.2674	0.26716667	82.5806311
8	4O4	0.2149	0.2158	0.2154	0.21536667	85.958011
10	4O5	0.2041	0.2043	0.2047	0.20436667	86.6752152

Table A 5: Absorbance measurements and percent decolouration of OR2 using 3 mm hole diameter orifice plate in the HC jet loop system at an inlet pressure of 300 kPa

Time (min)	Sample	Abs 1	Abs 2	Abs 3	Abs	% Decolouration
0	3O0	1.2781	1.2769	1.2759	1.27696667	0
2	3O1	0.708	0.7073	0.7077	0.70766667	44.5822131
4	3O2	0.3811	0.3821	0.382	0.38173333	70.1062414
6	3O3	0.2077	0.2074	0.2071	0.2074	83.7583858
8	3O4	0.15	0.1501	0.1504	0.15016667	88.2403613
10	3O5	0.1501	0.15	0.1501	0.15006667	88.2481923

Table A 6: Absorbance measurements and percent decolouration of OR2 using 2 mm hole diameter orifice plate in the HC jet loop system at an inlet pressure of 300 kPa

Time (min)	Sample	Abs 1	Abs 2	Abs 3	Abs	% Decolouration
0	2O0	1.6387	1.6378	1.6362	1.63756667	0
2	2O1	0.713	0.7131	0.7132	0.7131	56.4536813
4	2O2	0.4121	0.4118	0.412	0.41196667	74.8427545
6	2O3	0.2357	0.2362	0.2359	0.23593333	85.5924441
8	2O4	0.1738	0.1746	0.1744	0.17426667	89.3581941
10	2O5	0.1708	0.17	0.1701	0.1703	89.6004234

Table A 7: Absorbance measurements and percent decolouration of OR2 using the 10 mm throat diameter venturi in the HC jet loop system at an inlet pressures of 200 kPa, 300 kPa and 400 kPa

VENTURI ALONE						
200 kPa						
Time (min)	Sample	Abs 1	Abs 2	Abs 3	Abs	% Decolouration
0	2PV00	1.5321	1.5349	1.5402	1.53573333	0
2	2PV02	1.1329	1.1438	1.1345	1.13706667	25.95936795
4	2PV04	1.1032	1.1029	1.1038	1.1033	28.15810036
6	2PV06	0.9854	0.9832	0.9818	0.98346667	35.96110436
8	2PV08	0.917	0.9165	0.9218	0.91843333	40.19578052
10	2PV10	0.8534	0.8529	0.8533	0.8532	44.44347977
300 kPa						
Time (min)	Sample	Abs 1	Abs 2	Abs 3	Abs	% Decolouration
0	3PV00	1.509	1.5067	1.5057	1.50713333	0
2	3PV02	1.0248	1.0249	1.0243	1.02466667	32.01220861
4	3PV04	0.9181	0.9181	0.9181	0.9181	39.08302738
6	3PV06	0.7697	0.7701	0.7692	0.76966667	48.9317468
8	3PV08	0.6814	0.6822	0.682	0.68186667	54.75737603
10	3PV10	0.643	0.6433	0.6422	0.64283333	57.34728182
400 kPa						
Time (min)	Sample	Abs 1	Abs 2	Abs 3	Abs	% Decolouration
0	4PV00	1.5129	1.5142	1.5144	1.51383333	0
2	4PV02	0.9395	0.9289	0.9293	0.93256667	38.39700539
4	4PV04	0.8219	0.8344	0.8352	0.8305	45.13927117
6	4PV06	0.7534	0.7509	0.7512	0.75183333	50.33579214
8	4PV08	0.6608	0.6593	0.659	0.6597	56.42188704

10	4PV10	0.6239	0.625	0.6256	0.62483333	58.72509083

Table A 8: Absorbance measurements and percent decolouration of OR2 using the 2 mm hole diameter orifice plate in the HC jet loop system at an inlet pressures of 200 kPa, 300 kPa and 400 kPa

ORIFICE PLATE						
200 kPa						
Time (min)	Sample	Abs 1	Abs 2	Abs 3	Abs	% Decolouration
0	2POp00	1.6024	1.603	1.6041	1.60316667	0
2	2POp02	0.9023	0.9224	0.909	0.91123333	43.1604117
4	2POp04	0.7782	0.7767	0.7902	0.7817	51.2402537
6	2POp06	0.5056	0.5094	0.5093	0.5081	68.3064768
8	2POp08	0.3976	0.3954	0.3894	0.39413333	75.4153238
10	2POp10	0.3105	0.3097	0.3099	0.31003333	80.6611914
300 kPa						
Time (min)	Sample	Abs 1	Abs 2	Abs 3	Abs	% Decolouration
0	3POp00	1.6387	1.6378	1.6362	1.63756667	0
2	3POp02	0.713	0.7131	0.7132	0.7131	56.4536813
4	3POp04	0.4121	0.4118	0.412	0.41196667	74.8427545
6	3POp06	0.2357	0.2362	0.2359	0.23593333	85.5924441
8	3POp08	0.1738	0.1746	0.1744	0.17426667	89.3581941
10	3POp10	0.1708	0.17	0.1701	0.1703	89.6004234
400 kPa						
Time (min)	Sample	Abs 1	Abs 2	Abs 3	Abs	% Decolouration
0	4POp00	1.6173	1.618	1.6183	1.61786667	0
2	4POp02	0.6535	0.6587	0.6592	0.65713333	59.3827262
4	4POp04	0.3445	0.3439	0.3476	0.34533333	78.655019
6	4POp06	0.1978	0.1966	0.1983	0.19756667	87.7884457
8	4POp08	0.1565	0.1546	0.1561	0.15573333	90.3741553
10	4POp10	0.1423	0.1456	0.1438	0.1439	91.1055711

Table A 9: Absorbance measurements and percent decolouration of OR2 using the combination of the 10 mm throat diameter venturi and 2 mm hole diameter orifice plate in the HC jet loop system at an inlet pressures of 200 kPa, 300 kPa and 400 kPa

VENTURI + ORIFICE PLATE						
200 kPa						
Time (min)	Sample	Abs 1	Abs 2	Abs 3	Abs	% Decolouration
0	2PVOp00	1.5467	1.5456	1.549	1.5471	0
2	2PVOp02	0.9935	0.9917	0.9937	0.99296667	35.8175511
4	2PVOp04	0.8234	0.836	0.8345	0.8313	46.2672096
6	2PVOp06	0.6875	0.6743	0.6821	0.6813	55.9627691
8	2PVOp08	0.5597	0.5565	0.5642	0.56013333	63.7946265
10	2PVOp10	0.4964	0.4987	0.4932	0.4961	67.9335531
300 kPa						
Time (min)	Sample	Abs 1	Abs 2	Abs 3	Abs	% Decolouration
0	3PVOp00	1.5387	1.5426	1.5462	1.5425	0
2	3PVOp02	0.8726	0.9035	0.8837	0.8866	42.5218801
4	3PVOp04	0.7118	0.7551	0.7262	0.73103333	52.6072393
6	3PVOp06	0.485	0.4923	0.4834	0.4869	68.4343598
8	3PVOp08	0.481	0.4517	0.4691	0.46726667	69.7071853
10	3PVOp10	0.4701	0.434	0.4513	0.4518	70.7098865
400 kPa						
Time (min)	Sample	Abs 1	Abs 2	Abs 3	Abs	% Decolouration
0	4PVOp00	1.5254	1.5256	1.5239	1.52496667	0
2	4PVOp02	0.8552	0.8539	0.8493	0.8528	44.0774662
4	4PVOp04	0.6207	0.6198	0.6197	0.62006667	59.3390019
6	4PVOp06	0.5351	0.5329	0.5394	0.5358	64.8648058
8	4PVOp08	0.4169	0.4175	0.4178	0.4174	72.6289099
10	4PVOp10	0.3925	0.3978	0.3954	0.39523333	74.0824936

Table A 10: Absorbance measurements and percent decolouration of OR2 using the 10 mm throat diameter venturi in the HC jet loop system at an inlet pressure of 400 kPa

VENTURI ALONE						
400 kPa						
Time (min)	Sample	Abs 1	Abs 2	Abs 3	Abs	% Decolouration
0	4PV00	1.5129	1.5142	1.5144	1.51383333	0
2	4PV02	0.9395	0.9289	0.9293	0.93256667	38.3970054
4	4PV04	0.8219	0.8344	0.8352	0.8305	45.1392712
6	4PV06	0.7534	0.7509	0.7512	0.75183333	50.3357921
8	4PV08	0.6608	0.6593	0.659	0.6597	56.421887
10	4PV10	0.6239	0.625	0.6256	0.62483333	58.7250908

Table A 11: Absorbance measurements and percent decolouration of OR2 using the 2 mm hole diameter orifice plate in the HC jet loop system at an inlet pressure of 400 kPa

ORIFICE PLATE						
400 kPa						
Time (min)	Sample	Abs 1	Abs 2	Abs 3	Abs	% Decolouration
0	4POp00	1.6173	1.618	1.6183	1.61786667	0
2	4POp02	0.6535	0.6587	0.6592	0.65713333	59.3827262
4	4POp04	0.3445	0.3439	0.3476	0.34533333	78.655019
6	4POp06	0.1978	0.1966	0.1983	0.19756667	87.7884457
8	4POp08	0.1565	0.1546	0.1561	0.15573333	90.3741553
10	4POp10	0.1423	0.1456	0.1438	0.1439	91.1055711

Table A 12: Absorbance measurements and percent decolouration of OR2 using the combination of the 10 mm throat diameter venturi and 2 mm hole diameter orifice plate in the HC jet loop system at an inlet pressure 400 kPa

VENTURI + ORIFICE PLATE						
400 kPa						
Time (min)	Sample	Abs 1	Abs 2	Abs 3	Abs	% Decolouration
0	4PVOp00	1.5254	1.5256	1.5239	1.52496667	0
2	4PVOp02	0.8552	0.8539	0.8493	0.8528	44.0774662
4	4PVOp04	0.6207	0.6198	0.6197	0.62006667	59.3390019
6	4PVOp06	0.5351	0.5329	0.5394	0.5358	64.8648058
8	4PVOp08	0.4169	0.4175	0.4178	0.4174	72.6289099
10	4PVOp10	0.3925	0.3978	0.3954	0.39523333	74.0824936

Table A 13: Quantification of OH radical in the HC jet loop system using the 10 mm throat diameter venturi

VENTURI ALONE				
400 kPa				
Time (min)	Abs 1	Abs 2	Intensity Av	Concentration (ppm)
0	0	0	0	0
2	38626600	38873400	77500000	15.5
4	45314400	46185600	91500000	18.3
6	50175800	50824200	101000000	20.2
8	57500000	57000000	114500000	22.9
10	60661000	60839000	121500000	24.3

Table A 14: Quantification of OH radical in the HC jet loop system using the 2 mm hole diameter orifice plate

ORIFICE PLATE

400 kPa				
Time (min)	Abs 1	Abs 2	Intensity Av	Concentration (ppm)
0	0	0	0	0
2	60269000	60731000	121000000	24.2
4	70843220	71156780	142000000	28.4
6	76109800	75890200	152000000	30.4
8	78508000	78992000	157500000	31.5
10	80940000	80560000	161500000	32.3

Table A 15: Quantification of OH radical in the HC jet loop system using the combination of the 10 mm throat diameter venturi and 2 mm hole diameter orifice plate

VENTURI + ORIFICE PLATE				
400 kPa				
Time (min)	Abs 1	Abs 2	Intensity Av	Concentration (ppm)
0	0	0	0	0
2	45148000	45352000	90500000	18.1
4	54826400	54673600	109500000	21.9
6	58288000	58712000	117000000	23.4
8	64250000	64250000	128500000	25.7
10	68125040	67874960	136000000	27.2

Appendix B: Moody chart for determination of friction factor f (Beck & Collins, 2008)

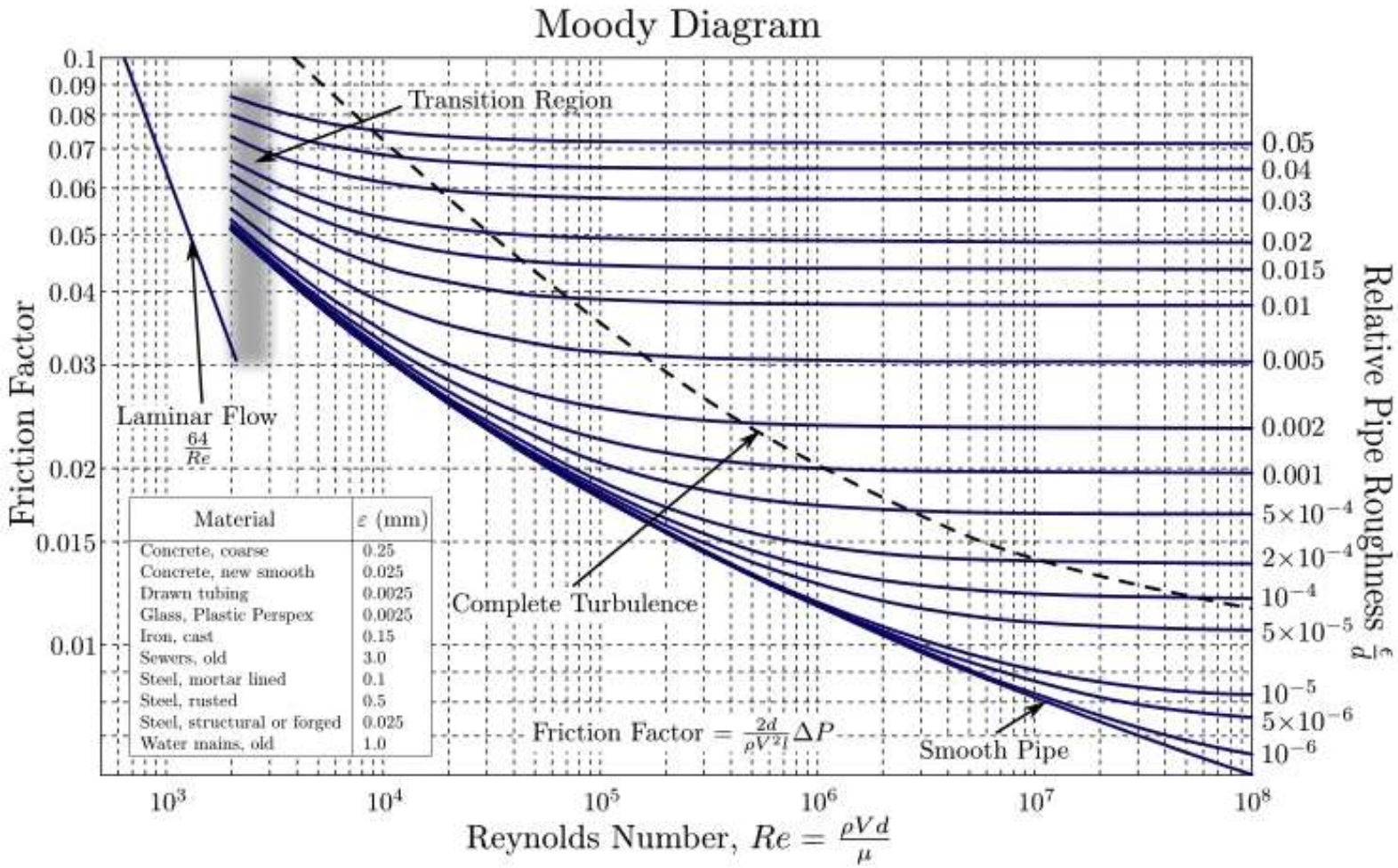
Moody Diagram
Friction Factor
Reynolds Number, $Re = \frac{\rho V d}{\mu}$
Relative Pipe Roughness $\frac{\epsilon}{d}$
Transition Region
Laminar Flow
$\frac{64}{Re}$
Complete Turbulence
Friction Factor = $\frac{2d}{\rho V^2 l}\Delta P$
Smooth Pipe
0.1
0.09
0.08
0.07
0.06
0.05
0.04
0.03
0.02
0.015
0.01
10^3
10^4
10^5
10^6
10^7
10^8
0.05
0.04
0.03
0.02
0.015
0.01
0.005
0.002
0.001
5×10^{-4}
2×10^{-4}
10^{-4}
5×10^{-5}
10^{-5}
5×10^{-6}
10^{-6}
Material | ε (mm)
Concrete, coarse | 0.25
Concrete, new smooth | 0.025
Drawn tubing | 0.0025
Glass, Plastic Perspex | 0.0025
Iron, cast | 0.15
Sewers, old | 3.0
Steel, mortar lined | 0.1
Steel, rusted | 0.5
Steel, structural or forged | 0.025
Water mains, old | 1.0